INFORMATION TO USERS

This reproduction was made from a copy of a document sent to us for microfilming. While the most advanced technology has been used to photograph and reproduce this document, the quality of the reproduction is heavily dependent upon the quality of the material submitted.

The following explanation of techniques is provided to help clarify markings or notations which may appear on this reproduction.

1. The sign or "target" for pages apparently lacking from the document photographed is "Missing Page(s)". If it was possible to obtain the missing page(s) or section, they are spliced into the film along with adjacent pages. This may have necessitated cutting through an image and duplicating adjacent pages to assure complete continuity.

2. When an image on the film is obliterated with a round black mark, it is an indication of either blurred copy because of movement during exposure, duplicate copy, or copyrighted materials that should not have been filmed. For blurred pages, a good image of the page can be found in the adjacent frame. If copyrighted materials were deleted, a target note will appear listing the pages in the adjacent frame.

3. When a map, drawing or chart, etc., is part of the material being photographed, a definite method of "sectioning" the material has been followed. It is customary to begin filming at the upper left hand corner of a large sheet and to continue from left to right in equal sections with small overlaps. If necessary, sectioning is continued again—beginning below the first row and continuing on until complete.

4. For illustrations that cannot be satisfactorily reproduced by xerographic means, photographic prints can be purchased at additional cost and inserted into your xerographic copy. These prints are available upon request from the Dissertations Customer Services Department.

5. Some pages in any document may have indistinct print. In all cases the best available copy has been filmed.

University Microfilms International
300 N. Zeeb Road
Ann Arbor, MI 48106

Order Number 1330931

Determination of rock plasticity parameters by indentation experiment

Stanley, H. Mark, III, M.S.

Rice University, 1987

U·M·I
300 N. Zeeb Rd.
Ann Arbor, MI 48106

PLEASE NOTE:

In all cases this material has been filmed in the best possible way from the available copy. Problems encountered with this document have been identified here with a check mark __✓__.

1. Glossy photographs or pages _____
2. Colored illustrations, paper or print _____
3. Photographs with dark background _____
4. Illustrations are poor copy _____
5. Pages with black marks, not original copy _____
6. Print shows through as there is text on both sides of page _____
7. Indistinct, broken or small print on several pages __✓__
8. Print exceeds margin requirements _____
9. Tightly bound copy with print lost in spine _____
10. Computer printout pages with indistinct print _____
11. Page(s) _____ lacking when material received, and not available from school or author.
12. Page(s) _____ seem to be missing in numbering only as text follows.
13. Two pages numbered _____. Text follows.
14. Curling and wrinkled pages _____
15. Dissertation contains pages with print at a slant, filmed as received _____
16. Other _____

_____

_____

University
Microfilms
International

RICE UNIVERSITY

DETERMINATION OF ROCK PLASTICITY PARAMETERS BY INDENTATION EXPERIMENT

by

H. MARK STANLEY III

A THESIS SUBMITTED
IN PARTIAL FULFILLMENT OF THE
REQUIREMENTS FOR THE DEGREE

MASTER OF SCIENCE

APPROVED, THESIS COMMITTEE

John B. Cheatham, Jr., Professor of
Mechanical Engineering, Director

J. E. Merwin, Professor in the
Department of Civil Engineering

Y. C. Angel, Assistant Professor
in the Department of
Mechanical Engineering

Houston, Texas

September, 1986

ABSTRACT

Indentation tests are performed on samples of Indiana Limestone and Berea Sandstone under confining pressures ranging from 0 to 2500 psi. The force-displacement data from these experiments are analyzed by comparing them to numerical results obtained for a simplified theoretical model which assumes 1) rigid-perfectly plastic behavior, 2) a Mohr-Coulomb linear yield envelope, and 3) negligible lip formation. In addition, indentation is assumed to be a quasi-static, equilibrium process.

The two Mohr-Coulomb parameters cohesive strength (c) and angle of internal friction (ϕ) are bounded by consideration of the following two heuristic conditions:

1. The force-displacement curve generated by a perfectly rough assumption must be an upper bound to the experimentally observed curve.
2. The frictionless solution must be a lower bound.

These two conditions restrict ϕ and c to a narrow allowable region in ϕ-c space, and are applicable to more realistic yield conditions, as well.

ACKNOWLEDGEMENTS

It is a pleasure to record my gratitude to Dr. John Cheatham for his guidance and advice throughout the project. The financial assistance by Dr. Phil Patillo and the Amoco Production Company is greatly appreciated. Thanks go to Daan Hekma-Wierda for his excellent sample preparation, and to Linda Anderson for typing the manuscript.

Table of Contents

LIST OF FIGURES

NOMENCLATURE

C1,C2,C3	curve fit constants
c	cohesive strength
c*	an effective cohesion = c + wtan ϕ
D	tool displacement
F	force on tool
i,j	indices for numbering finite-difference mesh nodes
r,z, λ	radial, axial, and circumferential directions in cylindrical polar coordinates
w	confining pressure on the rock face
β	angle of tool face to the vertical axis
θ	angle between the direction of maximum principal stress and the radial direction
μ	$= \pi/4 - \phi/2$
ξ, η	characteristics to the stress equations
σ	$= \frac{\sigma_1 + \sigma_3}{2} + c \cot \phi$, the distance from the yield envelope apex to the center of the Mohr's circle
$\sigma_1, \sigma_2, \sigma_3$	principal stresses
σ_n	a normal stress
τ	shear strength
ϕ	angle of internal friction
χ	an auxiliary function = $\frac{1}{2} \cot \phi \, \ln \frac{\sigma}{c}$

I. INTRODUCTION

Triaxial testing is currently the accepted method of determining rock properties. Due to the tremendous effective confining pressures under an indentation tool, and the difficulty with which such pressures are achieved in triaxial testing, there is motivation to study the problem of extracting these properties by an indentation test. This thesis presents a method for determining certain rock plasticity parameters.

Several assumptions are made in the analyses that follow:

1. The rock is rigid-perfectly plastic. No strain-hardening or softening is allowed, and elastic deformations are negligible.
2. The yield condition is the Mohr-Coulomb linear envelope.
3. Lip formation at the surface is negligible, with regard both to rock-tool interaction and to boundary conditions.
4. The theoretically correct load on the tool for a given set of parameters is obtained by integrating the differential equations of plastic equilibrium.

Assumption 4 inherently disregards consideration of a flow rule for the material.

Since the Mohr-Coulomb condition has two parameters, the ideal result of this study would be to specify a unique value for each as a result of analyzing an indentation test. It is known, however, that this yield condition is only an approximation to real behavior. The goal of the thesis, then, is to develop a method of restricting the two parameters in some systematic way.

II. THEORETICAL BACKGROUND AND NUMERICAL PROCEDURE

Failure Envelope

For a rigid-plastic material, the criterion for plastic flow is known as the yield condition. Rocks are among a class of materials whose yielding is influenced by hydrostatic pressure. Coulomb (1773) introduced the simplest description of such a behavior, proposing that the shear strength varies linearly with mean stress (see Figure 2.1):

$$\tau = c + \sigma_n \tan\phi \tag{1}$$

where

- τ is the shear strength
- c is the cohesive strength
- σ_n is a normal stress
- ϕ is the angle of internal friction.

Note that sign convention here and throughout the paper is positive for compressive stresses.

Other yield surfaces have been proposed in order to more closely model materials of this class - most notably the modified von Mises criterion and a parabolic yield envelope - but the Coulomb criterion is used exclusively in the present study since 1) it is easy to analyze for the proposed solution methods and 2) linear regions represent fairly well the behavior of rocks for compressive mean stresses (Gnirk and Cheatham [10]). In fact, tensile mean stresses are not encountered in indentation testing, so it is impossible with

MOHR-COULOMB YIELD ENVELOPE

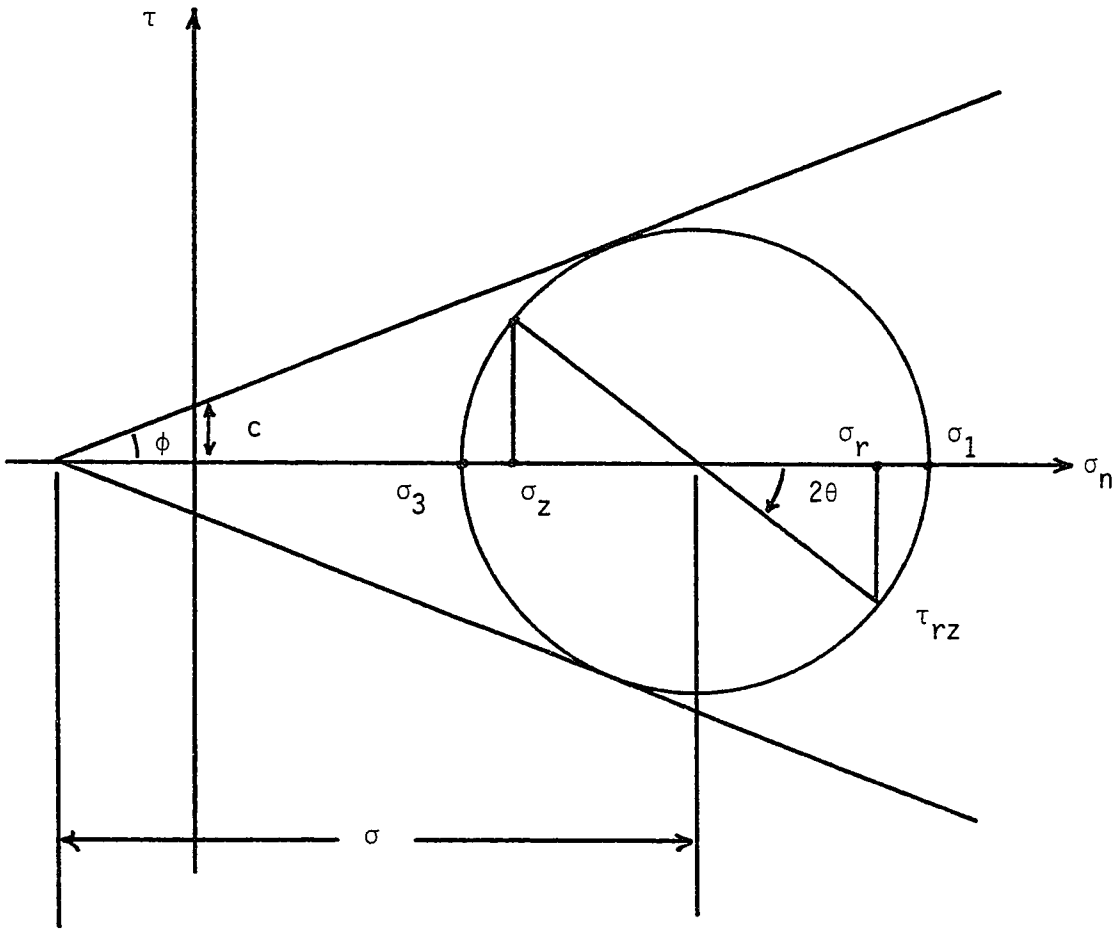

FIGURE 2.1

this method to deduce the shape of the failure envelope in the tensile region.

The Coulomb yield condition is often combined with Mohr's stress representation, so that yield is said to occur when the Mohr's circle contacts a failure envelope. Stress states represented by circles inside (not touching) the envelope result in rigid response, and circles outside of this envelope are not allowed.

Equations in Axial Symmetry

It has been shown (Harr [8]) that the solution to problems of limiting equilibrium reduces to the integration of the differential equations of equilibrium

$$\frac{\partial \sigma_r}{\partial r} + \frac{1}{r}\frac{\partial \tau_{r\lambda}}{\partial \lambda} + \frac{\partial \tau_{rz}}{\partial z} + \frac{(\sigma_r - \sigma_\lambda)}{r} = 0$$

$$\frac{\partial \tau_{r\lambda}}{\partial r} + \frac{1}{r}\frac{\partial \sigma_\lambda}{\partial \lambda} + \frac{\partial \tau_{z\lambda}}{\partial z} + \frac{2\tau_{r\lambda}}{r} = 0 \qquad (2)$$

$$\frac{\partial \tau_{rz}}{\partial r} + \frac{1}{r}\frac{\partial \tau_{z\lambda}}{\partial \lambda} + \frac{\partial \sigma_z}{\partial z} + \frac{\tau_{rz}}{r} = 0$$

combined with the stress relations given from the yield condition (Mohr-Coulomb in this case):

$$\begin{aligned} \sigma_r &= \sigma(1 + \sin\phi \cos 2\theta) - c \cot\phi \\ \sigma_z &= \sigma(1 - \sin\phi \cos 2\theta) - c \cot\phi \qquad (3) \\ \tau_{rz} &= \sigma \sin\phi \sin 2\theta \ . \end{aligned}$$

COORDINATE SYSTEMS*

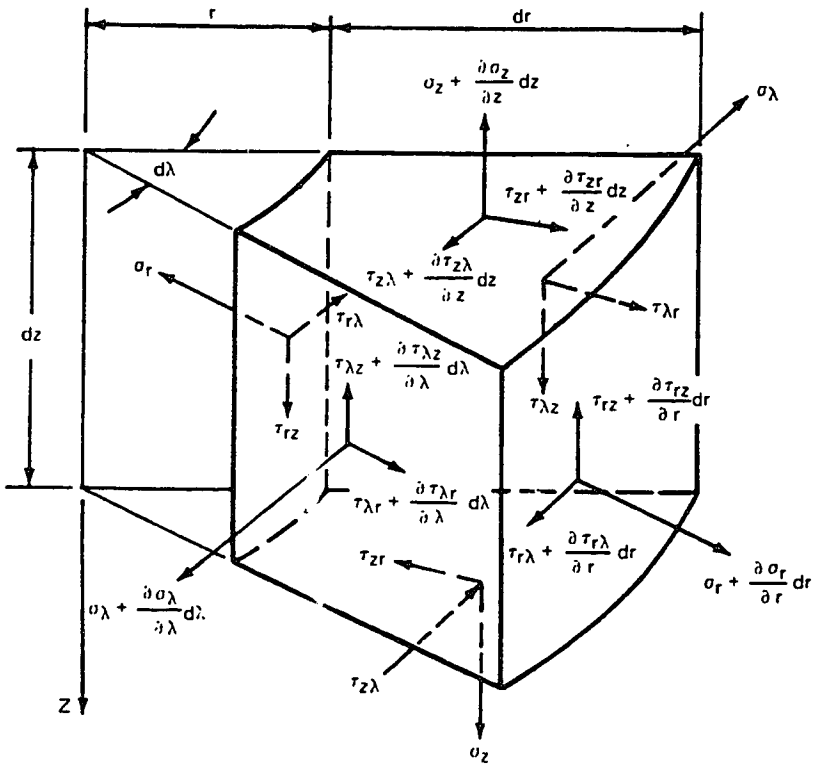

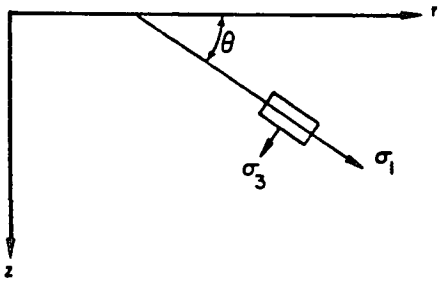

* after Karafiath and Nowatski [2]

FIGURE 2.2

Axial symmetry requires that the shear stresses $\tau_{r\lambda}$ and $\tau_{z\lambda}$ vanish, so that in an arbitrary r-z plane, equations (2) reduce to

$$\frac{\partial \sigma_r}{\partial r} + \frac{\partial \tau_{rz}}{\partial z} + \frac{(\sigma_r - \sigma_\lambda)}{r} = 0$$

$$\frac{\partial \tau_{rz}}{\partial r} + \frac{\partial \sigma_z}{\partial z} + \frac{\tau_{rz}}{r} = 0 \qquad (4)$$

A solution to the equations (3) and (4) depends not only on defining appropriate boundary conditions, but also on a further assumption known as the Haar and von Karman hypothesis (Cox, Eason, and Hopkins [12]), in which it is assumed that the circumferential stress σ_λ of equation (4) is equal to the minimum principal stress σ_3. Specifically:

$$\sigma_\lambda = \frac{\sigma_r + \sigma_z}{2} - \left[\left(\frac{\sigma_r - \sigma_z}{2}\right)^2 + \tau_{rz}^2\right]^{1/2} \qquad (5)$$

Cox, et al [12] suggest that stress distributions which agree with this hypothesis are appropriate to the indentation problem, but it should be recognized that other plastic stress states exist which permit axially symmetric flow. The solutions of the present study rely implicitly on the Haar and von Karman hypothesis.

Substitution of equations (3) and (5) into (4) yields

$$(1 + \sin\phi \cos 2\theta)\frac{\partial \sigma}{\partial r} - 2\sigma \sin\phi \sin 2\theta \frac{\partial \theta}{\partial r}$$
$$+ 2\sigma \sin\phi \cos 2\theta \frac{\partial \theta}{\partial z} + \sin\phi \sin 2\theta \frac{\partial \sigma}{\partial z}$$
$$+ \frac{1}{r}[\sigma \sin\phi(1 + \cos 2\theta)] = 0 \qquad (6a)$$

and

$$\sin\phi \sin 2\theta \frac{\partial \sigma}{\partial r} + 2\sigma \sin\phi \cos 2\theta \frac{\partial \theta}{\partial r}$$

$$+ (1 - \sin\phi \cos 2\theta) \frac{\partial \sigma}{\partial z} + 2\sigma \sin\phi \sin 2\theta \frac{\partial \theta}{\partial z}$$

$$+ \frac{1}{r}[\sigma \sin\phi \sin 2\theta] = 0 \qquad (6b)$$

Method of Characteristics Solution

In theory, it is possible to solve equations (6) based on a common numerical procedure such as a finite-difference approximation. There is, however, a further refinement which leads to simpler equations and quantities with physically obvious meaning: the method of characteristics (see Abbott [7], Smith [17]).

In this method, directions are sought along which the integration of the partial differential equations transforms to the integration of an equation involving total differentials only. Since there are two equations, two families of curves will result which satisfy these directions.

Multiplying the first of equations (6) by $\sin(\theta \pm \mu)$ and the second by $-\cos(\theta \pm \mu)$, dividing through by $\pm \cos\phi$, and adding, the following pair of equations is obtained ($\mu = \pi/4 - \phi/2$):

$$\begin{aligned} &\cos(\theta \mp \mu) \frac{\partial \sigma}{\partial r} + \sin(\theta \mp \mu) \frac{\partial \sigma}{\partial z} \\ &\mp 2\sigma \tan\phi \cos(\theta \mp \mu) \frac{\partial \theta}{\partial r} \\ &\mp 2\sigma \tan\phi \sin(\theta \mp \mu) \frac{\partial \theta}{\partial z} \\ &\pm \frac{\sigma \tan\phi}{r}[\sin(\theta \pm \mu) - \sin(\theta \mp \mu)] = 0 \end{aligned} \qquad (7)$$

A clever change of variables proposed by Sokolovski [16] brings equations (7) into characteristic form. Letting

$$\begin{aligned} \chi &= \frac{1}{2} \cot\phi \, \ln \frac{\sigma}{c} \\ \xi &= \chi + \theta \\ \eta &= \chi - \theta \end{aligned} \tag{8}$$

equations (7) become

$$\begin{aligned} \frac{\partial \xi}{\partial r} + \tan(\theta + \mu) \frac{\partial \xi}{\partial z} &= a = \frac{[\sin(\theta - \mu) - \sin(\theta + \mu)]}{2r \cos(\theta + \mu)} \\ \frac{\partial \eta}{\partial r} + \tan(\theta - \mu) \frac{\partial \eta}{\partial z} &= b = \frac{-[\sin(\theta + \mu) - \sin(\theta - \mu)]}{2r \cos(\theta - \mu)} . \end{aligned} \tag{9}$$

Along with the chain rule

$$\begin{aligned} d\xi &= \frac{\partial \xi}{\partial r} dr + \frac{\partial \xi}{\partial z} dz \\ d\eta &= \frac{\partial \eta}{\partial r} dr + \frac{\partial \eta}{\partial z} dz \end{aligned} \tag{10}$$

the system can be written in matrix form:

$$\begin{bmatrix} 1 & \tan(\theta + \mu) & 0 & 0 \\ 0 & 0 & 1 & \tan(\theta - \mu) \\ dr & dz & 0 & 0 \\ 0 & 0 & dr & dz \end{bmatrix} \begin{bmatrix} \frac{\partial \xi}{\partial r} \\ \frac{\partial \xi}{\partial z} \\ \frac{\partial \eta}{\partial r} \\ \frac{\partial \eta}{\partial z} \end{bmatrix} = \begin{bmatrix} a \\ b \\ d\xi \\ d\eta \end{bmatrix} \tag{11}$$

The solution of the characteristic slopes requires that the determinant of the coefficient matrix in (11) be zero (Abbott [7], p. 72):

$$dz^2 - [\tan(\theta - \mu) + \tan(\theta + \mu)]dr\, dz + [\tan(\theta - \mu)\tan(\theta + \mu)] = 0 \qquad (12)$$

Equation (12) is a quadratic equation for $\frac{dz}{dr}$, the slope of a characteristic line. The system (11) is classified as hyperbolic, parabolic, or elliptic, depending on whether the discriminant of the quadratic formula for (12) is positive, zero, or negative, respectively. In this case, the discriminant is

$$[\tan(\theta - \mu) - \tan(\theta + \mu)]^2 > 0 \qquad (13)$$

and, in fact, is equal zero only when $\phi = \pi/2$, which is meaningless. The system of equations (11) is therefore <u>hyperbolic</u> for the range of ϕ considered. Solving equation (12) yields the two real, distinct slopes associated with the characteristics ξ and η.

$$\frac{dz}{dr}\Big|_{\xi,\eta} = \tan(\theta \pm \mu) \qquad (14)$$

These two slopes may also be seen by use of the Mohr's circle pole, as in Figure 2.3. In the present case, the pole P is found by the intersection of a line through the minimum principal stress σ_3, inclined at an angle θ, with the stress circle. This is an

CHARACTERISTIC DIRECTIONS BY
MOHR'S CIRCLE POLE

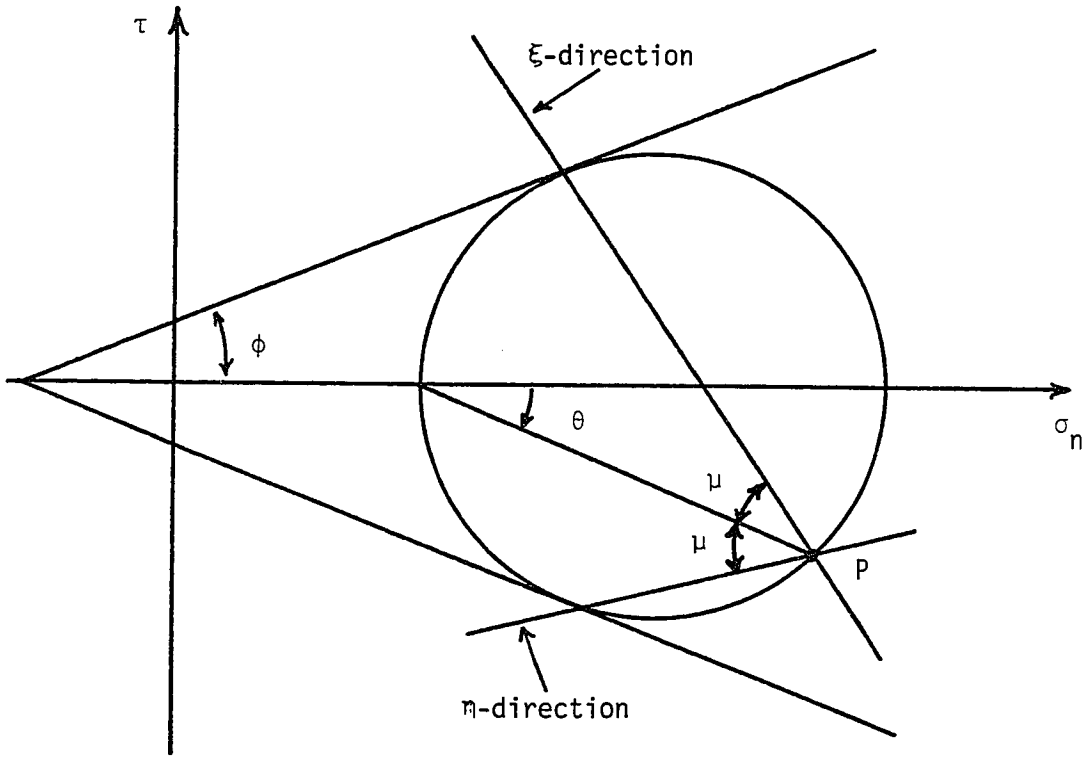

FIGURE 2.3

intuitively useful concept, since the lines drawn from the pole to the points of tangency to the yield envelope map directly into physical space as the characteristic slopes.

Setting all numerators of Cramer's solution to zero, the system (11) gives ordinary differential equations for the variation of ξ and η along the characteristics. The fundamental quantities of interest, however, are σ and θ. Using the relations (from equations (8)),

$$\sigma = c \exp[(\xi + \eta)\tan\phi]$$
$$\theta = \frac{\xi - \eta}{2} \tag{15}$$

the characteristic equations are given as

$$dz = dr \tan(\theta + \mu)$$

$$d\sigma + 2\sigma \tan\phi \, d\theta \tag{16a}$$
$$+ \frac{\sigma}{r}[\sin\phi dr + \tan\phi(1 - \sin\phi)dz] = 0$$

for the ξ-characteristics, and

$$dz = dr \tan(\theta - \mu)$$

$$d\sigma - 2\sigma \tan\phi \, d\theta \tag{16b}$$
$$+ \frac{\sigma}{r}[\sin\phi \, dr - \tan\phi(1 - \sin\phi)dz] = 0$$

for the η-characteristics.

Equations (16) are a generalization of the so-called Kötter's equations, which describe the variation of plastic stress along slip-lines in plane strain. Given the proper boundary conditions, these equations describe completely the values r, z, σ, and θ along their respective characteristic curves.

Finite-Difference Approximation to the Characteristic Equations

Since the characteristic equations (16) involve only total differentials, they are quite amenable to approximation by a finite-difference method. An arbitrary portion of a finite characteristic net is shown in Figure 2.4, showing a node-numbering system for the intersections of ξ and η characteristics. In this study, a simple backward-difference approximation is used. Thus equations (16) are replaced by the approximations

$$z_{i,j} - z_{i,j-1} = (r_{i,j} - r_{i,j-1})\tan(\theta_{i,j-1} + \mu)$$

$$\sigma_{i,j} - \sigma_{i,j-1} + 2\sigma_{i,j-1}\tan\phi(\theta_{i,j} - \theta_{i,j-1}) + \frac{\sigma_{i,j-1}B}{r_{i,j-1}} = 0 \qquad (17a)$$

for ξ-characteristics, and

$$z_{i,j} - z_{i-1,j} = (r_{i,j} - r_{i-1,j})\tan(\theta_{i-1,j} - \mu)$$

$$\sigma_{i,j} - \sigma_{i-1,j} - 2\sigma_{i-1,j}\tan\phi(\theta_{i,j} - \theta_{i-1,j}) + \frac{\sigma_{i-1,j}A}{r_{i-1,j}} = 0 \qquad (17b)$$

for η-characteristics where

$$A = \sin\phi(r_{i,j} - r_{i-1,j}) - \tan\phi(1 - \sin\phi)(z_{i,j} - z_{i-1,j})$$

$$B = \sin\phi(r_{i,j} - r_{i,j-1}) + \tan\phi(1 - \sin\phi)(z_{i,j} - z_{i,j-1}).$$

The first equations of (17a), (17b) constitute two equations in two unknowns, such that at the i,jth node (of Figure 2.4, for example):

$$z_{i,j} = z_{i-1,j} + \alpha_2(r_{i,j} - r_{i-1,j}) \tag{18}$$

or

$$z_{i,j} = z_{i,j-1} + \alpha_1(r_{i,j} - r_{i,j-1})$$

where

$$\alpha_1 = \tan(\theta_{i,j-1} + \mu)$$

$$\alpha_2 = \tan(\theta_{i-1,j} - \mu)$$

and

$$r_{i,j} = [z_{i-1,j} - z_{i,j-1} + \alpha_1 r_{i,j-1} - \alpha_2 r_{i-1,j}]/(\alpha_1 - \alpha_2). \tag{19}$$

Likewise, the second equations are solved algebraically to yield:

$$\sigma_{i,j} = [2\sigma_{i-1,j}\sigma_{i,j-1}(1 - \tan\phi(\theta_{i-1,j} - \theta_{i,j-1}))$$

$$- \sigma_{i-1,j}\sigma_{i,j-1}\{\frac{A}{r_{i-1,j}} + \frac{B}{r_{i,j-1}}\}]/[\sigma_{i,j-1} + \sigma_{i-1,j}] \tag{20}$$

A CHARACTERISTIC NETWORK

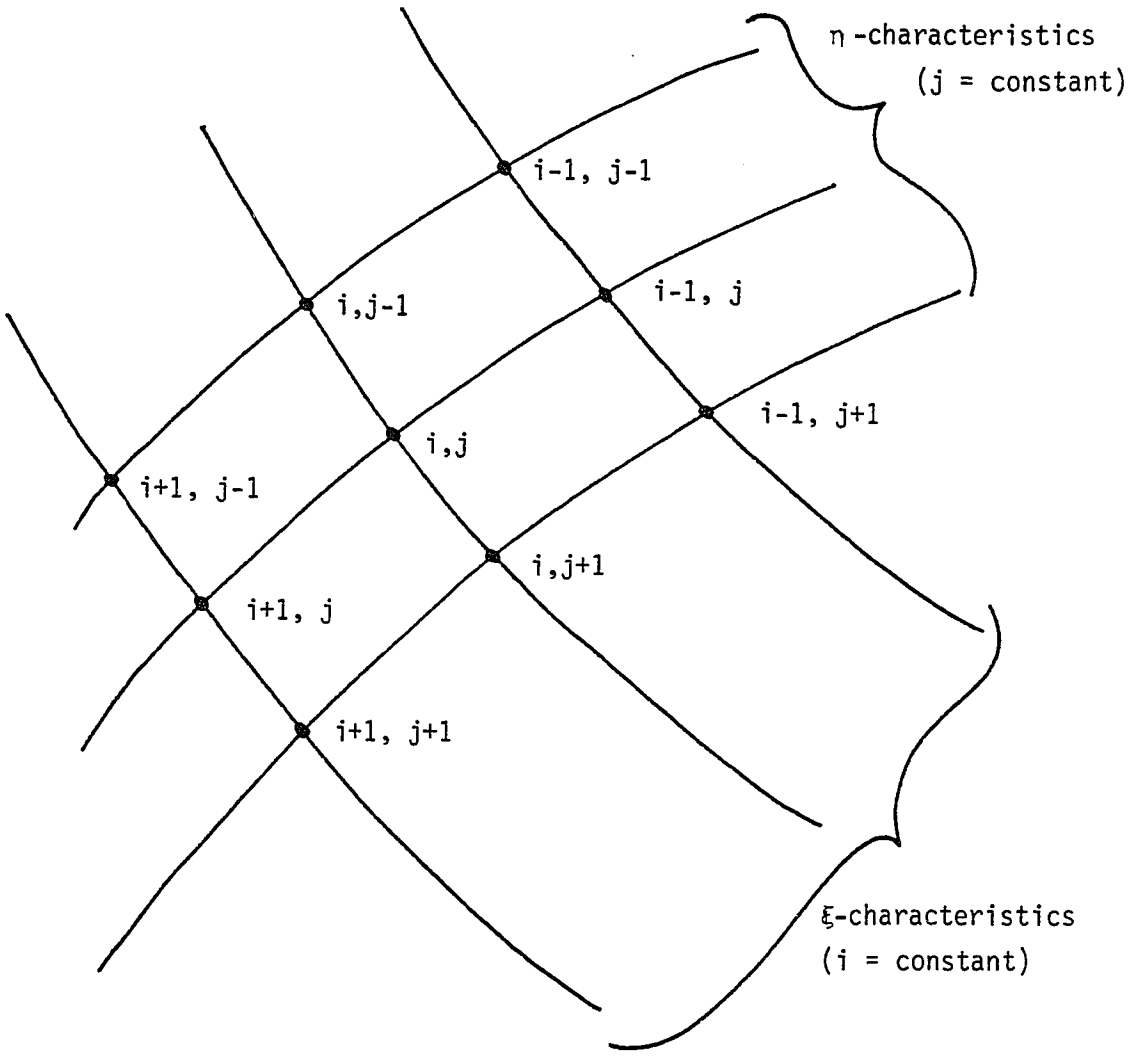

FIGURE 2.4

and

$$\theta_{i,j} = [\sigma_{i,j-1} - \sigma_{i-1,j} + 2\tan\phi(\sigma_{i-1,j}\ \theta_{i-1,j} + \sigma_{i,j-1}\ \theta_{i,j-1}) + \{\frac{\sigma_{i-1,j}}{r_{i-1,j}}^{A} - \frac{\sigma_{i,j-1}}{r_{i,j-1}}^{B}\}]/[2\tan\phi(\sigma_{i-1,j} + \sigma_{i,j-1})] \quad (21)$$

The preceding equations (18)-(21) are known as recurrence relations. For a given i,j node in the mesh, the values of r, z, σ, and θ are completely determined if they are known at the previous i- and j-characteristics. Characteristic meshes can now be constructed to provide such information along the problem boundaries.

Numerical Solutions

Procedure:

The implementation of a numerical solution now depends on a proper description of the boundary conditions at the free surface and at the tool-rock interface.

Along the free surface, for any choice of location r (z = 0), the boundary conditions are given by the fact that confining pressure represents a minimum principal stress. Since lip formation is neglected, the direction, θ, of the maximum principal stress is

$$\theta = 0 \quad (22)$$

The value of σ on the free boundary is given by

$$\sigma = \frac{c\ \cot\phi + w}{1 - \sin\phi} \quad (23)$$

Thus, for a given location, all four variables of the characteristic equations are specified.

At the tool-rock interface, σ is unknown. Indeed, it is the quantity to be established. A value for θ is given by the particular assumption made regarding friction along this boundary. Two types of frictional behavior are considered here: 1) a perfectly lubricated surface, in which the stress at the interface must be a (maximum) principal stress, then

$$\theta = \beta \tag{24}$$

or 2) a perfectly rough surface, in which the interface must itself be a characteristic line

$$\theta = \beta + \frac{\pi}{2} - \mu. \tag{25}$$

Solutions to indentation problems are generally obtained by progressing from the free surface boundary to the tool-rock interface. With reference to Figure 2.5, a description of a representative solution procedure for a cone is described:

1. The problem geometry is known. Assume the farthest extend of the slip line field and divide the boundary nodes equally into this length.
2. Now x, z, σ, and θ are known at the boundary nodes. This is the so-called Cauchy problem (all values known along a non-characteristic line).

3. Using the recurrence relations above, find all values at the nodal points in the passive zone.
4. Compute θ and σ at the singular point where many i-characteristics converge (equal increments of θ through the known total change in θ). Note there is an analytical solution at this point:

$$\sigma = \sigma_0 \exp[2\tan\phi\ \Delta\theta], \tag{26}$$

where σ_0 is the value on the free surface.

5. Use recurrence relations to solve the remaining radial zone.
6. Because θ is known at the rock-tool interface, the active zone corresponds to the so-called mixed boundary value problem (some values known on both characteristic and non-characteristic lines). After a boundary point has been solved, the standard recurrence relations solve the rest of the nodes along that particular i-characteristic.
7. The field is now complete. The final node of the active zone should be coincident with the tip of the cone. If it is not, the assumed extent of the slip line field must be adjusted until the final node and the wedge tip are at the same location (within some tolerance).

Results:

The above procedure is carried out on the Mechanical Engineering Department's Celerity C-1200 computer (see Appendix B for programs). The most obvious result is the construction of a characteristic net (or mesh) given by the r, z locations of each nodal point. Some of

these nets are plotted in the following figures for various conditions of tool geometry and friction conditions. The mesh boundaries are also the boundaries of the plastic region, with all material outside the boundary assumed rigid.

Notice (Figures 2.11, 2.12, 2.13) that the assumption of a perfectly rough interface introduces a "false cone" of rigid material underneath the punch when the cone half-angle is greater than 45°. The reason for this phenomenon is the condition that two characteristic lines must meet at the axis of symmetry at an angle not less than $\pi/4 - \phi/2$. Since real characteristic lines are slightly curved in this region, the rigid cap of material should also have a slight curvature. A close approximation, however, is to assume that the region is a true cone of half-angle $\pi/4 - \phi/2$ (this satisfying automatically the condition at the axis of symmetry).

The phenomenon of mesh overlap - seen to a slight extent in Figure 2.5 and more pronounced in Figures 2.10, 2.12, and 2.13 - is not explained. Clearly, the method of characteristics does not allow such an occurence, since it implies a physically inadmissible multivalued stress state. Karafiath and Nowatski [2] find that overlap is more likely to occur for sharp tool angles than for blunt, but offer no insight as to the causes. Since the resulting pressure profiles from these solutions compare well to those of non-overlapping solutions, the results are taken to be correct. Still, further study into the phenomenon is indicated, particularly to identify whether the problem is numerical or physical in nature.

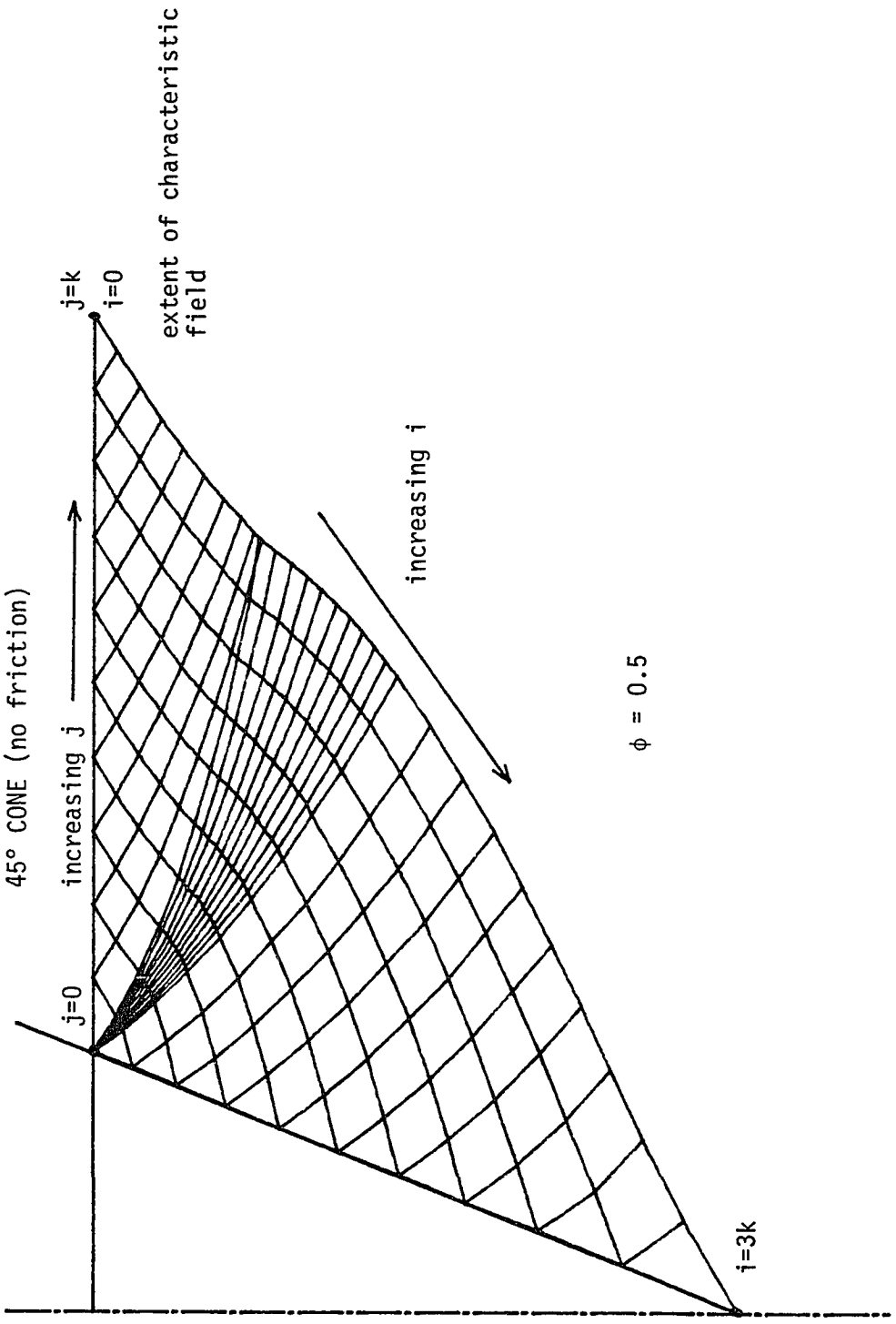
45° CONE (no friction)
increasing j
j=0
j=k
i=0
extent of characteristic field
increasing i
ϕ = 0.5
i=3k

FIGURE 2.5

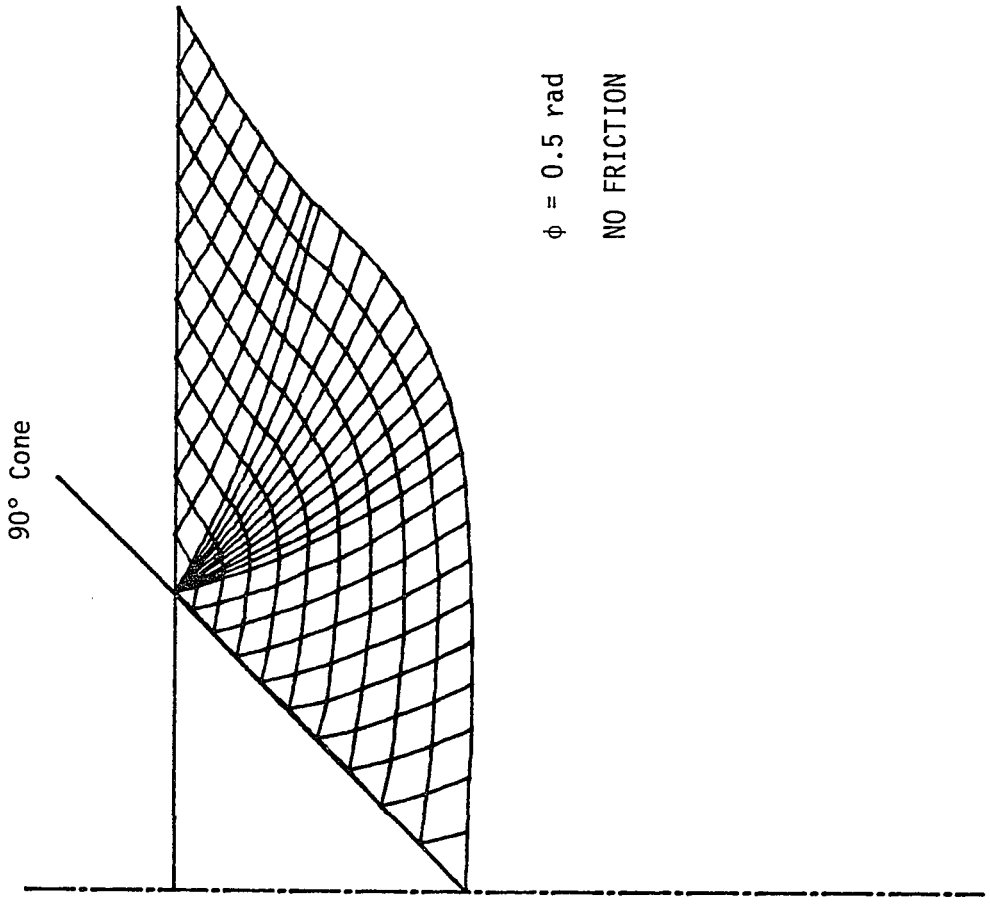

FIGURE 2.6

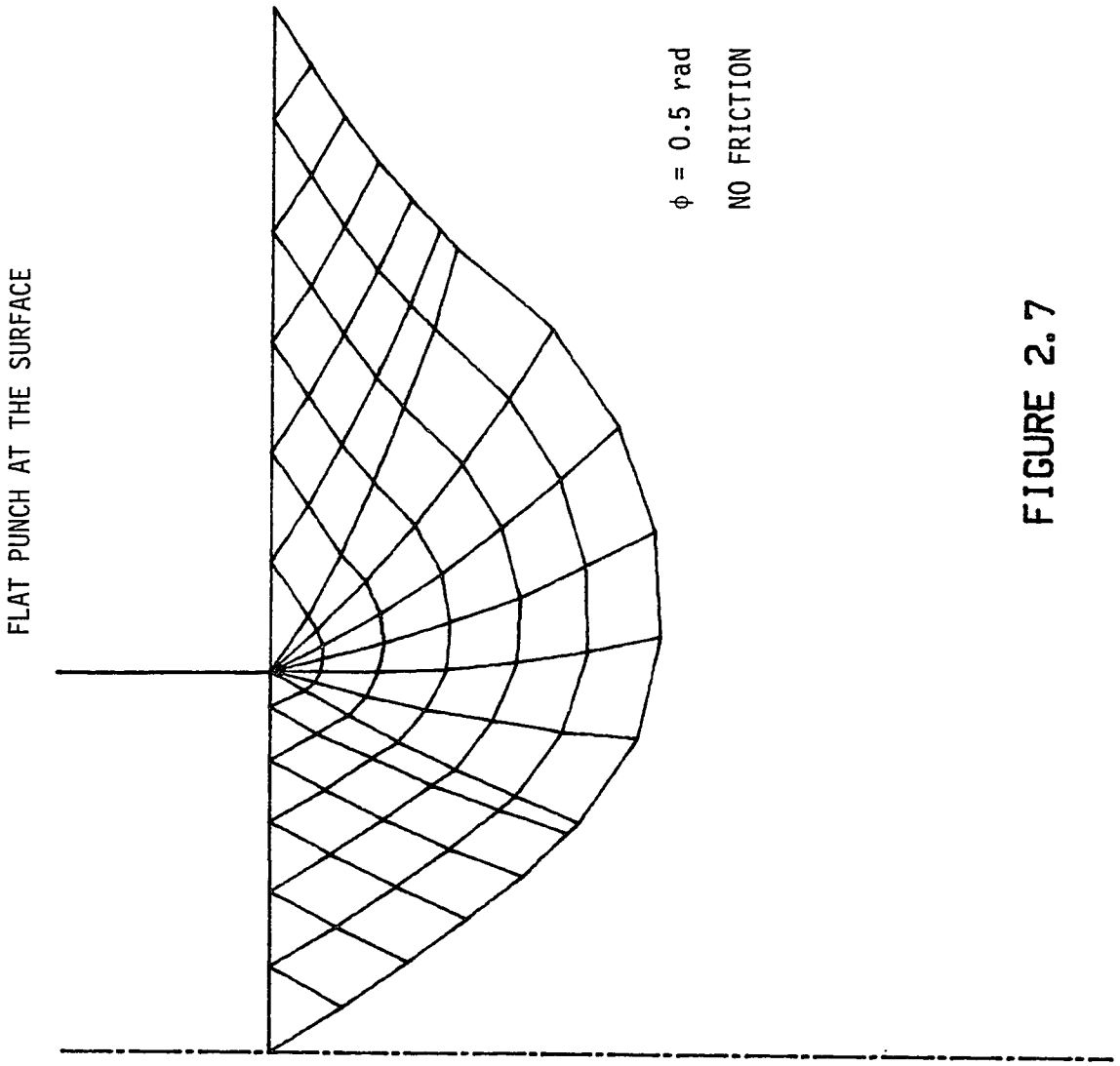

FIGURE 2.7

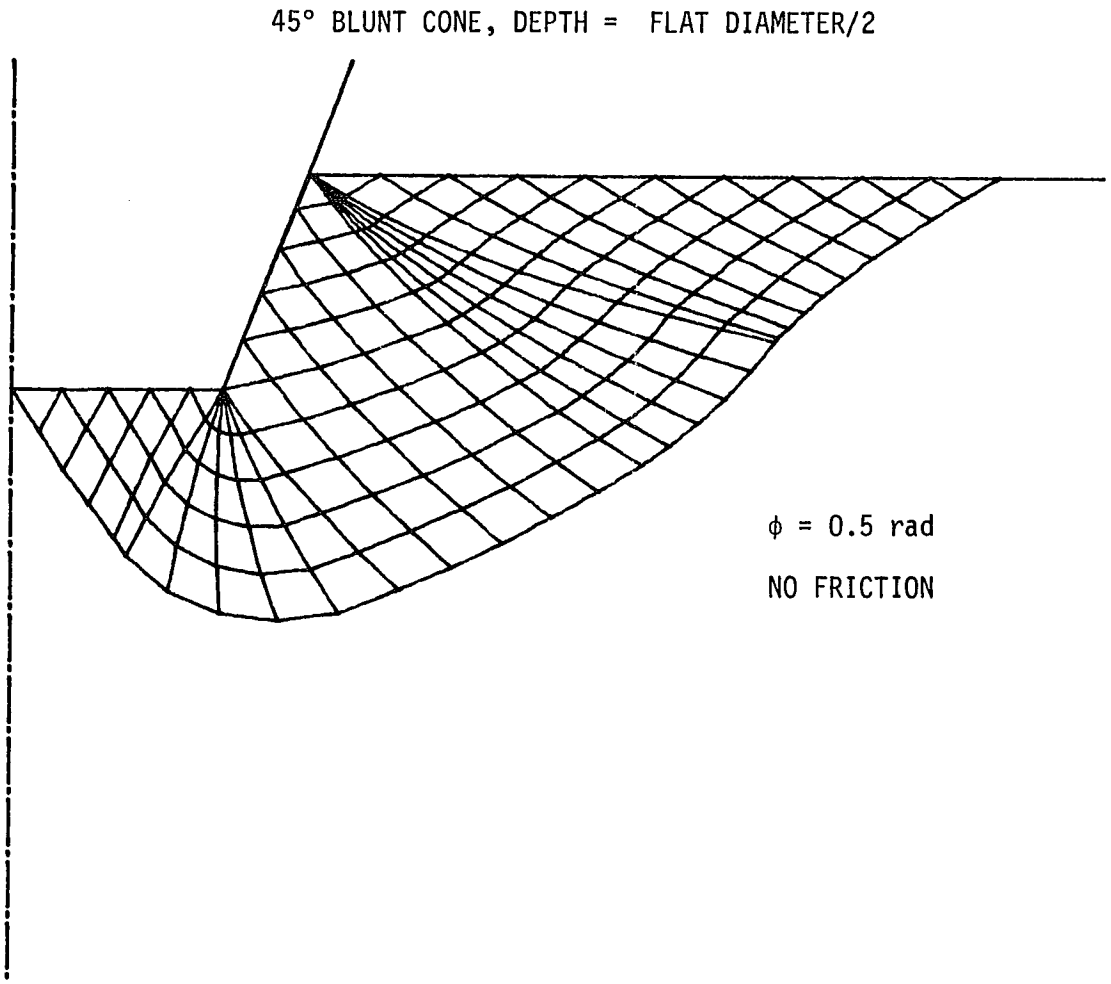

FIGURE 2.8

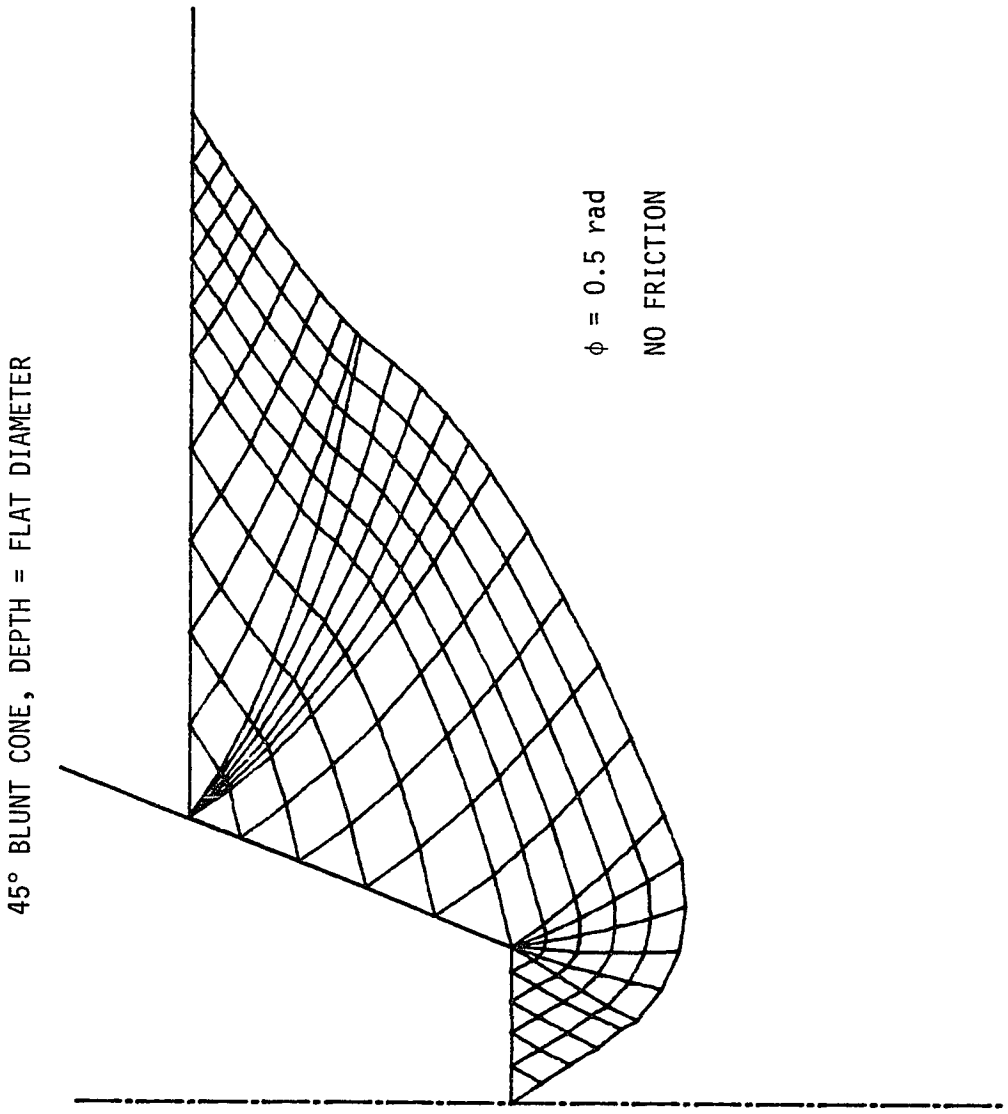

FIGURE 2.9

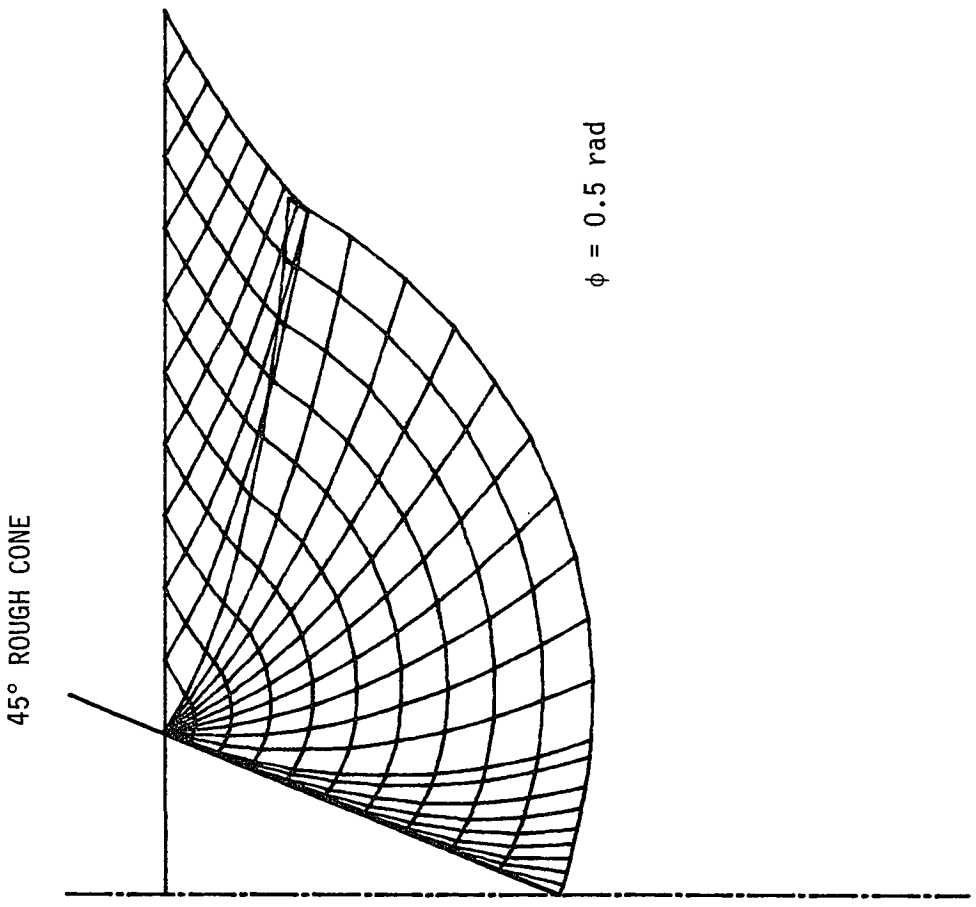

FIGURE 2.10

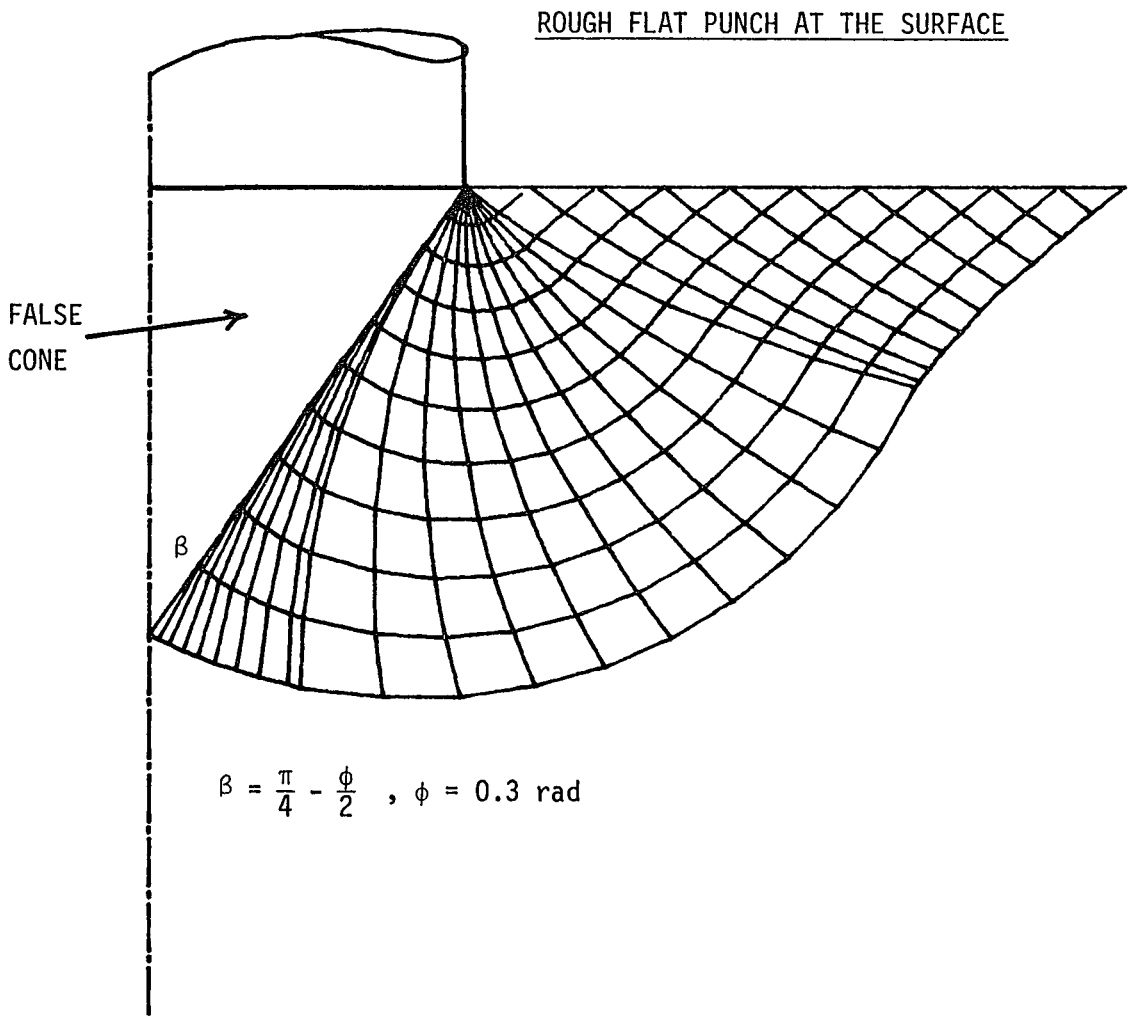
ROUGH FLAT PUNCH AT THE SURFACE
FALSE
CONE
β
$\beta = \frac{\pi}{4} - \frac{\phi}{2}$, ϕ = 0.3 rad

FIGURE 2.11

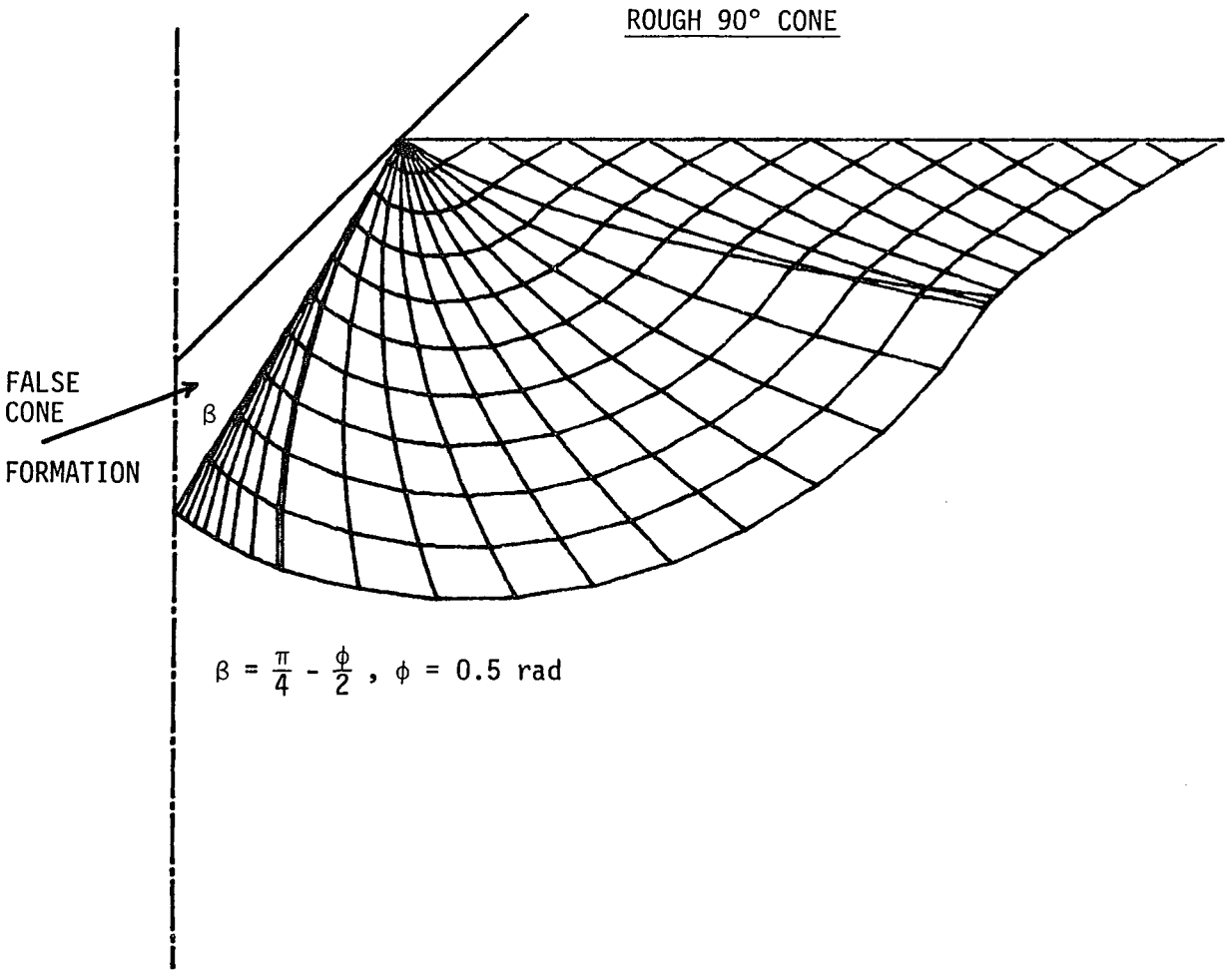
ROUGH 90° CONE
FALSE
CONE
FORMATION
β
$\beta = \frac{\pi}{4} - \frac{\phi}{2}$, ϕ = 0.5 rad

FIGURE 2.12

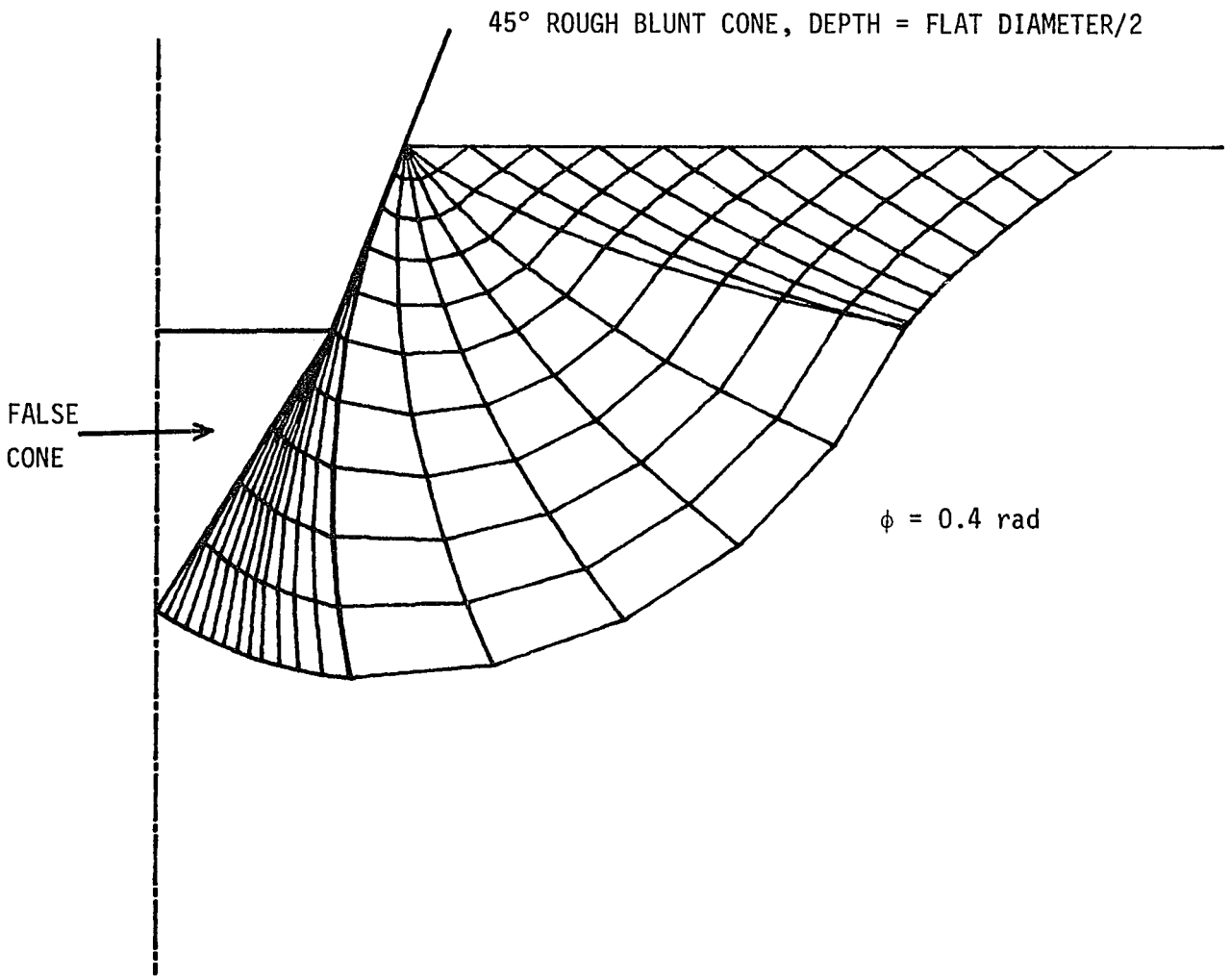
45° ROUGH BLUNT CONE, DEPTH = FLAT DIAMETER/2
FALSE
CONE
ϕ = 0.4 rad

FIGURE 2.13

The variable which is not shown in the characteristic nets is σ, but it is extremely important since it contains the stress quantities. Specifically, the normal pressure, σ_n, on the punch face of a smooth tool is given by

$$\sigma_n = \sigma(1 + \sin\phi) - c\cot\phi \qquad (27)$$

(by hypothesis $\tau = 0$)

whereas on the face of a perfectly rough tool,

$$\sigma_n = \sigma(1 - \sin\phi\cos 2\mu) - c\cot\phi$$
$$\tau = \sigma\sin\phi\sin 2\mu \qquad (28)$$

where $\mu = \pi/4 - \phi/2$.

In order to compare more easily the rough and smooth interfaces, it is useful to speak of an <u>effective pressure</u> on the surface of the rough tool. This pressure would consist of the actual normal pressure σ_n, and an equivalent normal pressure $\sigma_{n,eq}$ which would result in the same upward force as the shear stress τ. Thus, the equivalent pressure, $\sigma_{n,eq}$, should be such that

$$\tau\cos\beta = \sigma_{n,eq}\sin\beta$$

or

$$\sigma_{n,eq} = \tau/\tan\beta \qquad (29)$$

thus

$$\sigma_{n,effective} = \sigma_n + \sigma_{n,eq}.$$

A few of these pressure profiles are shown in the following graphs as a dimensionless pressure P/c^*, where $c^* = c + w\tan\phi$ is an effective cohesion, vs. r/r_o, where r_o is the radius at the rock

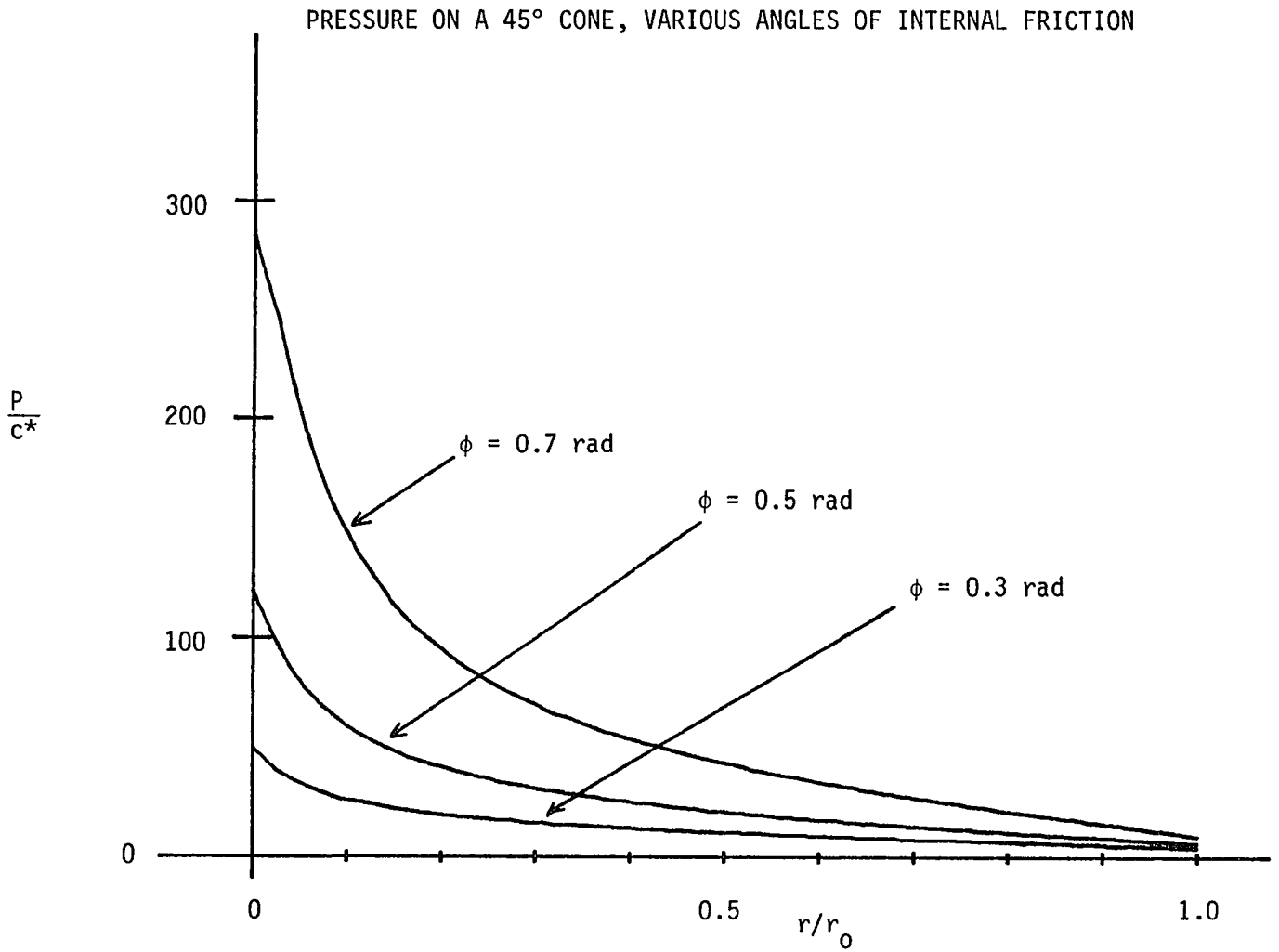
PRESSURE ON A 45° CONE, VARIOUS ANGLES OF INTERNAL FRICTION
300
200
100
0
P/c*
ϕ = 0.7 rad
ϕ = 0.5 rad
ϕ = 0.3 rad
0
0.5
1.0
r/r_o

FIGURE 2.14

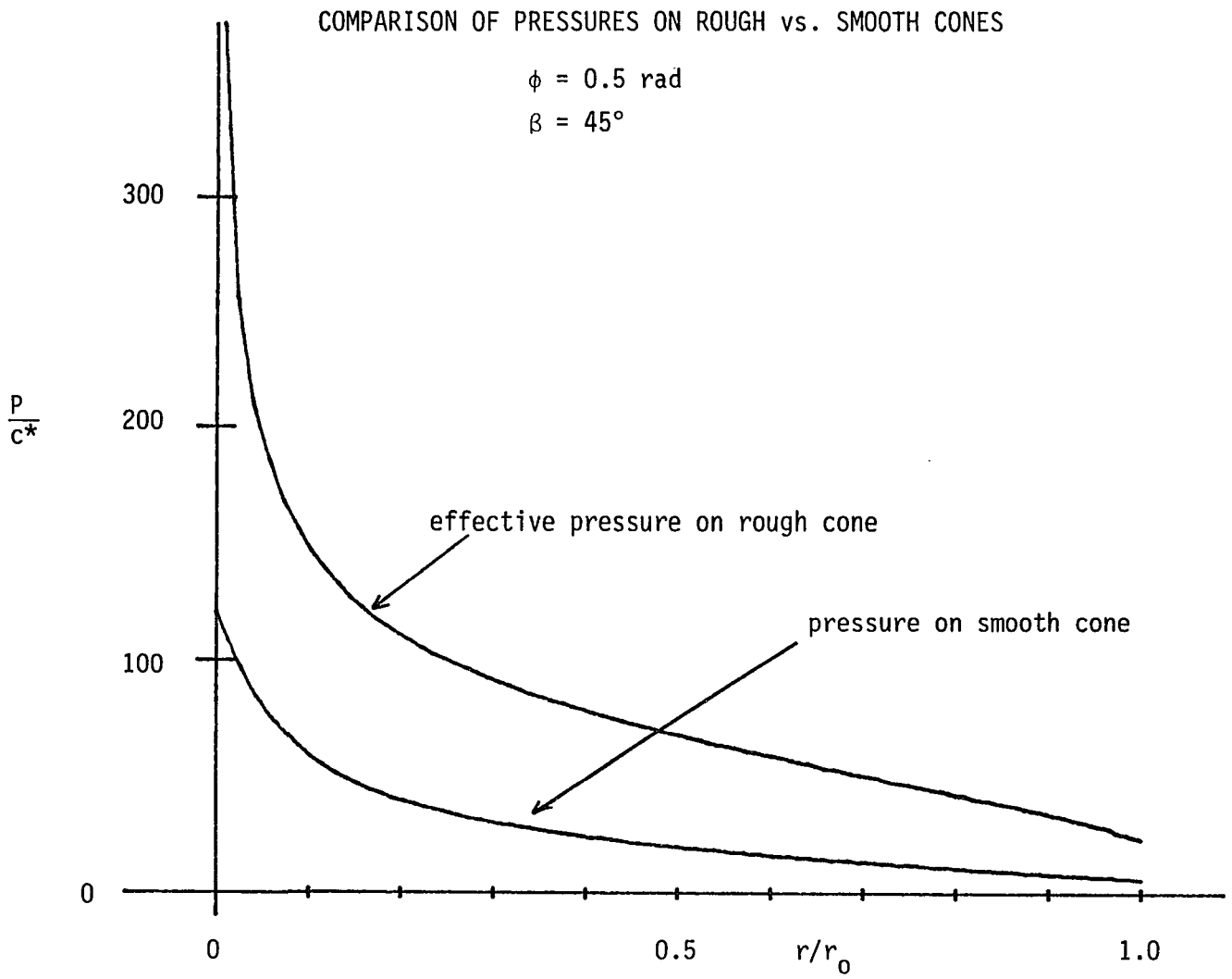
COMPARISON OF PRESSURES ON ROUGH vs. SMOOTH CONES
ϕ = 0.5 rad
β = 45°
300
200
100
0
$\frac{P}{c^*}$
effective pressure on rough cone
pressure on smooth cone
0
0.5
r/r_o
1.0

FIGURE 2.15

surface. Figure 2.14 shows the effect of increasing internal friction angle, and in Figure 2.15 it is seen that the rough interface predicts higher effective pressures (and thus, when integrated, higher overall forces) than the smooth case - an intuitively obvious fact.

Finally, it is noted that geometric similarity holds for flat punches on the surface and complete cones, but not for blunt cones. Solutions can be obtained for various values of ϕ and then scaled to the problem at hand when similarity holds, but for the other cases, new solutions must be computed at every depth of the indentation. The solution of Figure 2.9, for example, cannot be achieved by any "scaling" of Figure 2.8.

On the incompleteness of stress-characteristic solutions

Strictly speaking, the solution obtained by the stress characteristic networks is incomplete. Although such a field (if it can be found) may be completely determined by the stress boundary conditions, the force on the punch thus obtained is neither an upper nor a lower bound to the true, complete solution. The reasons for this are grounded in the theorems of limit analysis, and the fact that kinematical considerations are inherent to perfect plasticity.

The theorems of limit analysis are restated by Chen [14] as follows:

> Theorem I (Lower Bound Theorem) - If an equilibrium distribution of stress covering the whole body can be found which balances the applied loads on the stress boundary and is everywhere below yield; then the body will not collapse.

Thus, to show that the solution obtained by stress characteristics is at least a lower bound, it is necessary to extend the characteristic field into the rigid material below the plastic region, and determine that the yield condition is nowhere violated (statically admissible stress field). A method after Bishop is used by Cox, Eason, and Hopkins [12] to extend the characteristic field for the case of the flat punch, but this method would be extremely difficult in the present case, given the lack of simple geometry which exists for the flat punch.

> Theorem II (Upper Bound Theorem) - If a compatible mechanism of plastic deformation is assumed which satisfies the condition of no plastic work on the displacement boundary; then the loads determined by equating the rate at which external forces do work to the rate of internal dissipation will be either higher or equal to the actual limit load.

Using the stress characteristics to find this kinematically admissible velocity field of Theorem II requires a further assumption that the material behaves according to an associated flow rule (stress and strain characteristics coincide). In fact, many geologic materials exhibit non-associated flow characteristics (Desai and Siriwardane [15]). Furthermore, Chen [14] shows that proofs of Theorems I and II are a direct consequence of the associated flow assumption.

Given the difficulty of these limit analyses for all but the simplest geometries, Cox, et al [12] conclude their paper with the suggestion that the construction of complete solutions be omitted in problems of this type, advice which is undertaken here. It is noted in passing that the axisymmetric smooth flat punch solution is complete.

III. EXPERIMENTAL METHOD AND OBSERVATIONS

Apparatus

Indentation testing is carried out in the Mechanical Engineering department's Rock Mechanics Lab. Two kinds of rock are subjected to the various indentation experiments: Indiana Limestone and Berea Sandstone. The main purpose of these tests is to obtain a record of force vs. displacement for a variety of experimental conditions. Only three conditions are varied: rock type, tool profile, and confining pressure.

The main apparatus for these experiments is a large, thick-walled pressure vessel fitted with a hydraulic ram to force the tool into the rock (see Figure 3.1). The interior of the vessel holds a steel box containing a relatively large (4" x 3 1/2" x 12") rectangular rock sample. In order to obtain new testing sites on a particular rock sample, translating rods are brought out through O-ring seals in the thick end plates of the vessel, and are moved via a motor-driven power screw arrangement attached to one of the rods. Usually, it is possible to fit eight tests on a single rock sample.

The application of a confining pressure on the rock face is achieved by pressurizing the hydraulic oil in the vessel interior with a Sprague air-operated pump (oil pressure : air pressure = 150:1). Since they are permeable to the surrounding oil, the rock and surrounding Castone compound are covered with a silicone putty sealant (commonly known as "silly putty"), which forms a barrier between the oil and the dry rock (see Figure (3.2). Without this seal - or if the

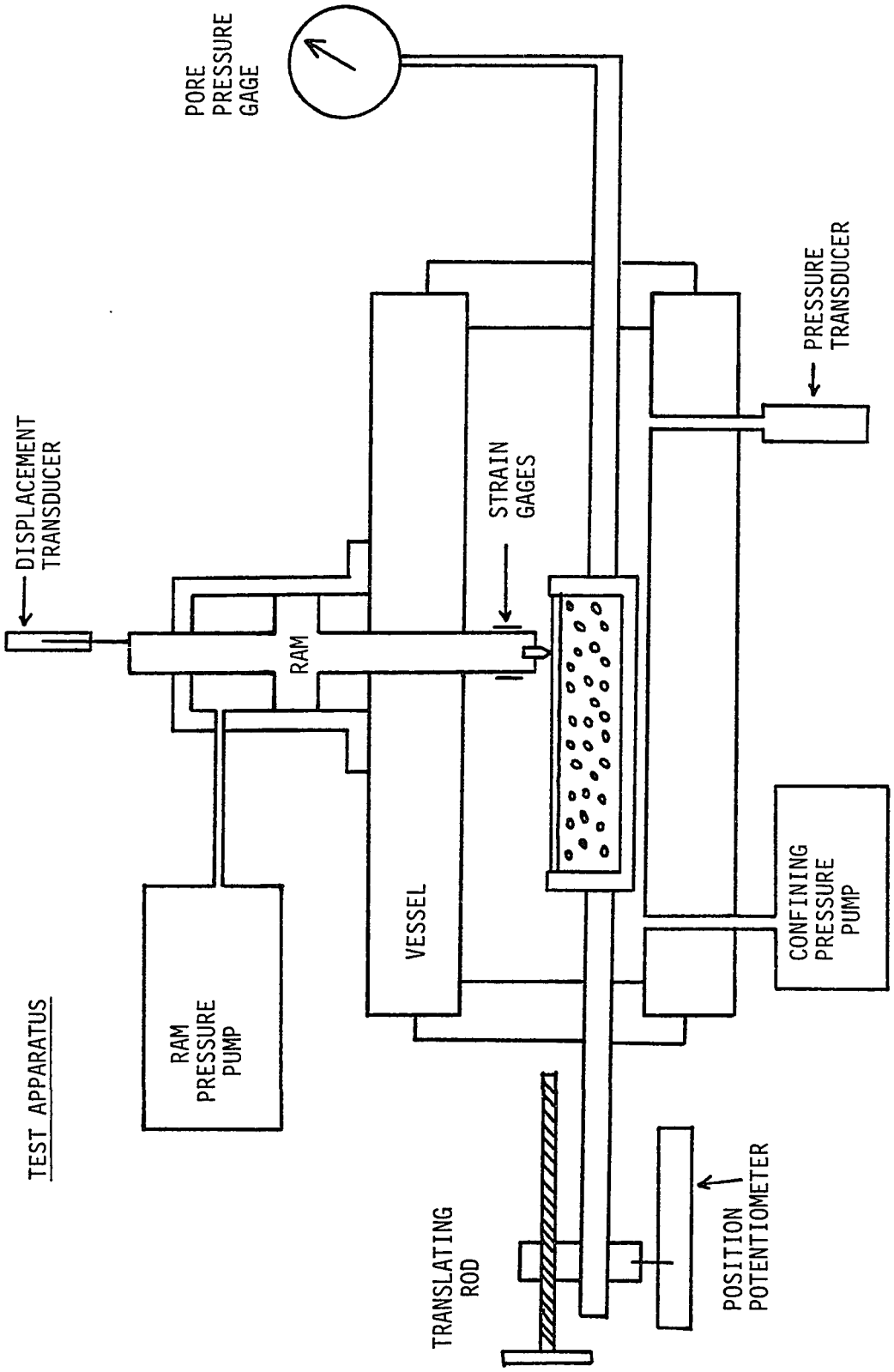
TEST APPARATUS
RAM PRESSURE PUMP
VESSEL
RAM
DISPLACEMENT TRANSDUCER
STRAIN GAGES
PORE PRESSURE GAGE
PRESSURE TRANSDUCER
CONFINING PRESSURE PUMP
TRANSLATING ROD
POSITION POTENTIOMETER

FIGURE 3.1

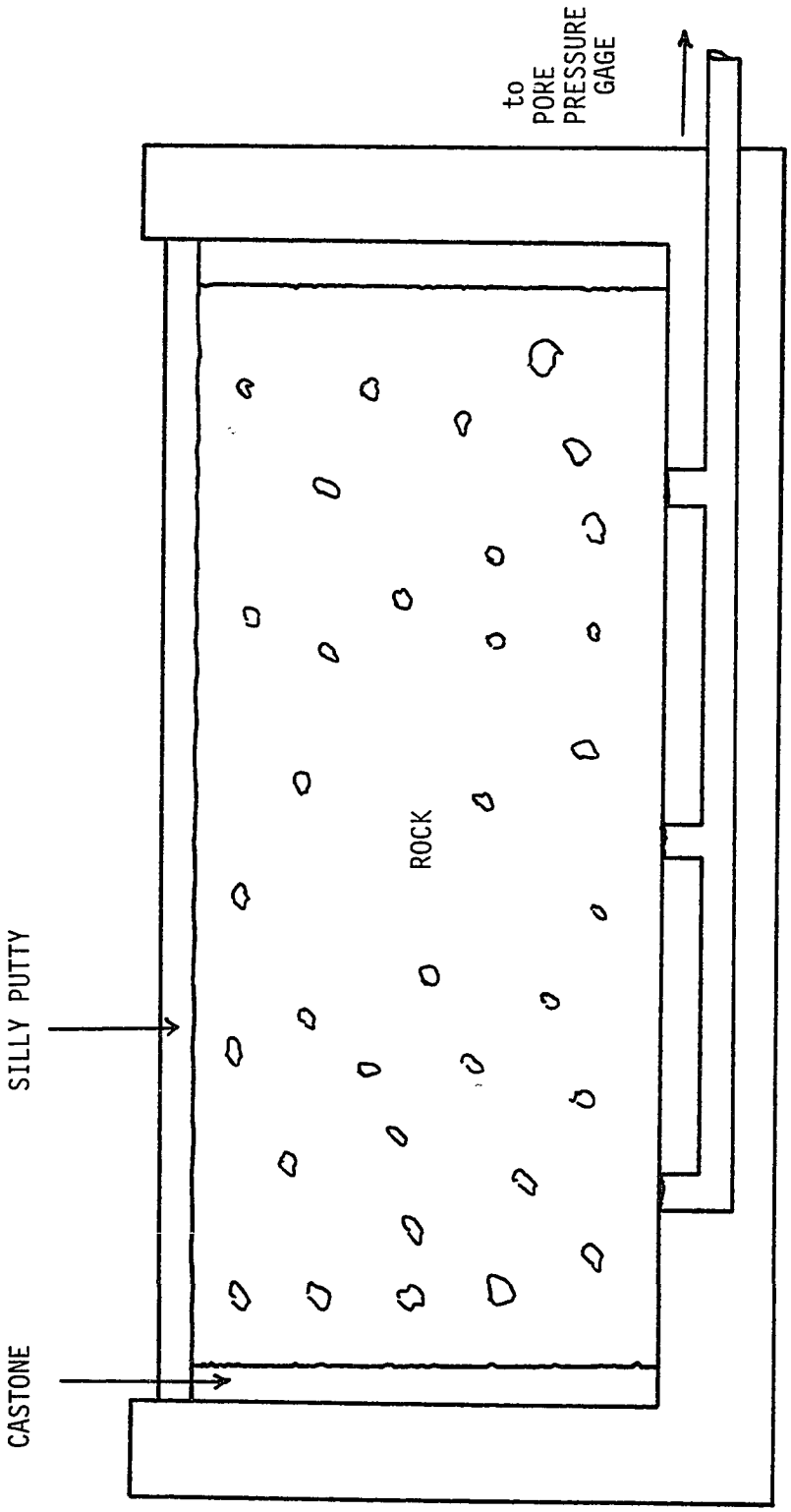

ROCK TRAY DETAIL

FIGURE 3.2

seal integrity is lost - the oil quickly forces its way into the rock, reducing the pressure differential across the rock face to zero. The (undesirable) result is an effectively-atmospheric confining pressure, with correspondingly brittle rock behavior. The present vessel can be safely operated at interior pressures of up to 10,000 psi, although no tests are run above 5,000 psi in this study. To avoid the possibility of injury from explosion, tests are run remotely from the next room.

Hardened steel tools of various profiles (see Figures 3.3 and 3.4) are placed in a fitting on the end of the ram and held in place by a set screw. In general, these tools can be of any shape, but tools in the present study are simple profiles amenable to analysis. The tool ram is part of a hydraulic piston, which is pressurized by a precision hand-operated Ruska pump during an indentation. This pump line is the only hydraulic connection between the testing room and operating room.

Data Acquisition

Since the testing vessel is operated remotely, various transducers are used to collect the relevant data (see Figure 3.5). These include: strain gages mounted on the ram to measure force, a linearly variable differential transformer (LVDT) to measure displacement at the top of the ram, a wire-wound potentiometer to determine the position of the rock tray within the vessel, and a strain gage pressure transducer for confining pressure measurement. In the case of the two strain gage devices and the LVDT, an excitation voltage is supplied by a Hewlett-Packard 6237B triple output power

TOOLS

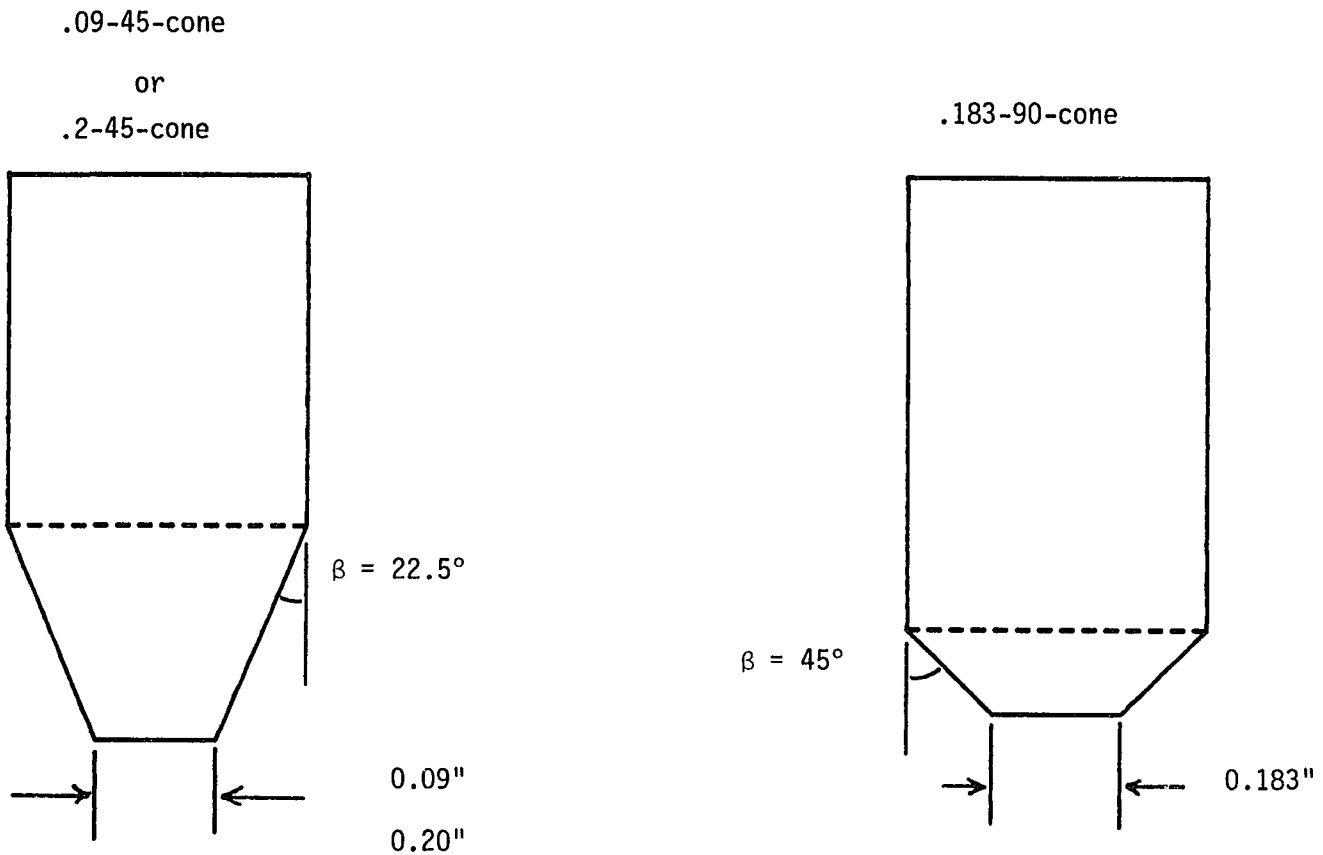

FIGURE 3.3

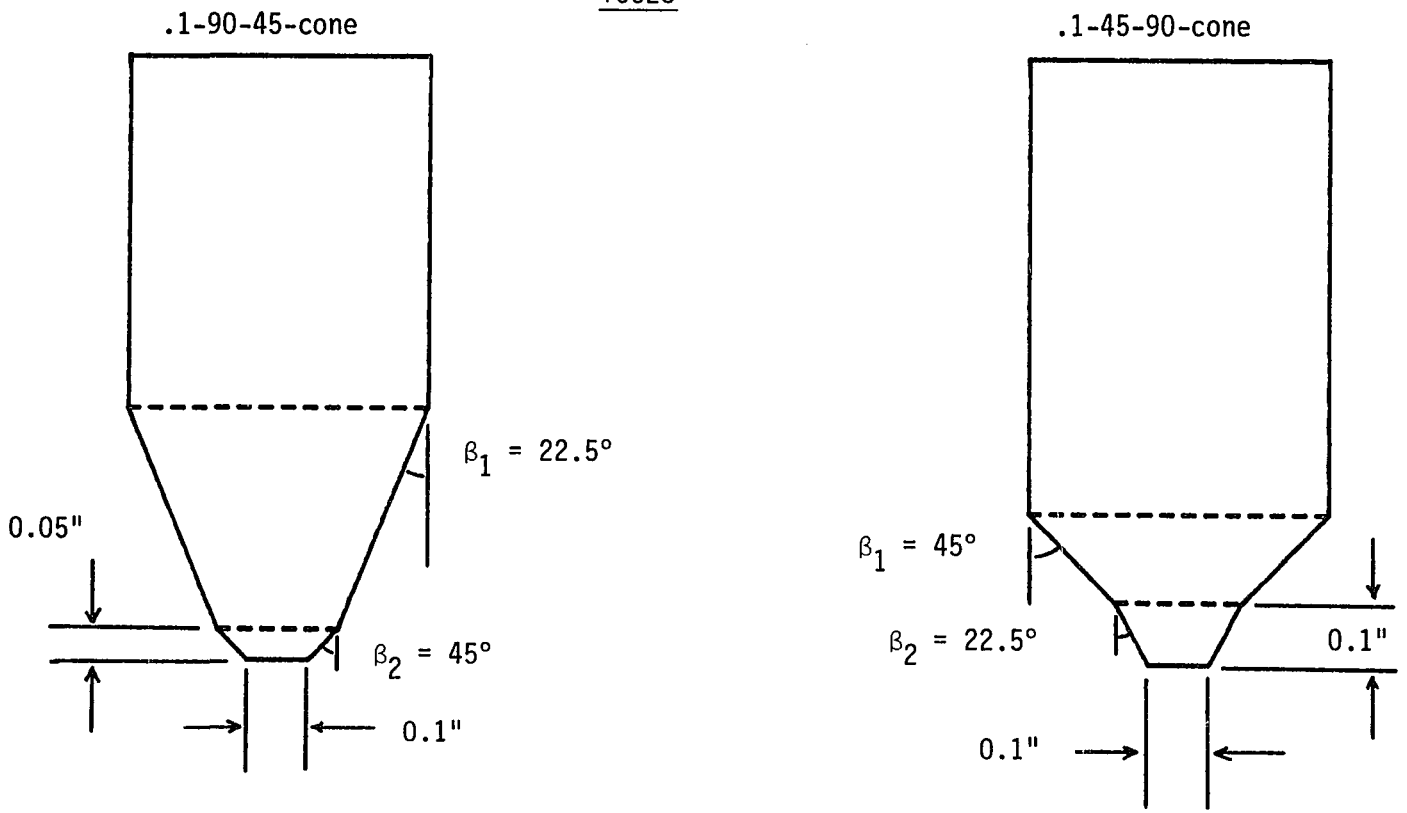
.1-90-45-cone
β_1 = 22.5°
0.05"
β_2 = 45°
0.1"
.1-45-90-cone
β_1 = 45°
β_2 = 22.5°
0.1"
0.1"

FIGURE 3.4

DATA ACQUISITION SCHEMATIC

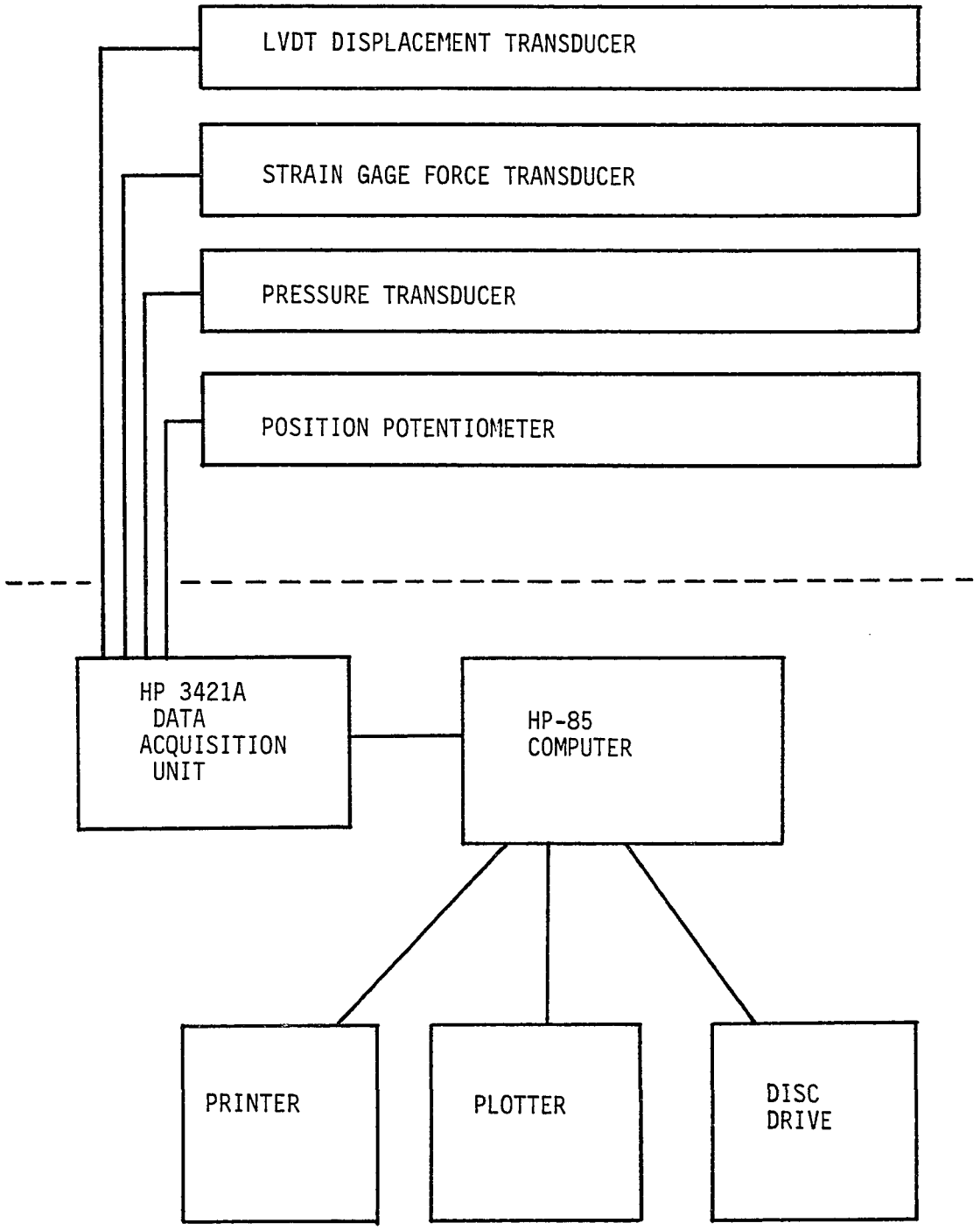

FIGURE 3.5

supply. Signal voltages (or potentiometer leads, as the case may be) are brought into a Hewlett-Packard 3421A Data Acquisition Unit, which measures and digitizes the voltages/resistance. A controlling computer, in the form of an HP-85, sends software commands to the 3421A, reads in the digitized data, and makes necessary calculations in order to translate the transducer signals into meaningful physical quantities. In addition, the plotting capabilities of the HP-85 are used to generate a simultaneous force-displacement curve on the screen as a test is conducted - a valuable indicator of test progress.

Repeatability

Variation of material properties between samples is of concern when testing "natural" materials such as rocks, since there is the possibility that results will be more strongly affected by such variation than by known experimental conditions. Although no rigorous analysis of sample variability is performed for this study, the empirical evidence suggests that the rocks under consideration display remarkable consistency in behavior. Figure 3.6 shows identical tests performed on two different samples of Indiana Limestone. Obviously, there is close agreement between the two curves, giving some measure of confidence in the results that follow.

Experimental Results

The following graphs present the primary (corrected) experimental data for tests using axially symmetric tools. Experimental variables, namely rock type, confining pressure, and tool geometry, appear with each plot (also a dataset number "nc" where n is the test number).

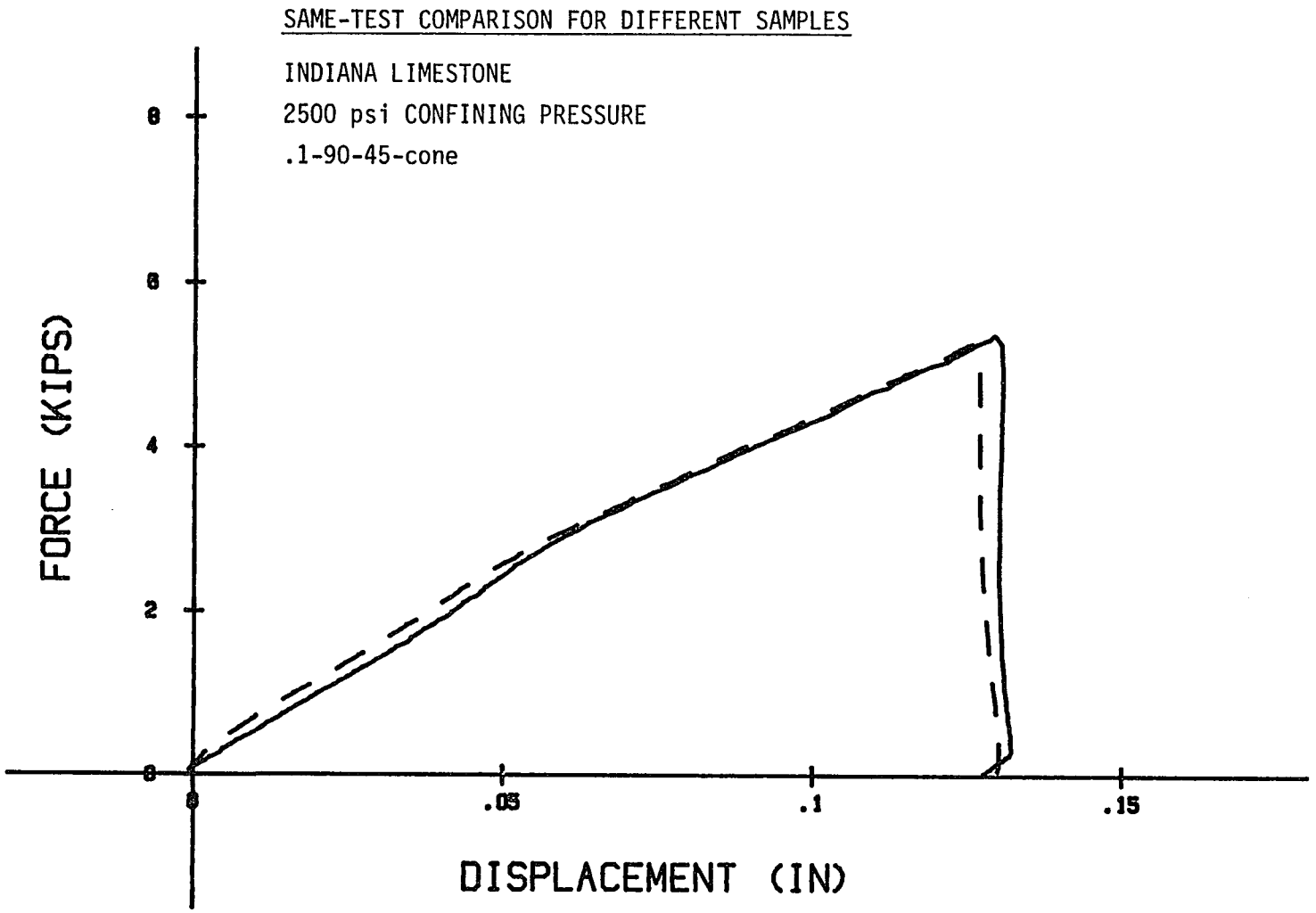
SAME-TEST COMPARISON FOR DIFFERENT SAMPLES
INDIANA LIMESTONE
2500 psi CONFINING PRESSURE
.1-90-45-cone
FORCE (KIPS)
8
6
4
2
0
0
.05
.1
.15
DISPLACEMENT (IN)

FIGURE 3.6

For the cases in which confining pressure is varied widely (Figures 3.8, 3.9), the zero-pressure tests clearly exhibit brittle behavior, as shown by the jagged, unpredictable curves. This response corresponds to the formation of large chips around the testing site which become completely separated from the intact rock. It is also clear that strength generally increases with increased confining pressure.

Note the abrupt change in slope in Figure 3.10 for the .1-45-90 cone. Since the 45° section of this tool has a depth of 0.1", the fact that the slope change occurs slightly before 0.1" displacement indicates that some lip formation is taking place, contrary to the assumption made for numerical solutions.

Tests shown in Figure 3.17-3.23 are carried out to extremely high force in order to observe the effect of an initial section. Thus, it is postulated that the response of the .1-45-90 cone in the displacement region > 0.1" (Figure 3.17) should correspond to the response of the .183-90 cone from zero displacement. In fact, the two curves (shifted by the 0.1" initial section) do not agree well except that the final slopes are nearly equal after a large "transition region". There is better agreement for the case of Berea Sandstone (compare Figures 3.20 and 3.21), but the transition region is still fairly large. Computation of characteristic nets for the dual-angle tools, not performed here, may provide some insight to this behavior.

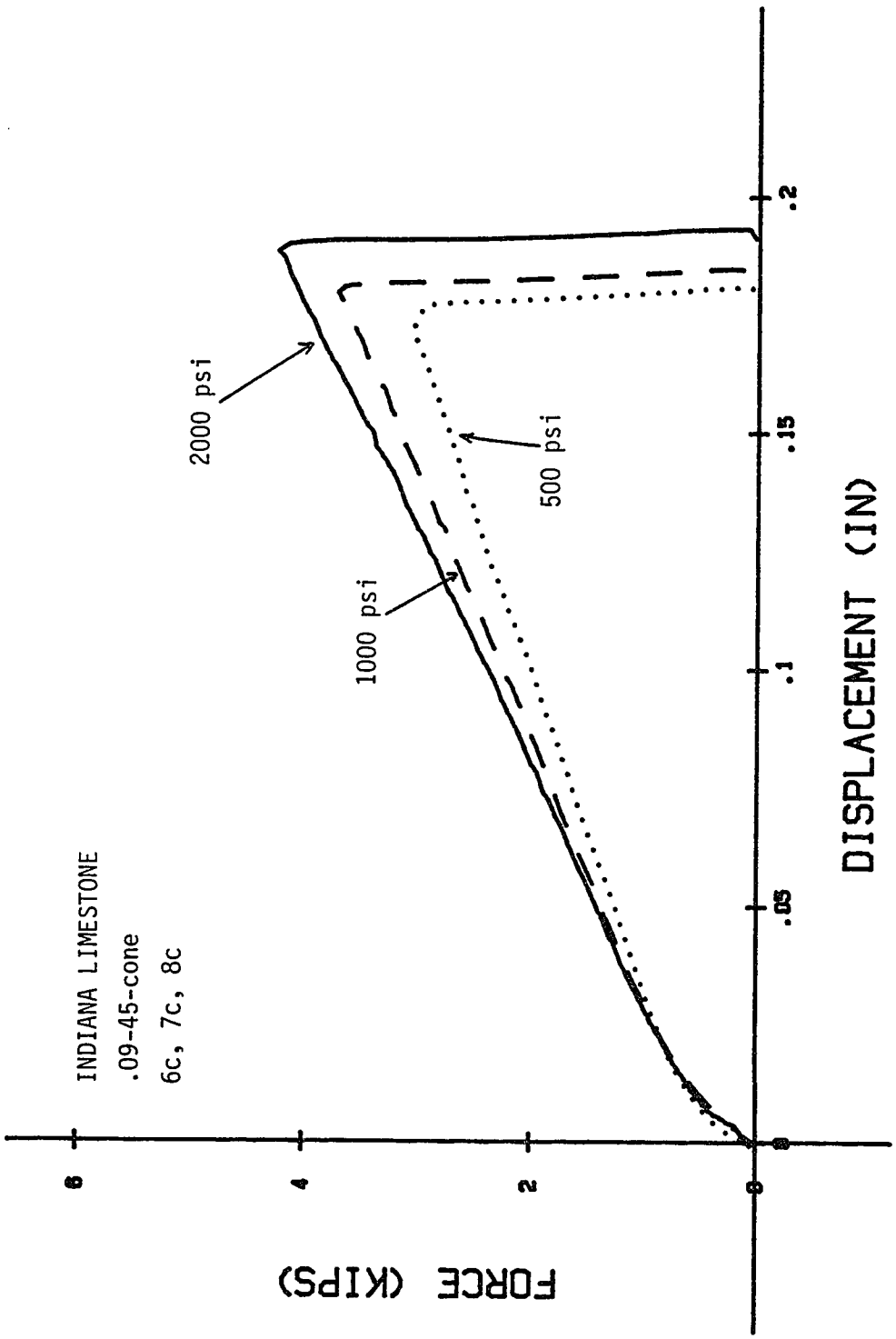
INDIANA LIMESTONE
.09-45-cone
6c, 7c, 8c
2000 psi
1000 psi
500 psi
FORCE (KIPS)
DISPLACEMENT (IN)
0
2
4
6
.05
.1
.15
.2

FIGURE 3.7

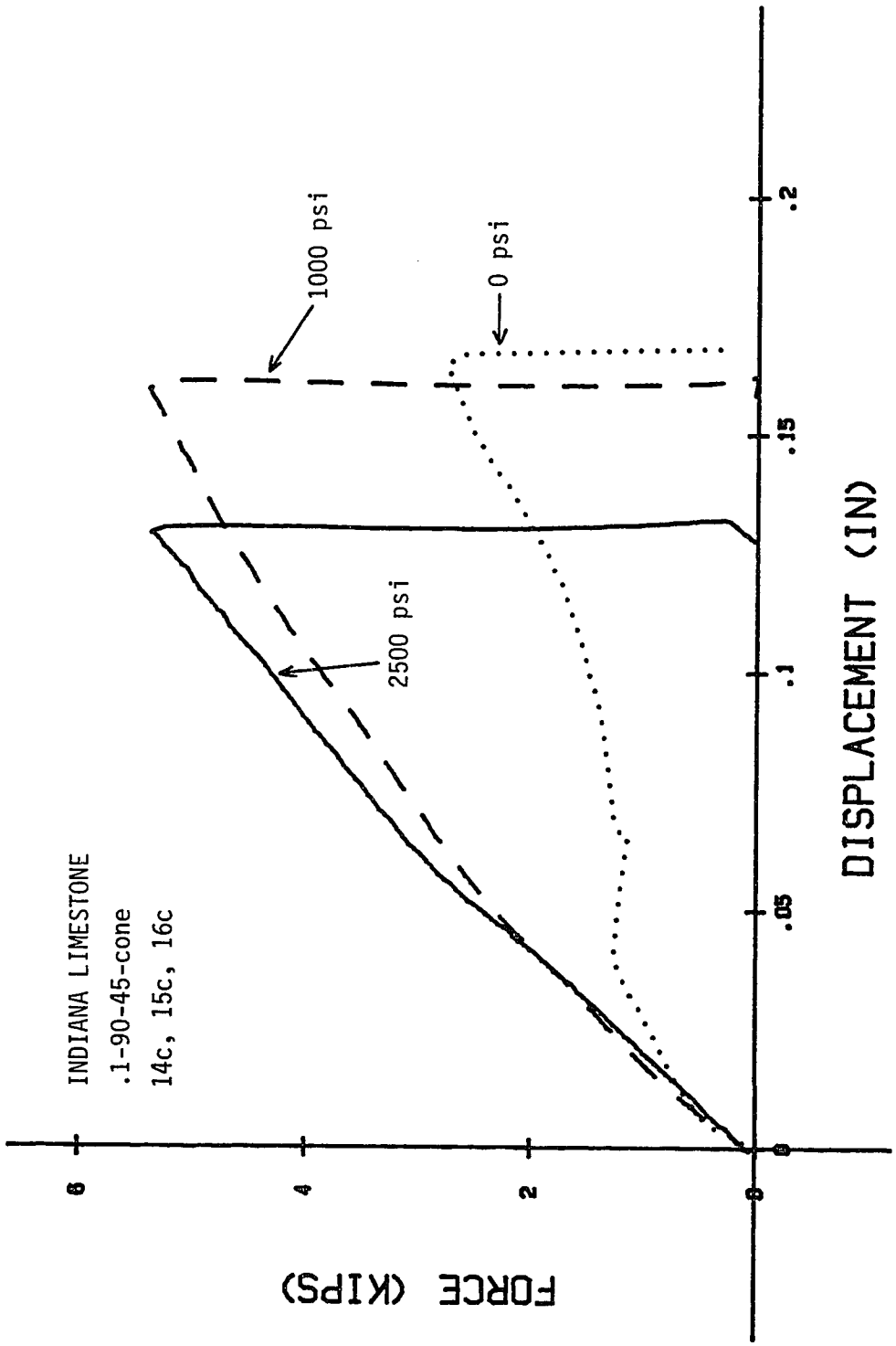
INDIANA LIMESTONE
.1-90-45-cone
14c, 15c, 16c
1000 psi
0 psi
2500 psi
FORCE (KIPS)
DISPLACEMENT (IN)
0
2
4
6
.05
.1
.15
.2

FIGURE 3.8

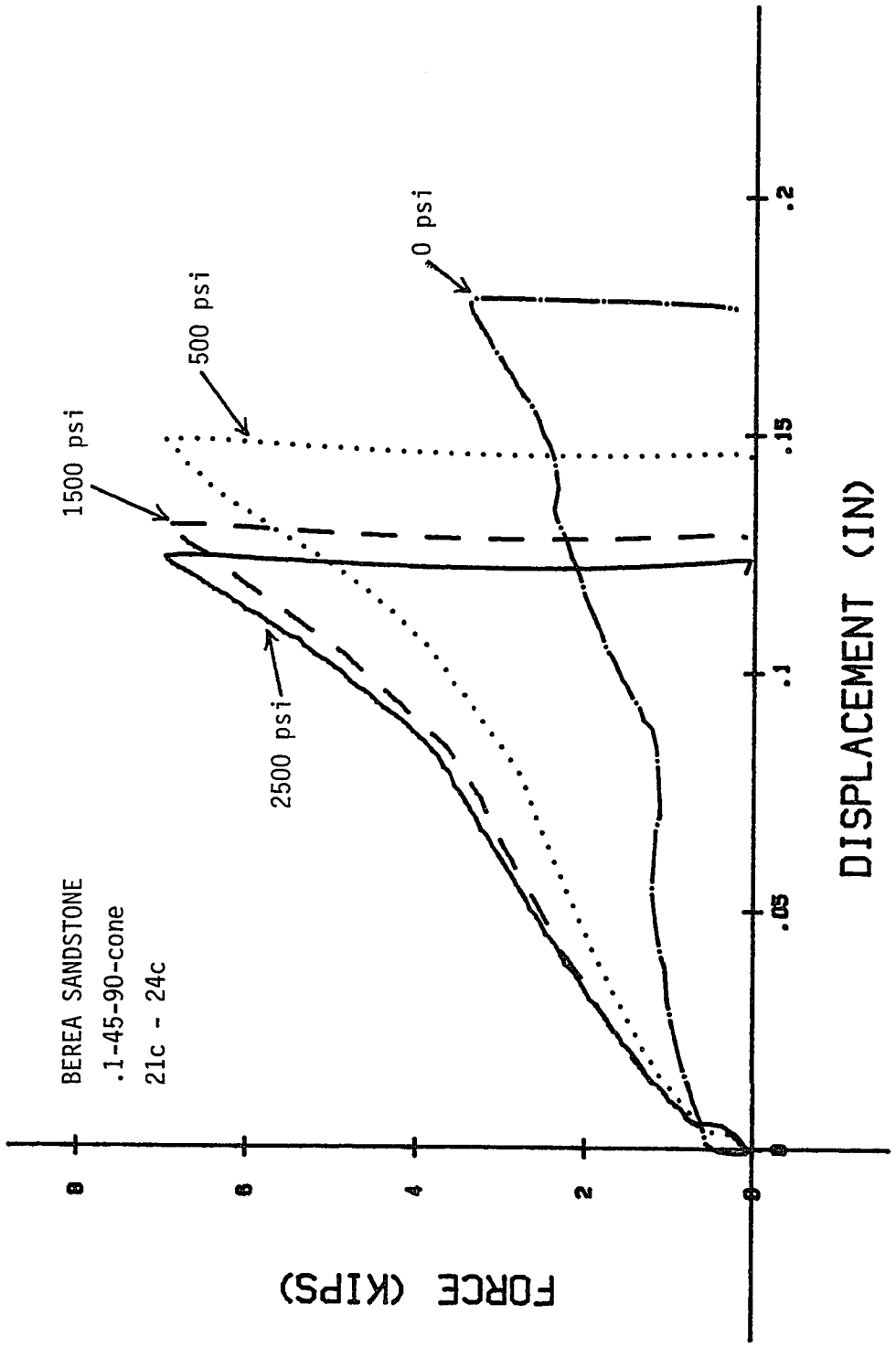
BEREA SANDSTONE
.1-45-90-cone
21c - 24c
1500 psi
500 psi
0 psi
2500 psi
FORCE (KIPS)
DISPLACEMENT (IN)
0
2
4
6
8
.05
.1
.15
.2

FIGURE 3.9

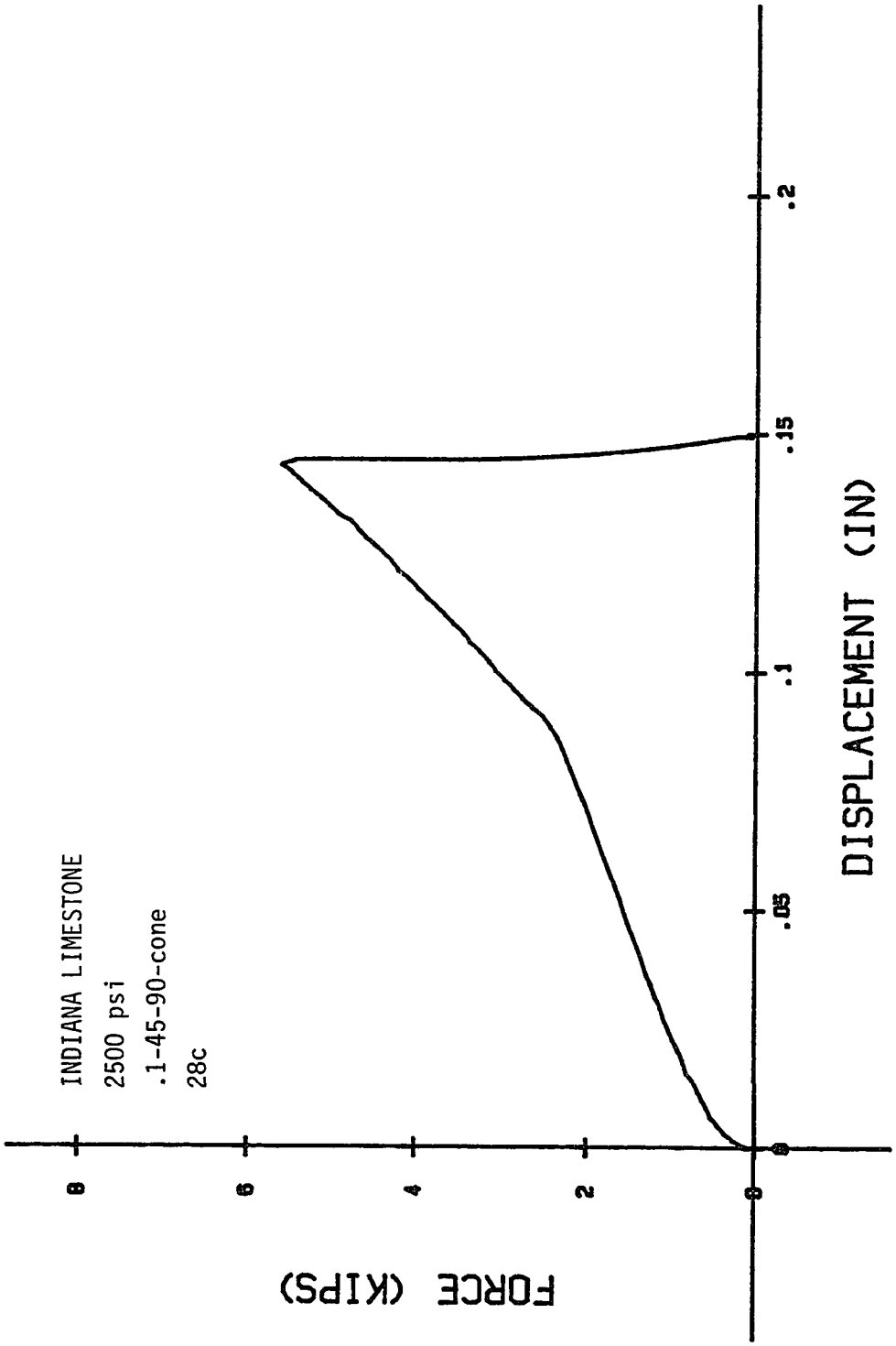
INDIANA LIMESTONE
2500 psi
.1-45-90-cone
28c
FORCE (KIPS)
0
2
4
6
8
0
.05
.1
.15
.2
DISPLACEMENT (IN)

FIGURE 3.10

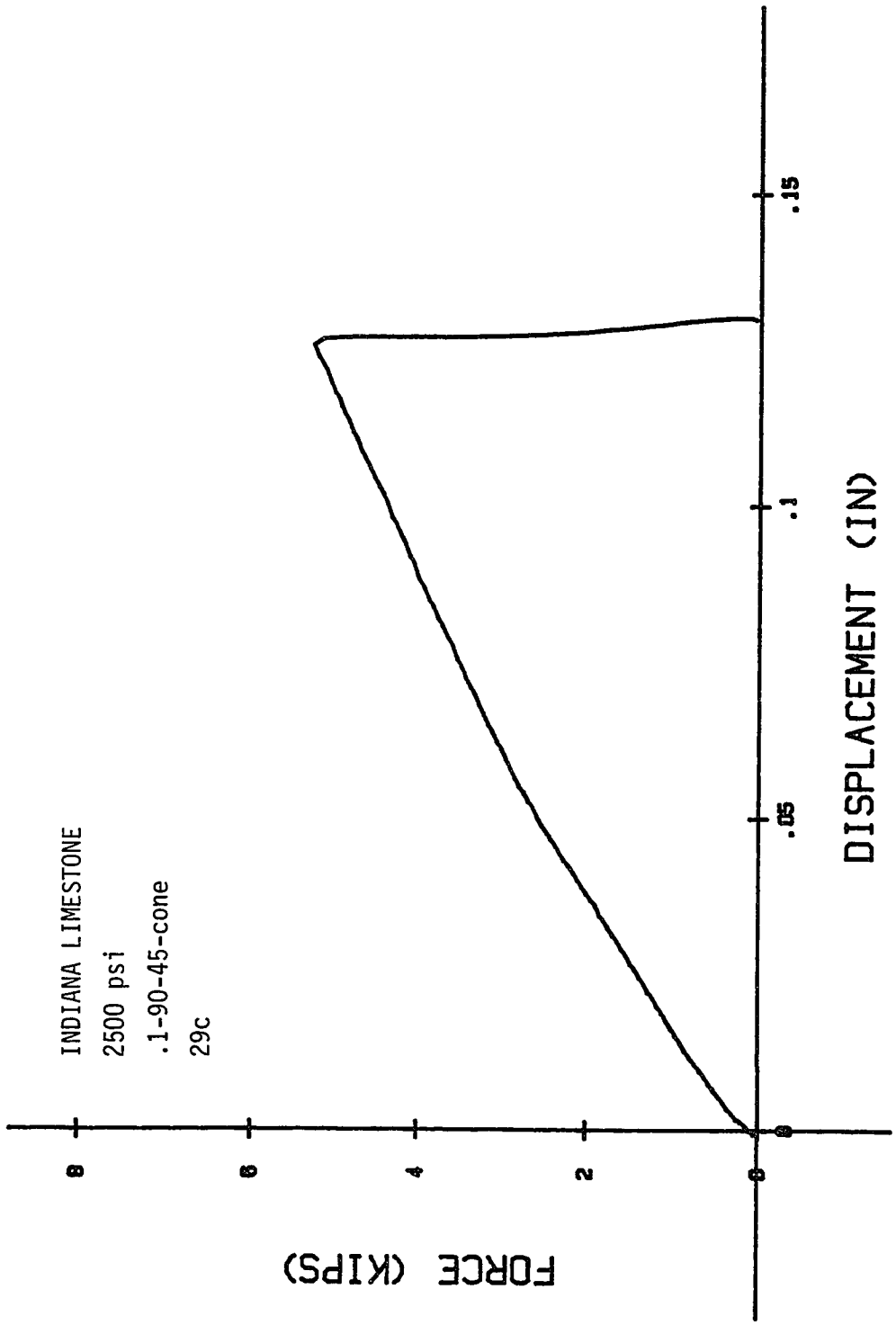
INDIANA LIMESTONE
2500 psi
.1-90-45-cone
29c
FORCE (KIPS)
0
2
4
6
8
0
.05
.1
.15
DISPLACEMENT (IN)

FIGURE 3.11

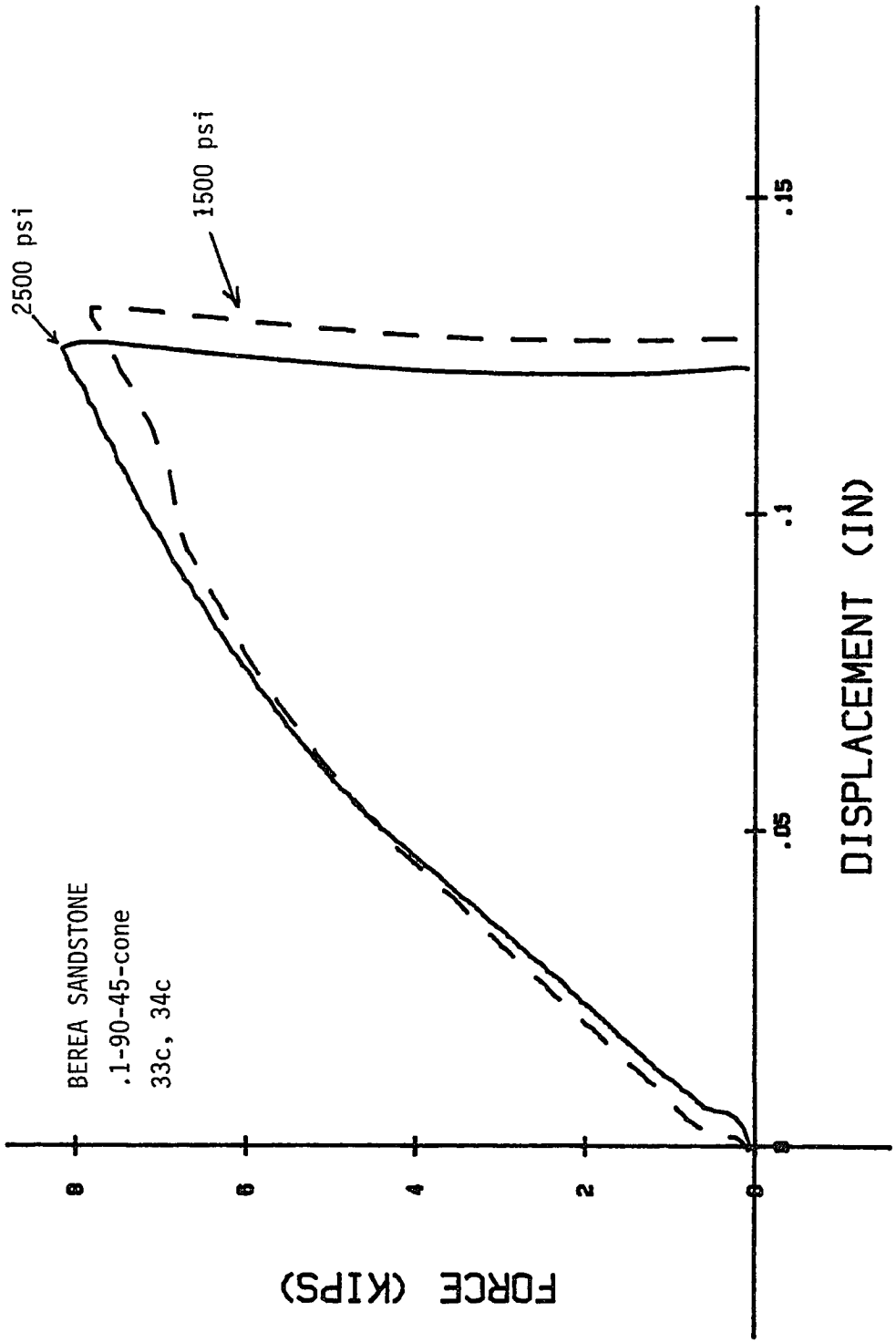
2500 psi
1500 psi
BEREA SANDSTONE
.1-90-45-cone
33c, 34c
FORCE (KIPS)
0
2
4
6
8
.05
.1
.15
DISPLACEMENT (IN)

FIGURE 3.12

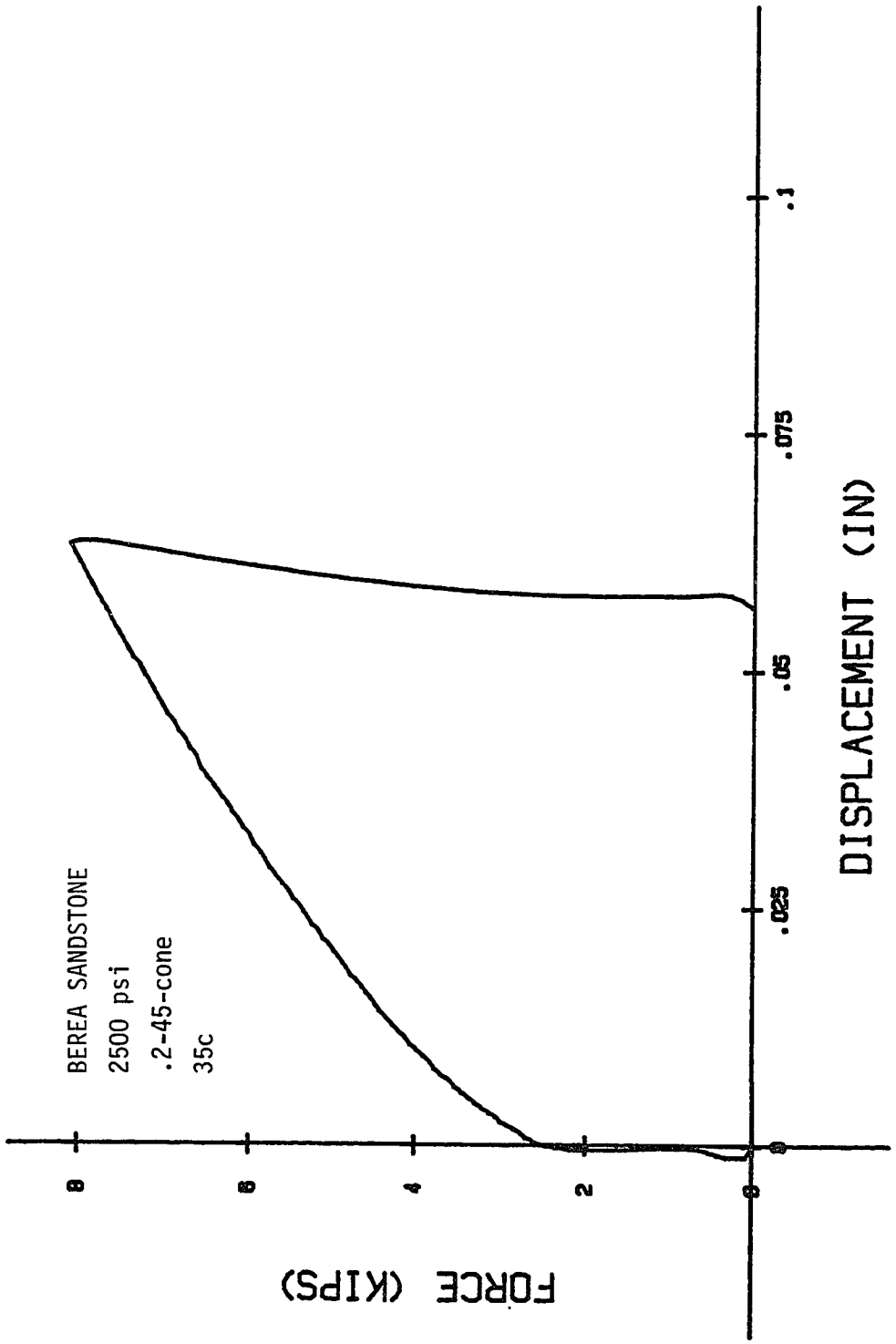
BEREA SANDSTONE
2500 psi
.2-45-cone
35c
FORCE (KIPS)
0
2
4
6
8
.025
.05
.075
.1
DISPLACEMENT (IN)

FIGURE 3.13

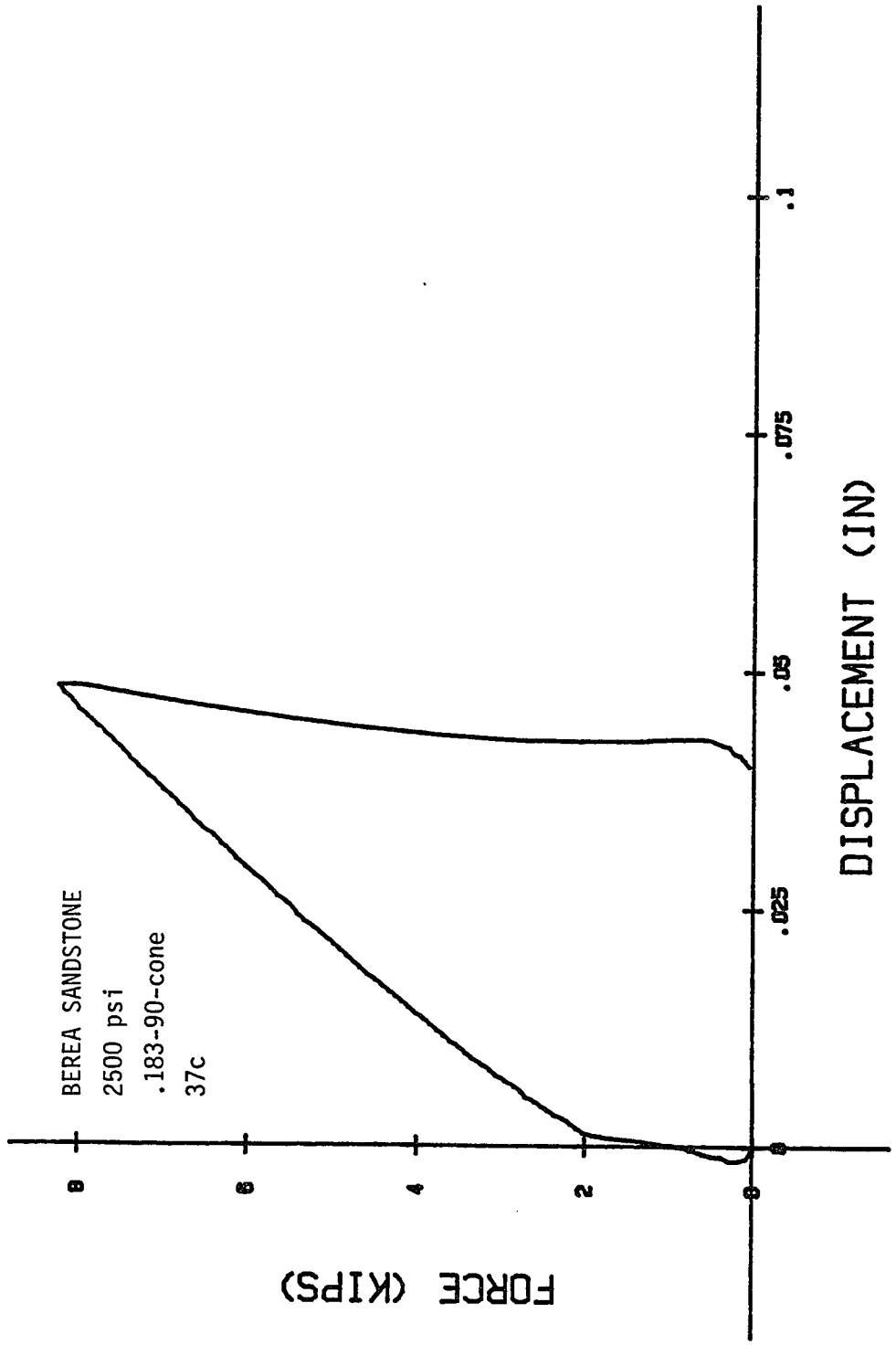
BEREA SANDSTONE
2500 psi
.183-90-cone
37c
FORCE (KIPS)
0
2
4
6
8
DISPLACEMENT (IN)
0
.025
.05
.075
.1

FIGURE 3.14

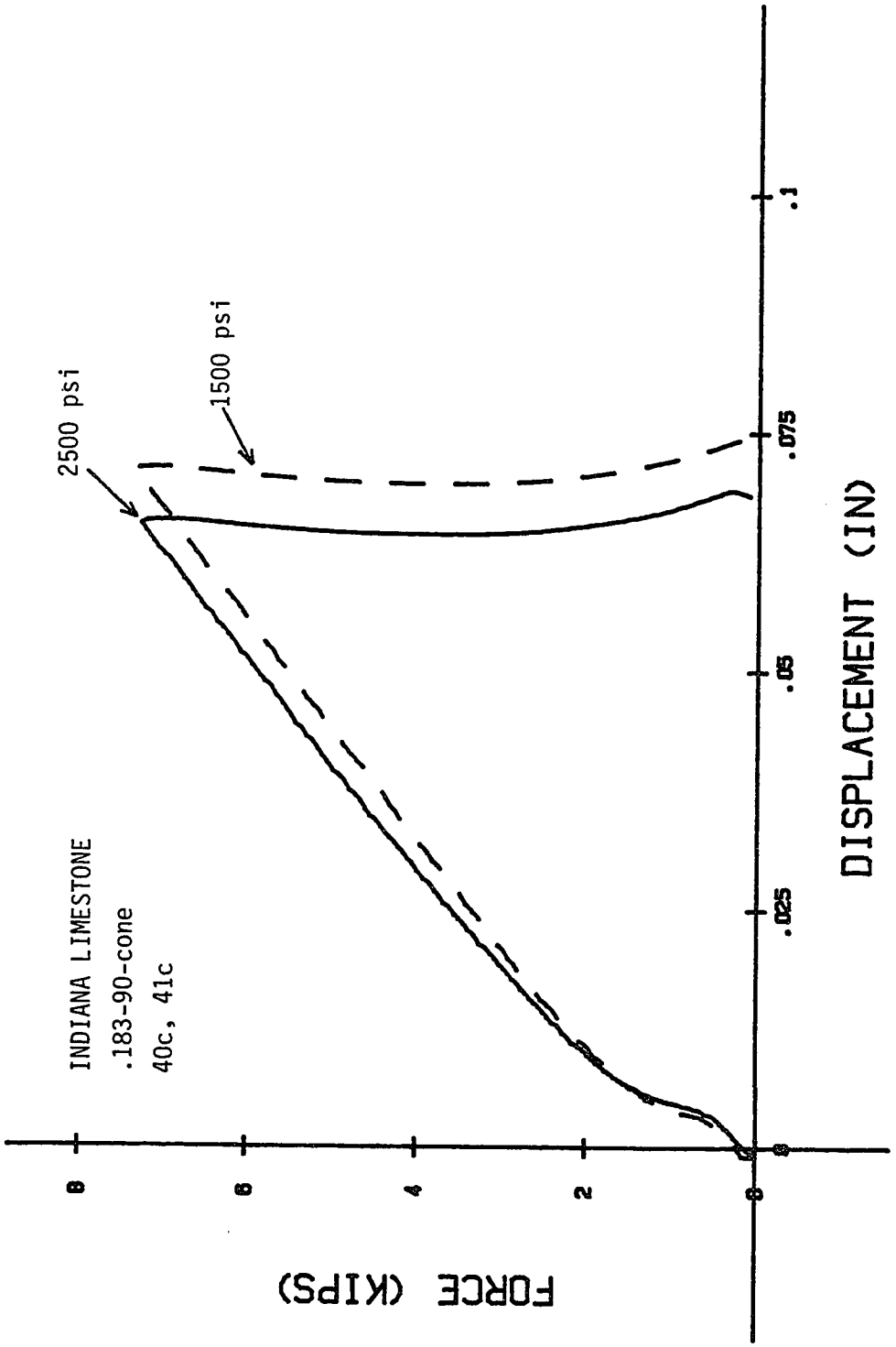
INDIANA LIMESTONE
.183-90-cone
40c, 41c
2500 psi
1500 psi
FORCE (KIPS)
0
2
4
6
8
0
.025
.05
.075
.1
DISPLACEMENT (IN)

FIGURE 3.15

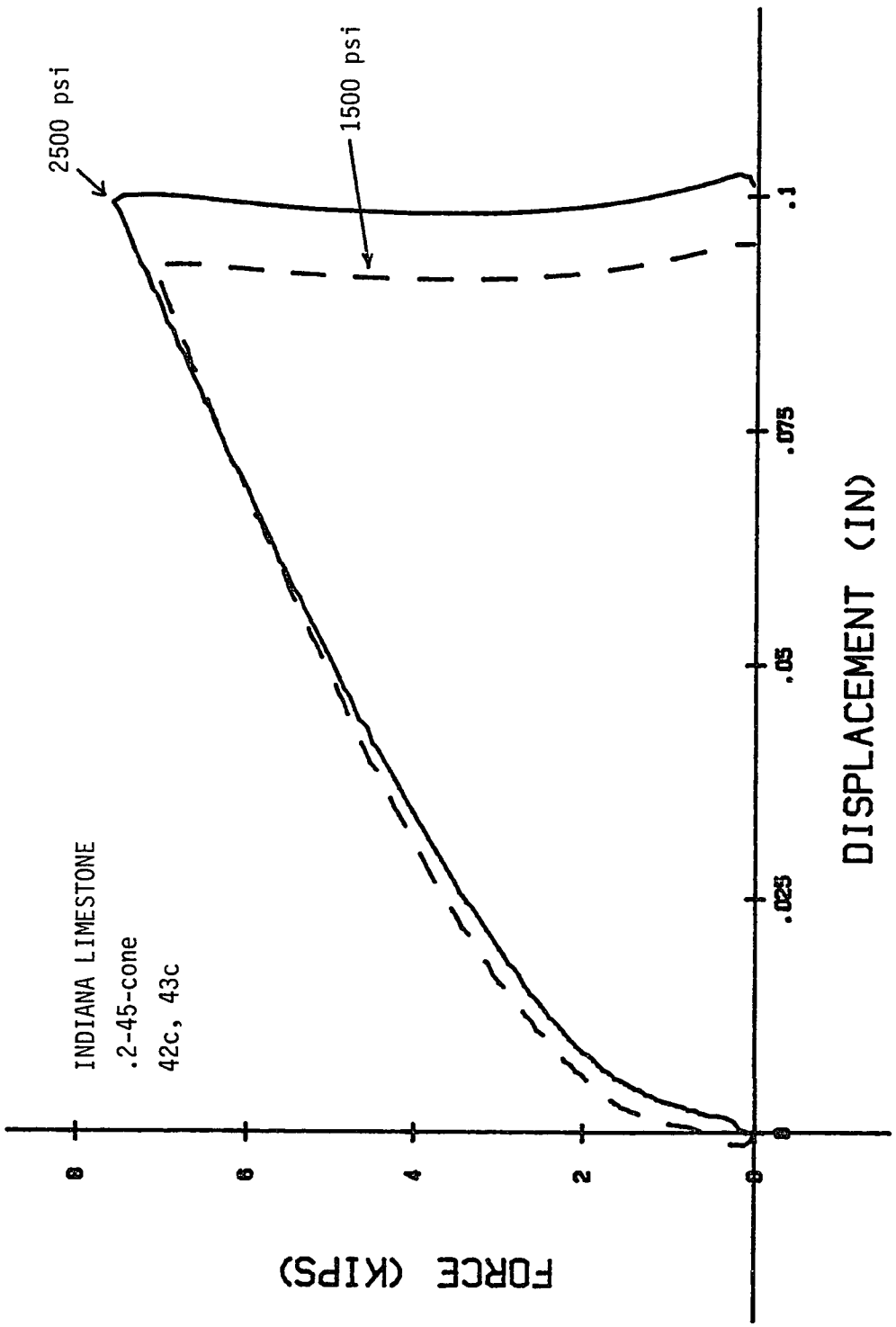
INDIANA LIMESTONE
.2-45-cone
42c, 43c
2500 psi
1500 psi
FORCE (KIPS)
0
2
4
6
8
0
.025
.05
.075
.1
DISPLACEMENT (IN)

FIGURE 3.16

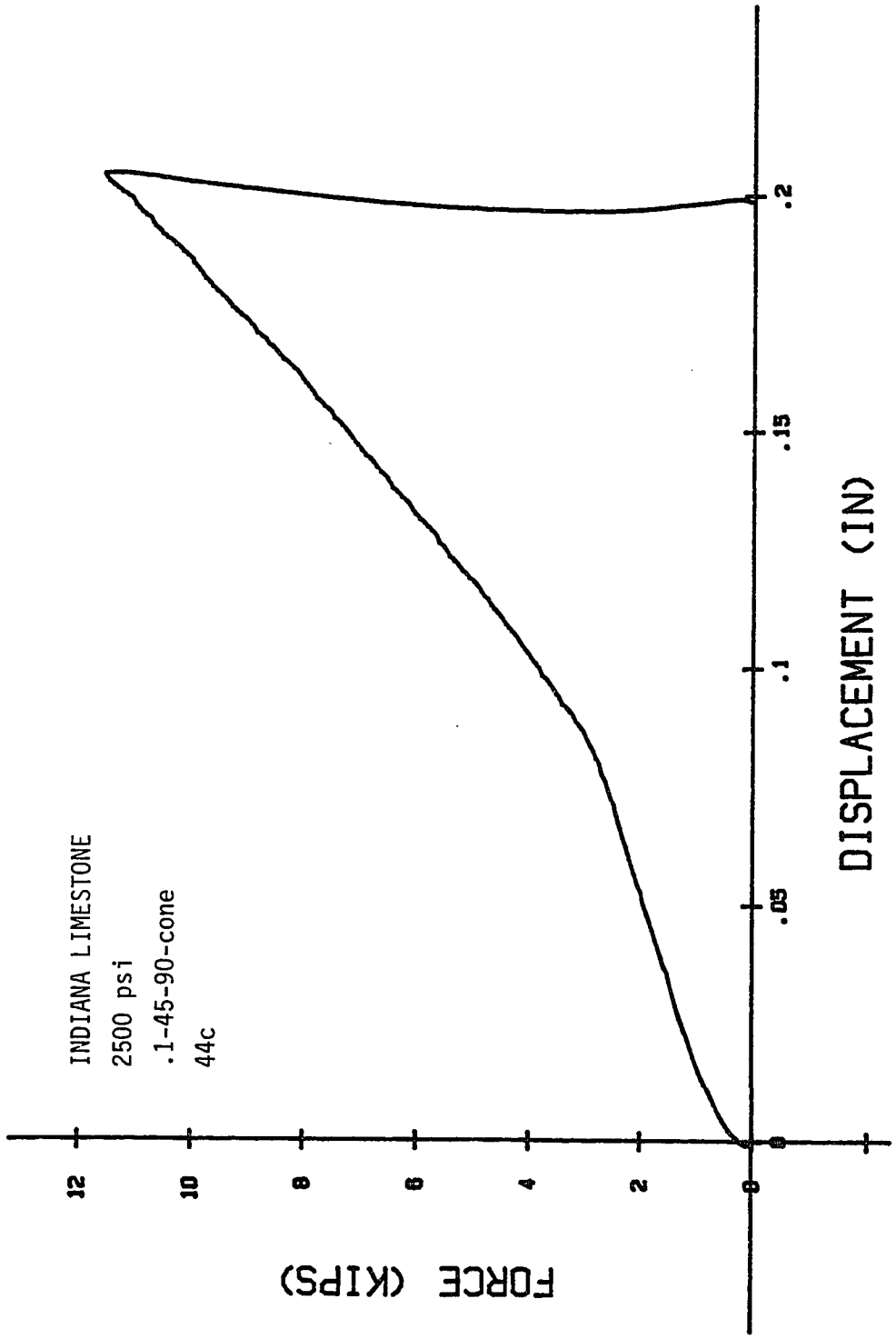
INDIANA LIMESTONE
2500 psi
.1-45-90-cone
44c
FORCE (KIPS)
12
10
8
6
4
2
0
0
.05
.1
.15
.2
DISPLACEMENT (IN)

FIGURE 3.17

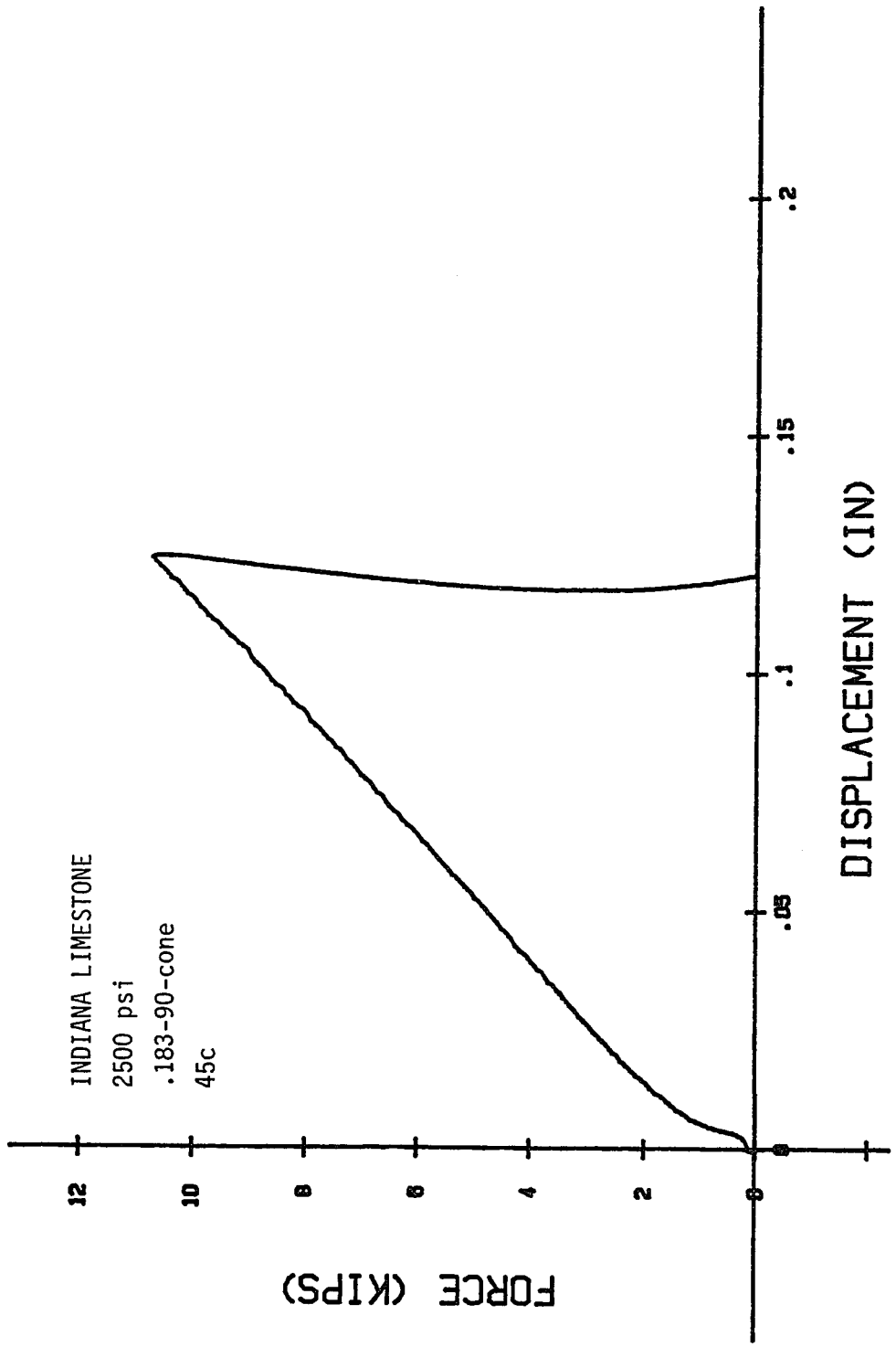
INDIANA LIMESTONE
2500 psi
.183-90-cone
45c
FORCE (KIPS)
12
10
8
6
4
2
0
0
.05
.1
.15
.2
DISPLACEMENT (IN)

FIGURE 3.18

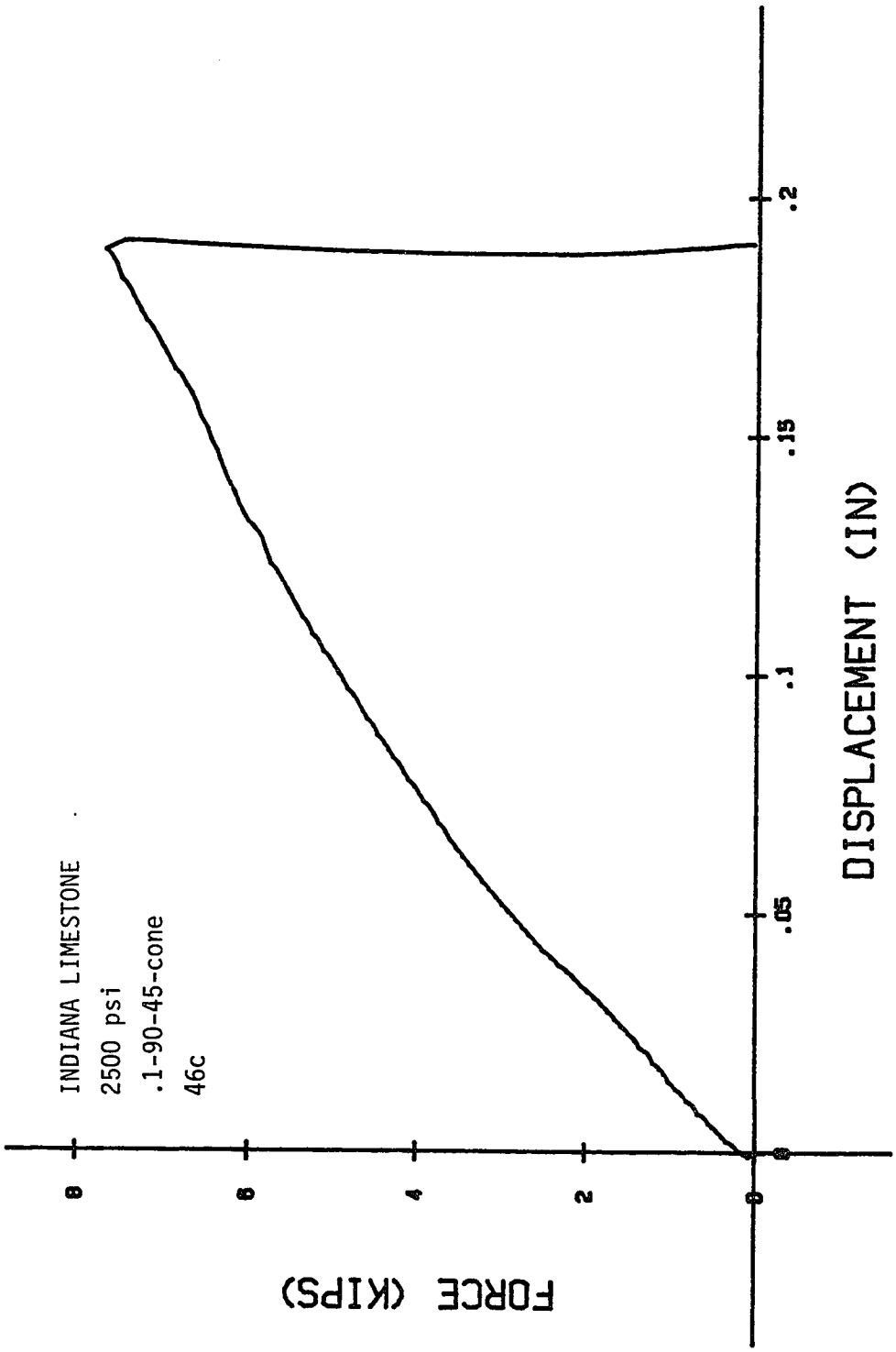
INDIANA LIMESTONE
2500 psi
.1-90-45-cone
46c
FORCE (KIPS)
0
2
4
6
8
DISPLACEMENT (IN)
0
.05
.1
.15
.2

FIGURE 3.19

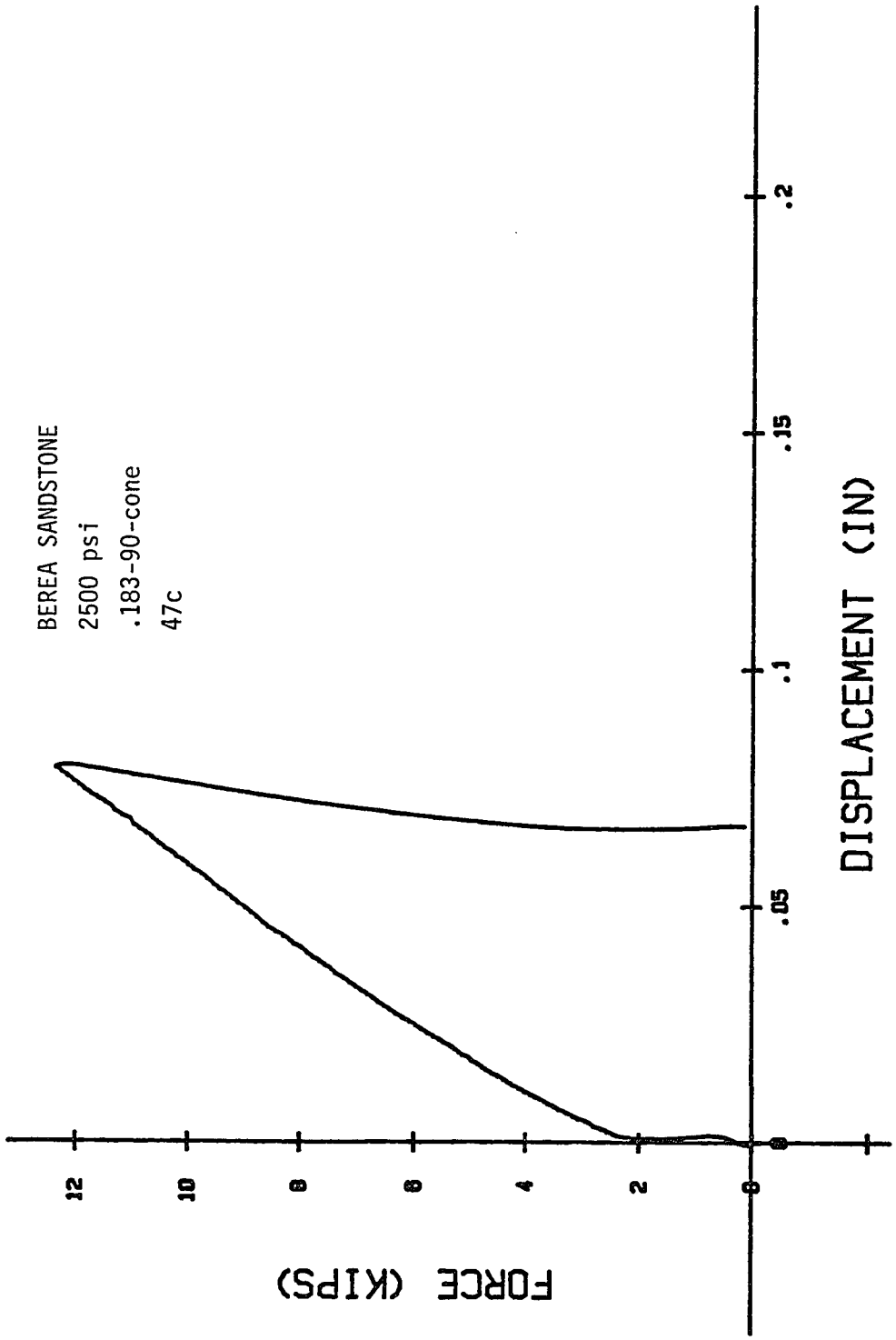
BEREA SANDSTONE
2500 psi
.183-90-cone
47c
FORCE (KIPS)
12
10
8
6
4
2
0
0
.05
.1
.15
.2
DISPLACEMENT (IN)

FIGURE 3.20

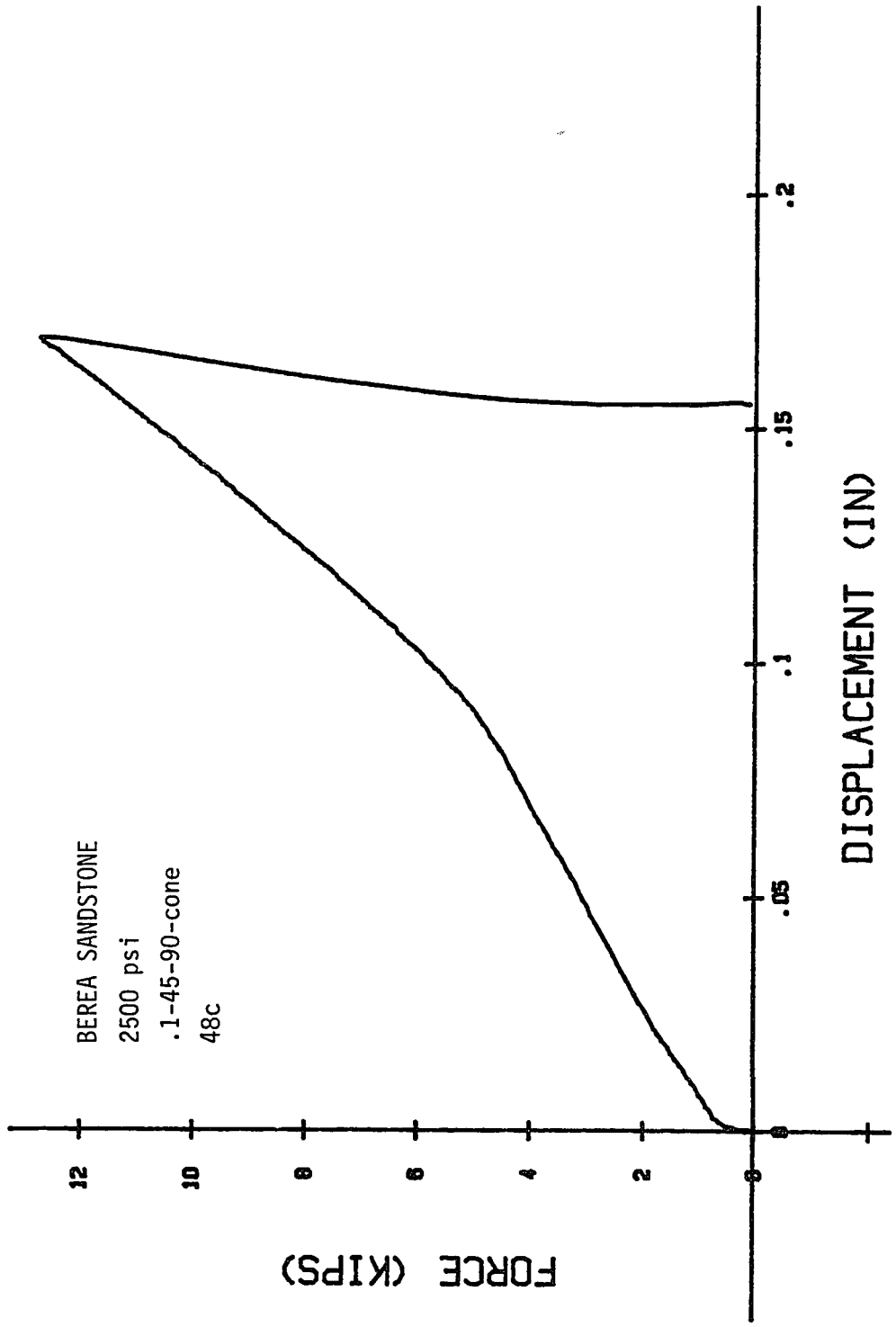
BEREA SANDSTONE
2500 psi
.1-45-90-cone
48c
FORCE (KIPS)
12
10
8
6
4
2
0
0
.05
.1
.15
.2
DISPLACEMENT (IN)

FIGURE 3.21

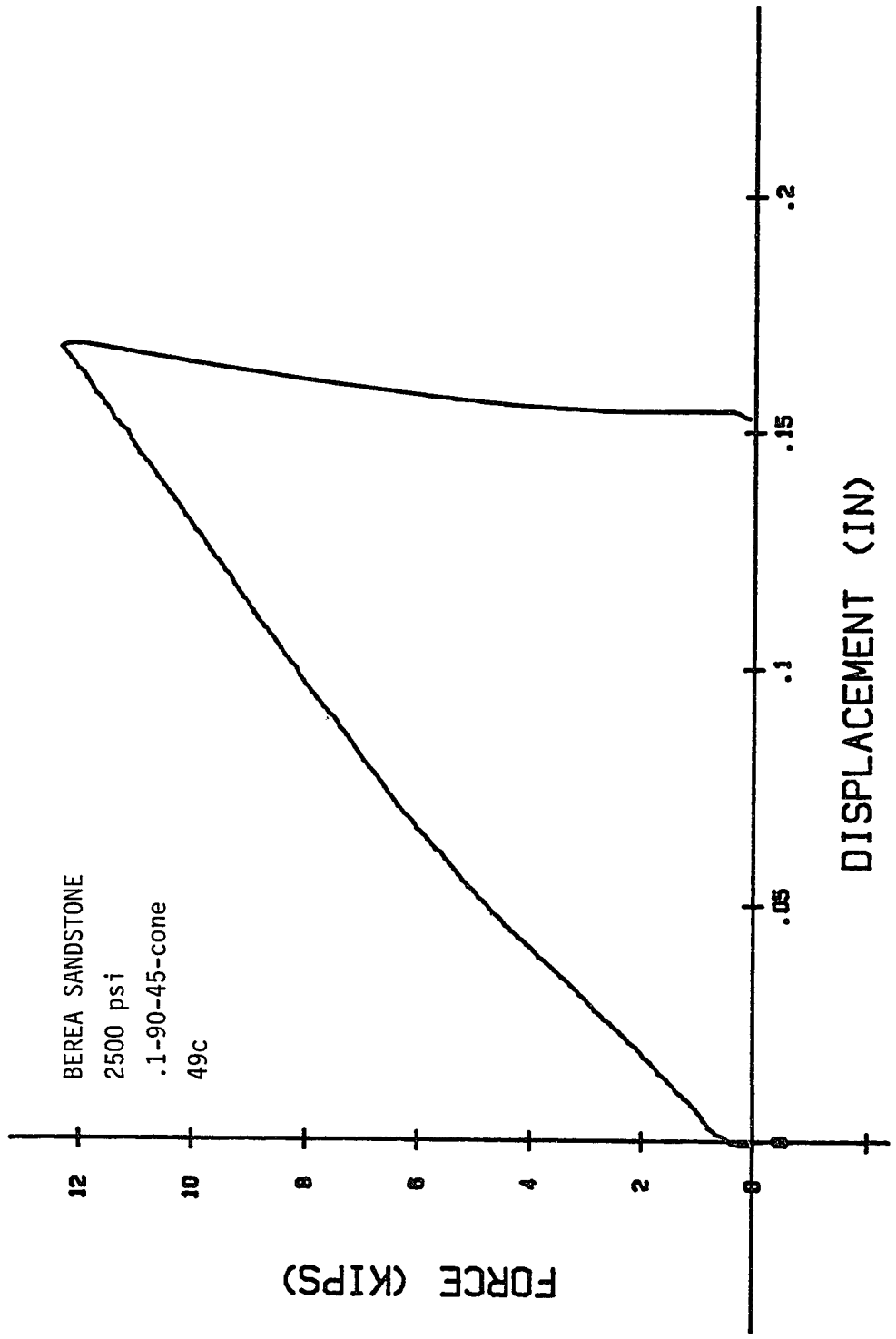
BEREA SANDSTONE
2500 psi
.1-90-45-cone
49c
FORCE (KIPS)
12
10
8
6
4
2
0
0
.05
.1
.15
.2
DISPLACEMENT (IN)

FIGURE 3.22

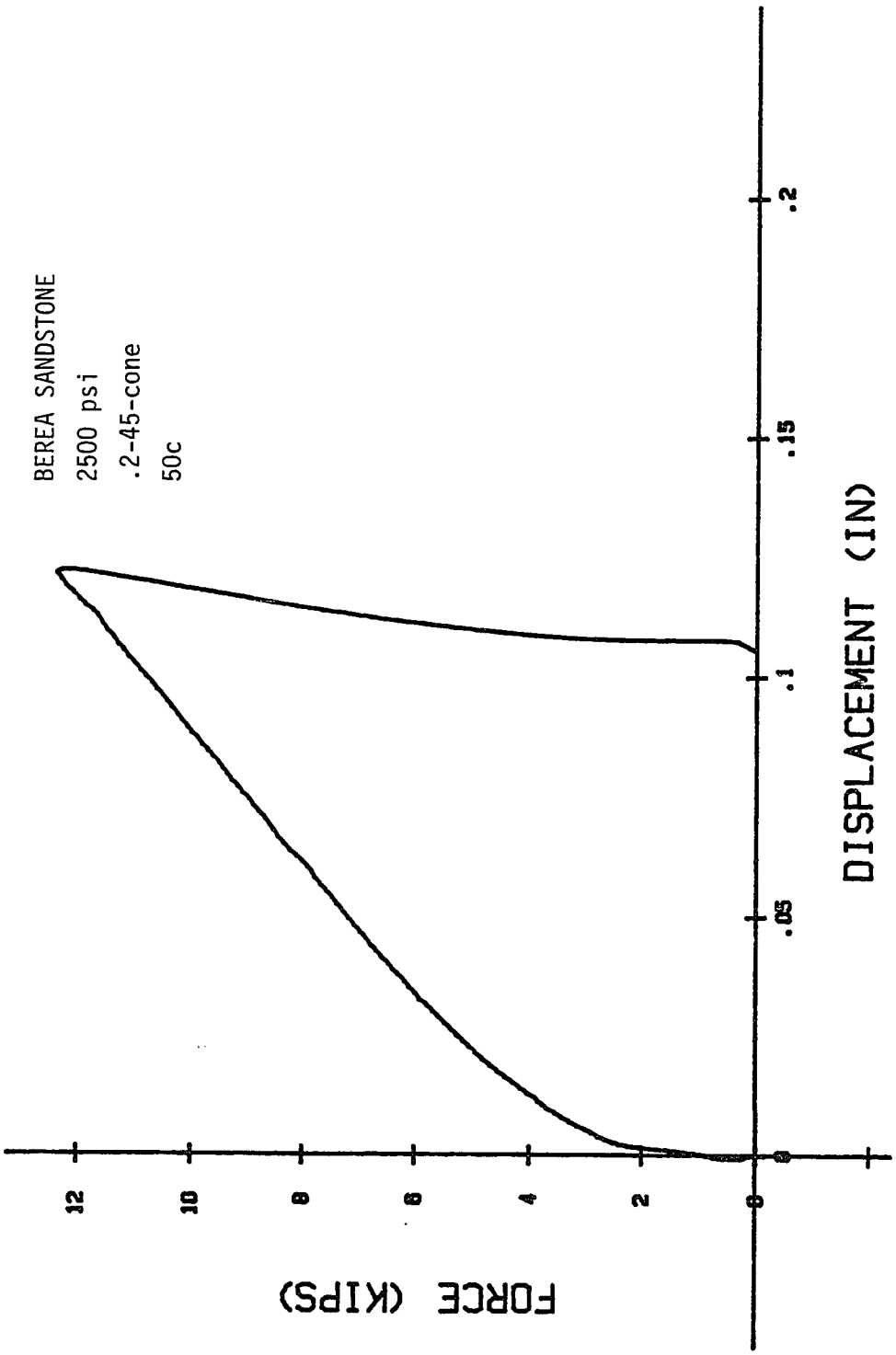
BEREA SANDSTONE
2500 psi
.2-45-cone
50c
FORCE (KIPS)
0
2
4
6
8
10
12
DISPLACEMENT (IN)
.05
.1
.15
.2

FIGURE 3.23

IV. RESTRICTION OF PLASTICITY PARAMETERS

Method

For a particular problem geometry, there exist now both a numerical solution and an experimental result. The experimental result is a single number: the force on the punch. The numerical solution, however, consists of a dimensionless pressure profile, P/c^*. This profile can be integrated using a combination of the trapezoidal rule and the theorem of Pappus-Guldinus (see Appendix B), to yield an "effective area", F/c^*, which gives a force on the tool for some choice of c^*.

If the material under consideration were to behave exactly according to a Mohr-Coulomb failure law, and lip formation could be neglected, and the interface were either perfectly rough or frictionless, then at every point in the indentation, the value of c^* necessary to equate predicted and actual force would be constant. This is not the case.

Consider a two-parameter space, as in Figure 4.2. For a given indentation problem, the values of c^* and ϕ are bounded by the following two conditions:

1. The force-displacement curve generated by the perfectly rough solution must be an upper bound to the experimentally observed curve.
2. The solution calculated for the frictionless interface must be a lower bound to the experimental curve.

These conditions imply that for a given ϕ, constant, and a given depth of indentation c* is restricted by

$$c^* \Big|_\phi > \frac{F_{experiment}}{(F/c^*)_{rough}} \quad \text{(lower bound for c*)} \qquad (30)$$

and

$$c^* \Big|_\phi < \frac{F_{experiment}}{(F/c^*)_{smooth}} \quad \text{(upper bound for c*)} \qquad (31)$$

Furthermore, since the proposed yield condition is, in general, not equal to the actual, equations (20), (21) constitute only local lower and upper bounds. It is necessary to check these bounds at every depth of indentation to find the maximum (global) lower bound and the minimum (global) upper bound for a given ϕ. When this procedure has been carried out for each value of ϕ, the upper and lower bound curves should envelope a (hopefully small) area of allowable ϕ-c* existence. The smallness of this area is an indication of the accuracy with which the proposed yield surface corresponds to the rock's actual yield condition. Figure 4.1 shows one such ideal result for a hypothetical two-parameter yield condition, the parameters given by A and B.

Example 1: Indiana Limestone, 2000 psi confining pressure, .09-45-cone (test 8c).

From the test curve, the following values are obtained at the dimensionless depth d/r:

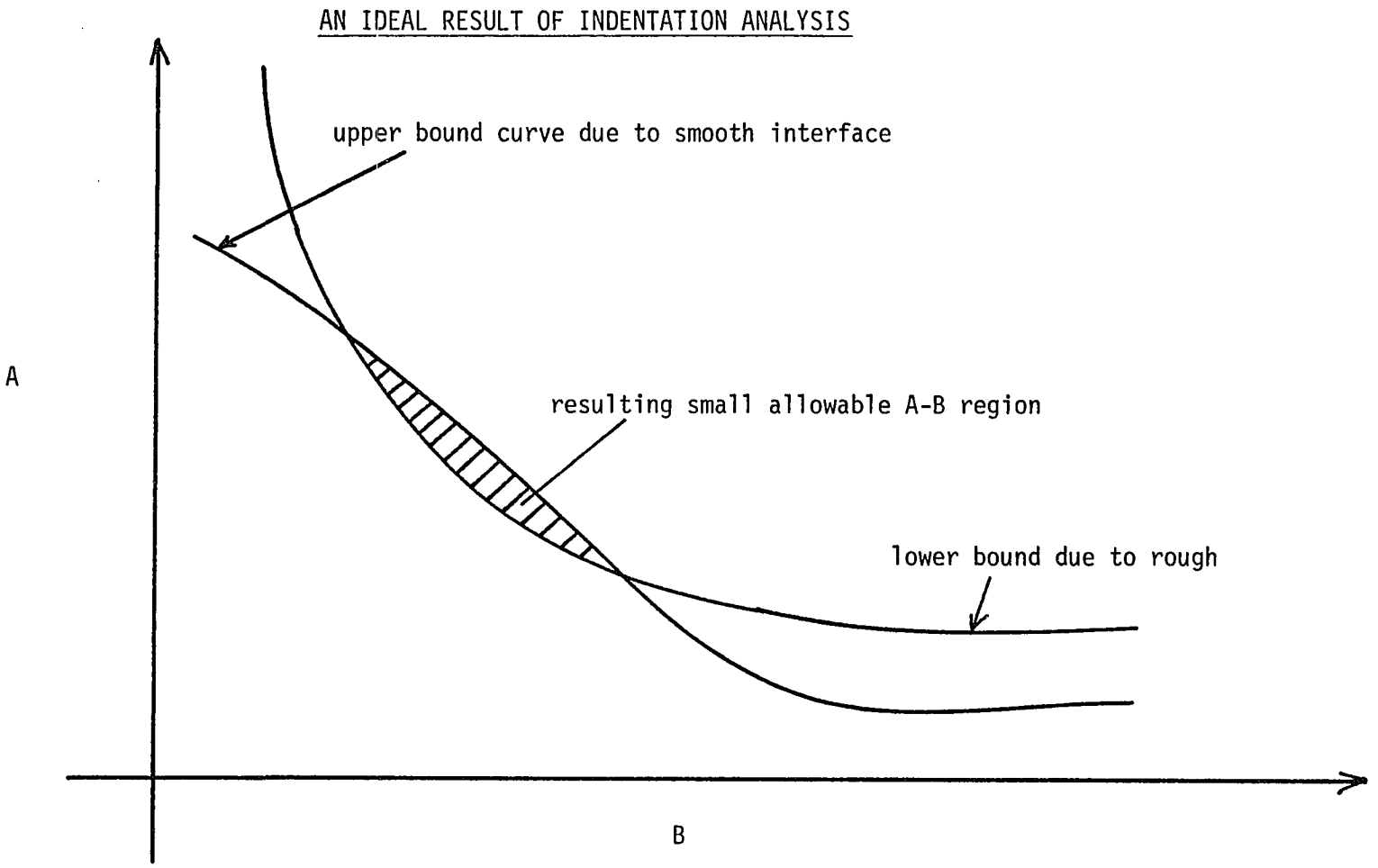
AN IDEAL RESULT OF INDENTATION ANALYSIS
upper bound curve due to smooth interface
A
resulting small allowable A-B region
lower bound due to rough
B

FIGURE 4.1

d/r	F(lbf)
0.5	860
1.0	1330
4.0	4070

Program force.c is used to integrate the pressure curves for this tool at several values of ϕ for each of the above depth ratios. The smooth case gives for F/c*:

Table 4.1

	d/r		
ϕ(rad)	0.5	1.0	4.0
0.1	.0677	.0884	.0271
0.2	.0956	.124	.365
0.3	.142	.182	.512
0.4	.221	.283	.756
0.5	.372	.474	1.20
0.6	.680	.861	2.05
0.7	1.40	1.76	3.95
0.8	3.33	4.15	8.81

According to the above method, it is necessary to find the minimum c* allowed at each depth increment for a particular value of ϕ: the global minimum for c* is then the minimum of these values. For example, at ϕ = 0.4

$$c^*_{max,0.5} = 860/.221 = 3891 \text{ psi}$$

$$c^*_{max,1.0} = 1330/.283 = 4700 \text{ psi}$$

$$c^*_{max,4.0} = 4070/.756 = 5383 \text{ psi}$$

The minimum value of c^*_{max} is thus 3891 psi. If this process is performed at each value of ϕ (0.1 to 0.8), the following results are obtained for c^*_{max}:

Table 4.2

ϕ (rad)	c^*_{max} (psi)
0.1	12703
0.2	8995
0.3	6056
0.4	3891
0.5	2312
0.6	1265
0.7	614
0.8	258

The rough case is treated analogously, giving the following values for c^*_{min} (take the maximum of all depths):

Table 4.3

ϕ (rad)	c^*_{min} (psi)
0.1	10900
0.2	7470
0.3	4850
0.4	2995
0.5	1720
0.6	910
0.7	430
0.8	175

It is notable that the critical depth/radius ratio for the rough case is 1.0, not 0.5. Tables 4.2 and 4.3 are the points on upper and lower bound curves, respectively, for c* plotted versus ϕ. This plot is shown in Figure 4.2a. Note that while the c-ϕ pairs are, indeed, restricted to a narrow band, each parameter may still take on a rather large range.

Example 2: Berea Sandstone, 2500 psi confining pressure, .1-45-90 cone (test 48c).

Table 4.4 and Figure 4.2b show similar results.

RESULT FOR INDENTATION OF INDIANA LIMESTONE

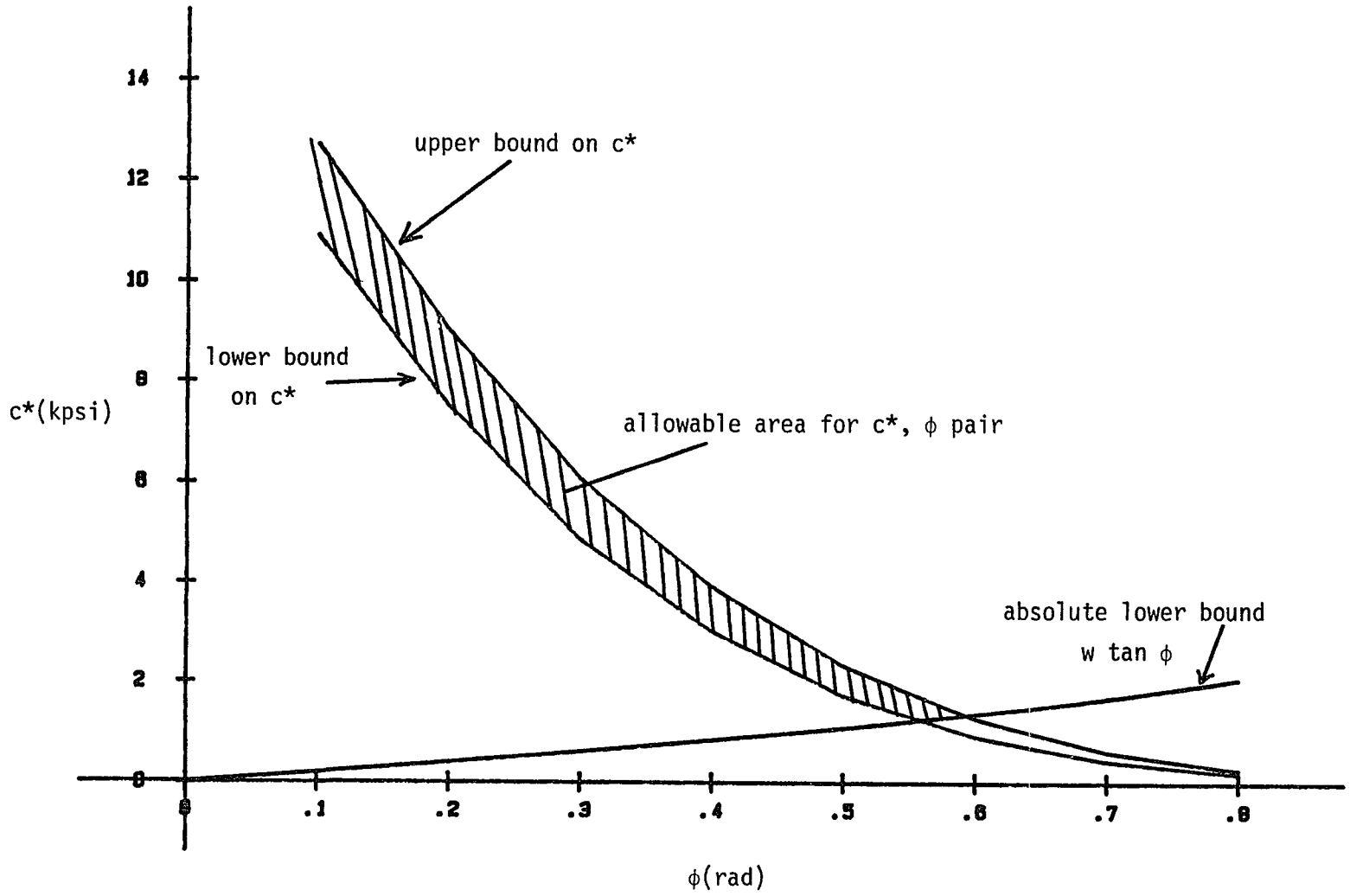

FIGURE 4.2a

Table 4.4

ϕ(rad)	c^*_{min}(psi)	c^*_{max}(psi)
0.1	22210	23150
0.2	15160	16400
0.3	9890	11060
0.4	6110	7090
0.5	3520	4220
0.6	1880	2300
0.7	900	1120
0.8	370	470

Although these results mean that the rock plasticity parameters are not uniquely specified (on the surface a negative result), they are in fact the correct results for the Mohr-Coulomb envelope. If one is restricted to a linear envelope, there exist many choices of this straight line which could be used to approximate a "real" failure envelope, and due to the fact that the rough and smooth predictions diverge widely from the observed curve as indentation progresses, all of these choices will envelope the test results. Figure 4.3 shows this divergence for a particular choice of $\phi = 0.5$ as applied to the curve of the example (test 8c). Even for this arbitrary choice of ϕ, the predictions are not too bad. Apparently, the rough case more closely approximates the true curve - a result which is expected. The choice of a finite coefficient of friction would, of course, fall somewhere between the two curves, but would not be expected to resolve the ambiguity in the choice of c and ϕ.

RESULT FOR INDENTATION OF BEREA SANDSTONE

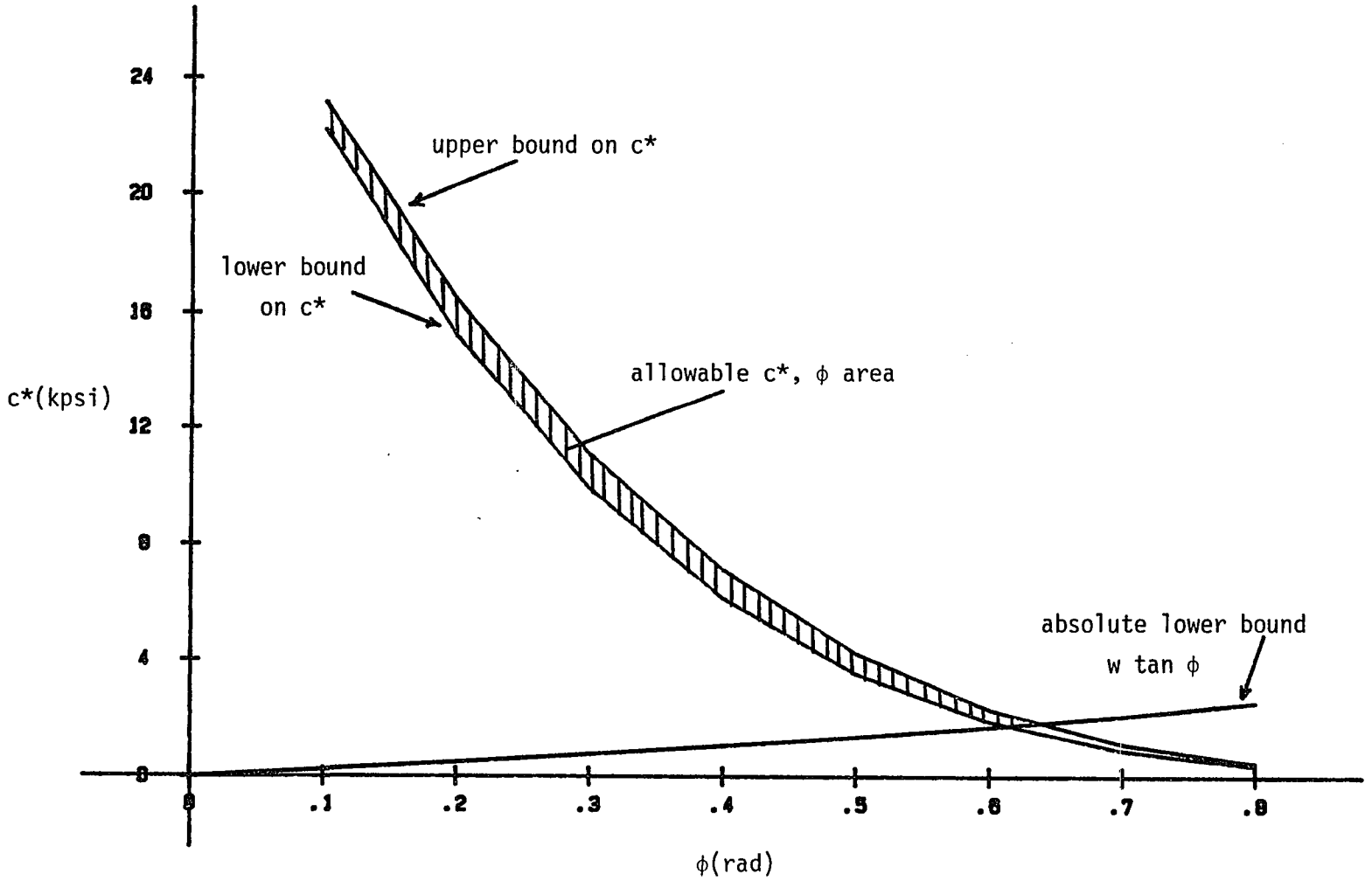

FIGURE 4.2b

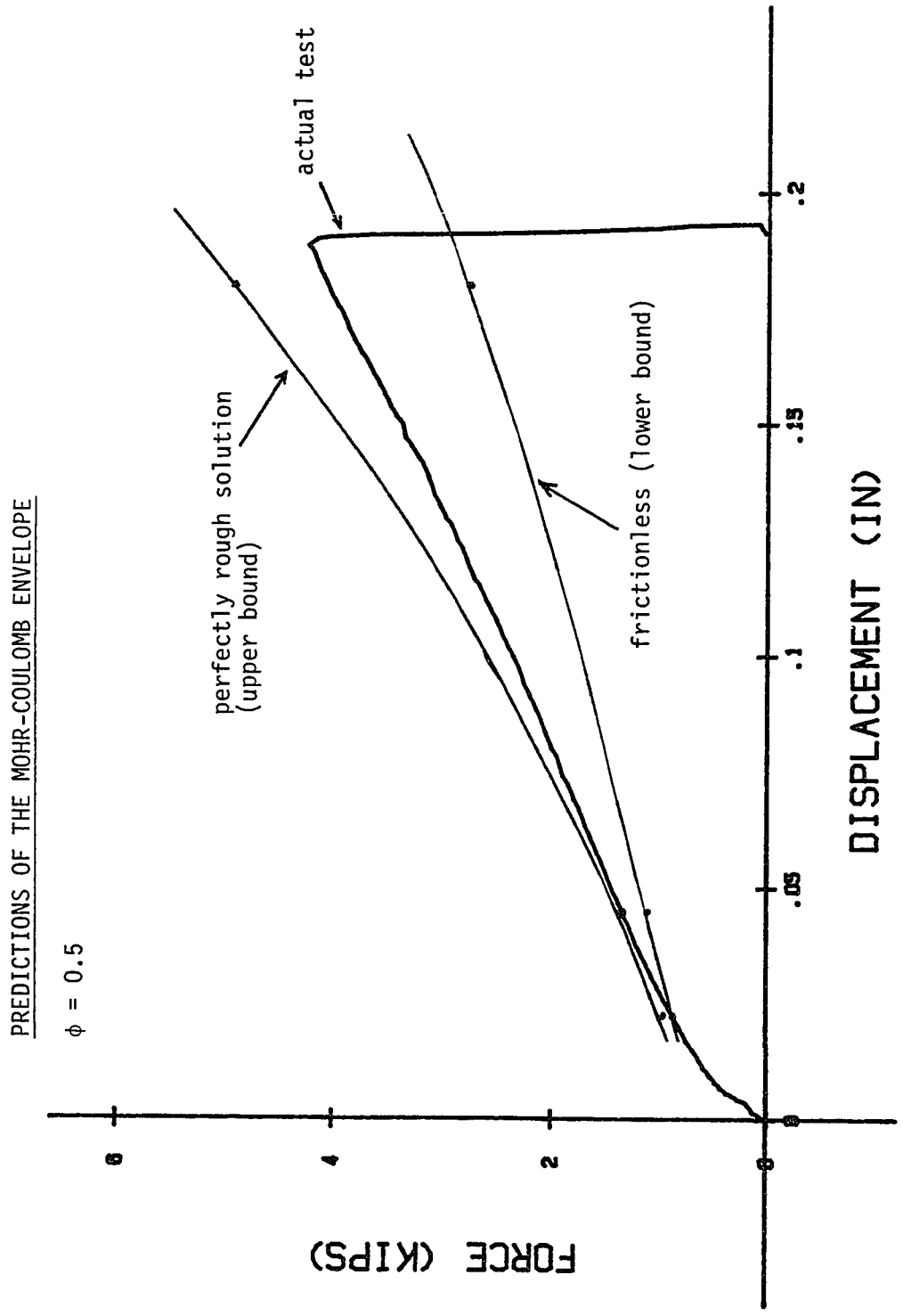
PREDICTIONS OF THE MOHR-COULOMB ENVELOPE
ϕ = 0.5
perfectly rough solution
(upper bound)
actual test
frictionless (lower bound)
FORCE (KIPS)
DISPLACEMENT (IN)
0
2
4
6
.05
.1
.15
.2

FIGURE 4.3

V. SUMMARY AND CONCLUSIONS

Laboratory tests are conducted on samples of Indiana Limestone and Berea Sandstone by indenting them with axially symmetric steel tools of various profiles. In order to achieve plastic (rather than brittle) behavior, confining pressures of up to 2500 psi are applied to the face of the sample. A record of force vs. displacement is obtained for each test. The goal of the thesis is to use the results of such a test to determine the parameters of a particular proposed yield condition.

In the present case, a Mohr-Coulomb linear yield envelope is chosen for simplicity of analysis. Further, the rock-tool interface is regarded as either frictionless or perfectly rough, and lip formation at the surface is neglected. The differential equations of plastic equilibrium are integrated for these assumptions at various values of ϕ, the angle of internal friction. The ultimate result of this integration is an effective area F/c^* for each value of ϕ (F is the total force on the tool; c^* - the effective cohesion - contains c, the cohesive strength). Since the true force is known by experiment, this effective area is used to establish bounds on c^* at a particular value of ϕ, using the condition that the frictionless and perfectly rough numerical solutions must everywhere envelope the experimental curve.

As a result of this method, the Mohr-Coulomb parameters are confined to a narrow allowable region in ϕ-c^* space, rather than uniquely specified. It is concluded, therefore, that the Mohr-Coulomb yield condition is a poor approximation for the entire yield envelopes

of these rocks, even though it may be an acceptable model in certain regions of mean stress. The narrowness of the allowable regions, however, indicates that plasticity parameters can be adequately restricted merely by consideration of perfectly rough and smooth interfaces.

There exists from this study a good database with which to compare other theoretical models. The general method outlined in section IV provides a means of bounding plasticity parameters for any such proposed yield envelope. This thesis, then, provides a base for the future work suggested below:

1. Propose a parabolic yield condition. It is amenable to the method of characteristics, contains only two plasticity parameters, and much more closely approximates "real" envelopes over all ranges of mean stress.
2. Construct characteristic nets for the dual-angle tools, since they may provide more restrictive conditions to the plasticity parameters.
3. Analyze the transition region between angles of a dual-angle cone. 1 and 2, above, may provide considerable insight here. Lip formation may be an important component of the transition.

A method of characteristics solution to the parabolic yield condition can be substituted almost directly into the programs provided by this thesis, and is the single most important improvement to make. Hopefully, such a refinement will lead to a very small allowable region of parameters, in which case the extraction of triaxial data from an indentation test is complete.

REFERENCES

[1] R. Hill, The Mathematical Theory of Plasticity, Clarendon Press, Oxford (1950).

[2] L. L. Karafiath and E. A. Nowatski, Soil Mechanics for Off-Road Vehicle Engineering, Trans Tech Publications, Clausthal, Germany (1978).

[3] J. R. Booker and E. H. Davis, "Stability Analysis by Plasticity Theory", Chapter 21 in Numerical Methods in Geotechnical Engineering, C. S. Desai and J. T. Christian, eds., McGraw-Hill (1977).

[4] P.-A. Lindgrist and L. Hai-Hui, "Behaviour of the Crushed Zone in Rock Indentation", Rock Mechanics and Rock Engineering, v. 16, n. 3 (1983), pp. 199-207.

[5] P. S. Symonds, "The Determination of Stresses in Plastic Regions in Problems of Plane Flow", Journal of Applied Physics, v. 20 (1949), pp. 107-112.

[6] M. Sh. Stein, "Some Exact Solutions of the Equations of Ideal Plasticity in the Case of Axial Symmetry", Prikladnaya Mechanika, vo. 19 n. 10 (1983), pp. 41-46.

[7] M. B. Abbott, An Introduction to the Method of Characteristics, American Elsevier, New York (1966).

[8] M. E. Harr, Foundations of Theoretical Soil Mechanics, McGraw-Hill (1966).

[9] A. W. Jenike and R. T. Shield, "On the Plastic Flow of Coulomb Solids Beyond Original Failure", Journal of Applied Mechanics (1959), pp. 599-602.

[10] P. F. Gnirk and J. B. Cheatham, Jr., "An Experimental Study of Single Bit-Tooth Penetration into Dry Rock at Confining Pressures of 0 to 5000 psi", Trans. AIME, v. 234 (1965), pp. II 117-130.

[11] L. L. Karafiath, "Cone Resistance in Sand by Incremental Method", Journal of Terramechanics, vo. 17 n. 2 (1980), pp. 101-113.

[12] A. D. Cox, G. Eason, and H. G. Hopkins, "Axially Symmetric Plastic Deformation in Soils", Phil. Trans. Roy. Soc. (London), v. 254 n. 1036 (1961), pp. 1-45.

[13] I. F. Collins, "The algebraic-geometry of slip line fields with applications to boundary value problems", Proc. Roy. Soc. A, vo. 303 (1968) pp. 317-338.

[14] Wai-Fah Chen, Limit Analysis and Soil Plasticity, Elsevier (1975).

[15] C. S. Desai and H. J. Siriwardane, "Concept of Correction Functions to Account for Non-Associative Characteristics of Geologic Media", Int. J. Num. & Anal. Meth. in Geomechanics, v. 4 no. 4 (1980), p. 377-387.

[16] V. V. Sokolovskii, Statics of Granular Media, Pergamon Press (1965).

[17] G. D. Smith, Numerical Solution of Partial Differential Equations: Finite Difference Methods, Clarendon Press (1985).

APPENDIX A

CORRECTING FOR SYSTEM ELASTICITY

The raw test data for an indentation test consist of a force, a displacement, and a time for each force-displacement pair. Since the time measurement lags the recording of force and displacement by a constant delay, it may be considered to be without error. The force is subject to typical strain gage errors, but since the gages are mounted immediately above the tool, the measurement is not subject to any systematic bias (such as friction).

The displacement reading, however, contains errors associated with "system elasticity". In order to determine the extent to which this elasticity is important, a test was performed on a steel block using a large, (1/2" x 1/2") flat tool (see Figure A1, solid curve).

The non-linear part of the loading curve at low loads is due to the suspension of the rock tray. The tray has a clearance from the vessel floor to facilitate motion along the length of the vessel. An application of small force (about 200 lbf) closes the clearance, after which the tray is far more rigid.

Even after the tray clearance closes, there is noticeable displacement with increasing load, only a negligible portion of which is due to compression of the steel block. In other words, the displacement measurement contains a systematic bias throughout the loading range.

Correction of the raw data curves is simple in theory: fit a curve to the elasticity test (steel block) and subtract displacements

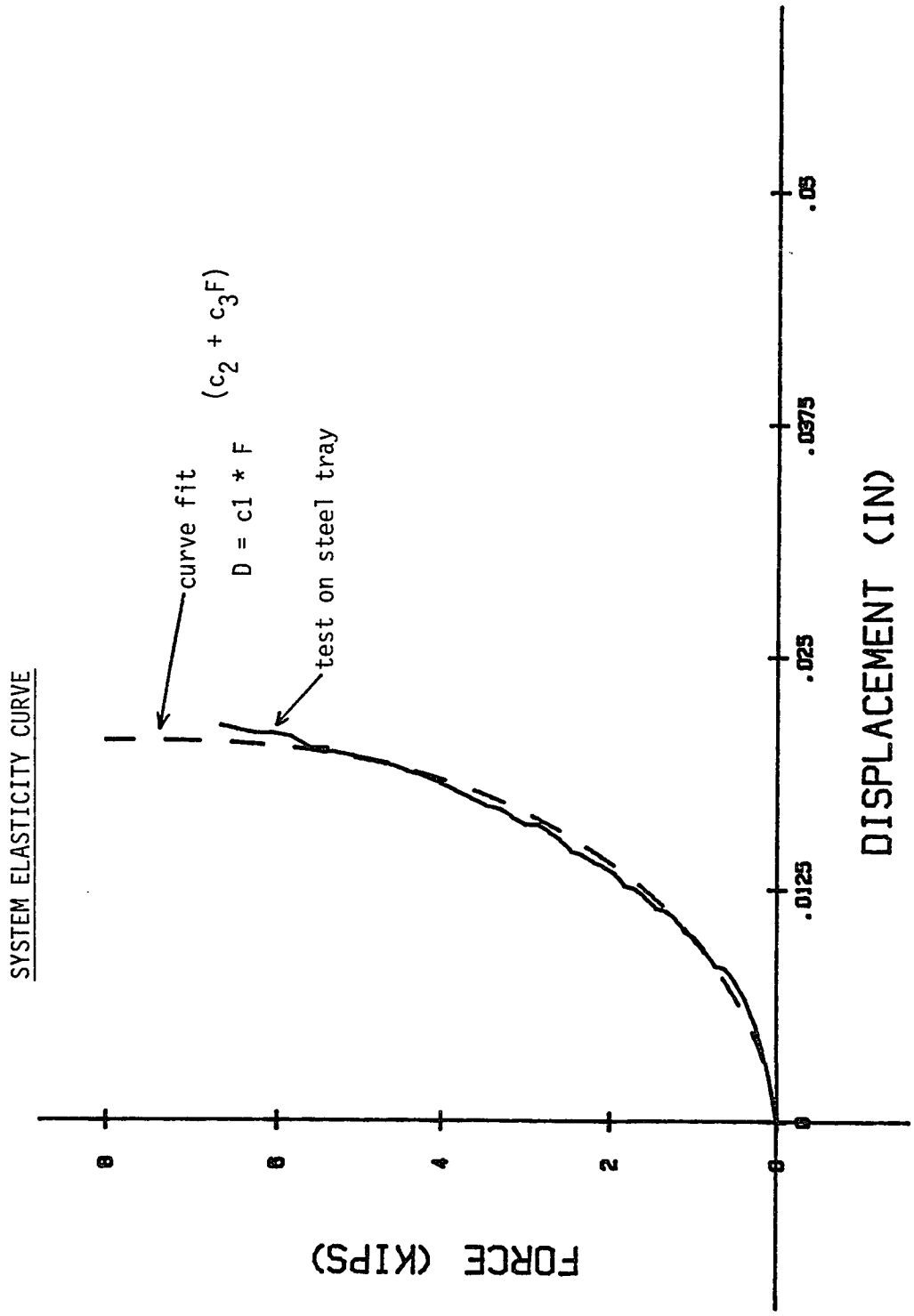
SYSTEM ELASTICITY CURVE
curve fit
$(c_2 + c_3F)$
D = c1 * F
test on steel tray
FORCE (KIPS)
8
6
4
2
0
.0125
.025
.0375
.05
DISPLACEMENT (IN)

FIGURE A1

from the raw data. The practicalities of curve fitting, however, made the search for a good fit difficult. A further problem is that, due to the nature of the curve, it is easier to fit the force to mathematical functions of displacement rather than vice-versa, but these functions are usually not (conveniently) invertible to yield displacement as a function of force. After a long search through polynomial, exponential, logarithmic, and power-curve basis functions, one was finally found that adequately represented the displacement as a function of force (see Figure A1, dashed curve):

$$D = C_1 F^{(C_2 + C_3 F)}$$

where

D = displacement in inches

and

F = force in pounds.

The three constants for a least-square fit are

$C_1 = 1.41884 \times 10^{-4}$

$C_2 = 0.62032$

$C_3 = -8.3744 \times 10^{-6}$

These constants were found using the SPEAKEZ command MULTIREG applied to the loading portion of the TRAY3 data set. All corrected datasets use this curve to make displacement corrections. A typical dataset correction is shown in Figure A2. If the rock were truly rigid, the corrected unloading part of the curve would be a vertical line. Finite elasticity would result in a slight left curvature - somewhat

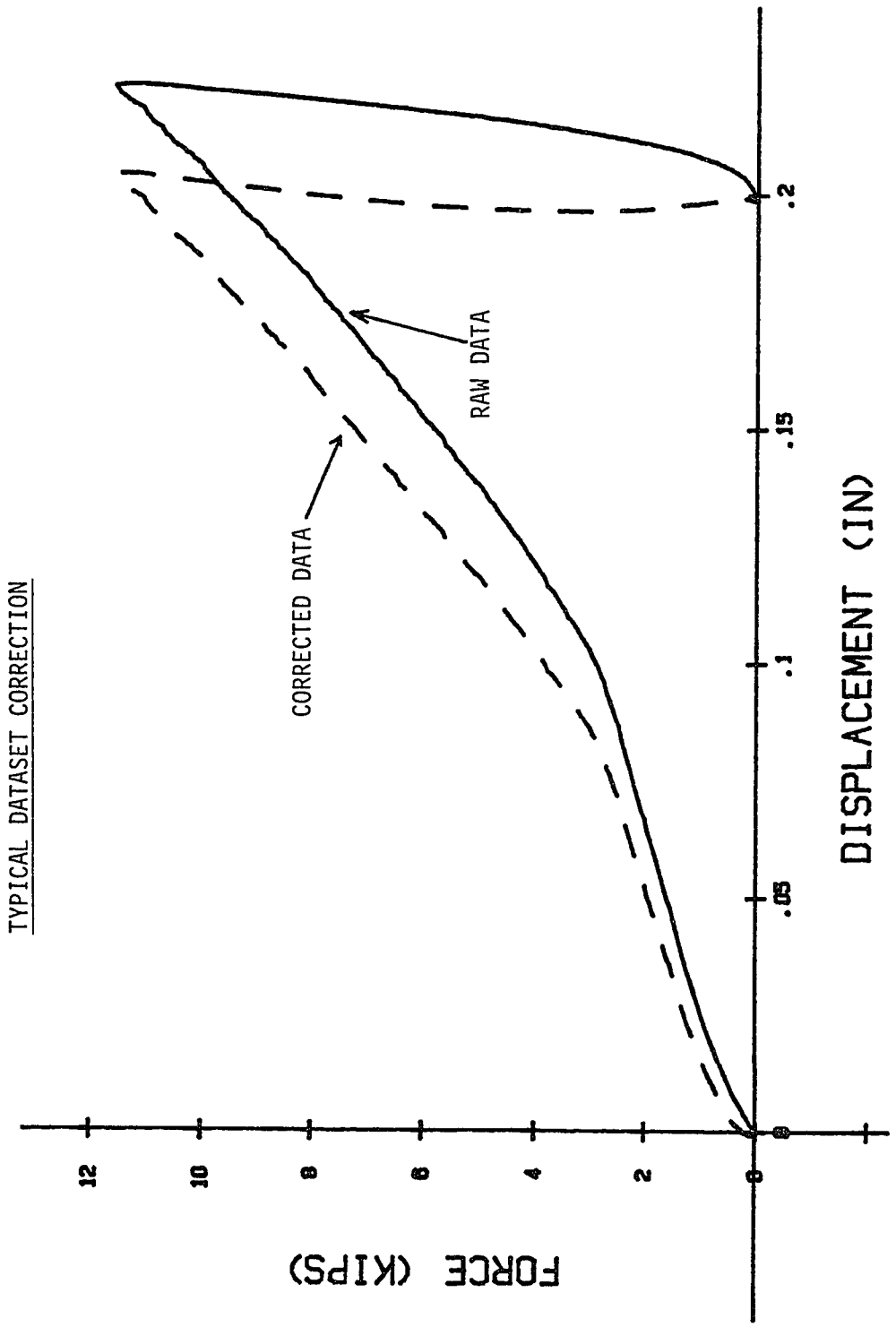
TYPICAL DATASET CORRECTION
CORRECTED DATA
RAW DATA
FORCE (KIPS)
12
10
8
6
4
2
0
.05
.1
.15
.2
DISPLACEMENT (IN)

FIGURE A2

like the raw data shown. The slight right curvature of the unloading in Figure A2 is due to overcorrection for elasticity at certain force levels.

APPENDIX B

COMPUTER PROGRAMS

Program	Computer	Purpose
"TEST6"	HP-85	main testing program controls HP-3421A files data points
"CORRECT"	HP-85	applies system elasticity curve fit to raw data
"GPLOT"	HP-85	reads and plots a dataset
"cone.c"	Celerity	solve the characteristic net for the cone indentation problem, calculate pressure profile
"bluntcone.c"	Celerity	characteristic net and pressures for a flat-ended cone
"force.c"	Celerity	obtain F/c* for a given pressure profile

```
10 ! MAIN TESTING PROGRAM
20 OPTION BASE 1
30 REAL P0,F0,D0,T0,P1,F1,D1,T1
40 REAL A4,A6,A8,A9,V3,V4,V5,V6,V7,V8,R9
50 REAL X(500,3)
60 ! (force,displacement,time)
70 DIM N$[6],D$[8],R$[20],C$[311]
80 INTEGER I,N,I2
90 CLEAR
100 ! ...here are the calibration        constants...
110 P0=5789010 ! psi/vrel
120 T0=5.69957 ! ohm/inch
130 D0=1.23089 ! inch/vrel
140 F0=15750000 ! lbf/vrel
150 !
160 ! ... zeroing routine
170 DISP "SET ALL INSTRUMENTS TO ZERO,     THEN HIT CONT"
180 PAUSE
190 OUTPUT 709 ;"F1RA1Z0N4LS3-8;T3"
200 ENTER 709 ; V3,V4,V5,V6,V7,V8
210 OUTPUT 709 ;"CLS9"
220 OUTPUT 709 ;"F3R2Z0N4T2"
230 CLEAR
240 ENTER 709 ; R9
250 ! set up plot axes now
260 GCLEAR
270 SCALE -.03,.23,-500,8300
280 AXES .05,1000
290 LDIR 0
300 LORG 6
310 CSIZE 3
320 FOR S=0 TO .2 STEP .05
330 MOVE S,-100
340 LABEL S
350 NEXT S
360 LORG 8
370 FOR S=0 TO 8000 STEP 1000
380 MOVE 0,S
390 LABEL S/1000
400 NEXT S
410 !
420 ON KEY# 1," RAM" GOTO 520
430 ON KEY# 2,"ROCK" GOTO 620
440 ON KEY# 3,"PRES" GOTO 720
450 ON KEY# 4,"FORCE" GOTO 820
460 ON KEY# 5,"Z RAM" GOTO 920
470 ON KEY# 8,"BEGIN" GOTO 970
480 !
490 KEY LABEL
500 GOTO 500 ! waiting
510 !
520 ! ... read ram position ...
530 OUTPUT 709 ;"CLS8"
540 OUTPUT 709 ;"F1RA1Z0N4T1"
```

```
550 ENTER 709 ; A8
560 D1=(A8-V8)/V7*D0
570 KEY LABEL
580 DISP USING 590 ; D1
590 IMAGE ///,"RAM POSITION,= ",MD.DDD
600 GOTO 550
610 !
620 ! ...place rock correctly
630 OUTPUT 709 ;"CLS9"
640 OUTPUT 709 ;"F3R2Z0N4T1"
650 ENTER 709 ; A9
660 T1=(A9-R9)/T0
670 KEY LABEL
680 DISP USING 690 ; T1
690 IMAGE //,"ROCK POSITION = ",MD.DD
700 GOTO 650
710 !
720 ! ...get up to pressure
730 OUTPUT 709 ;"CLS4"
740 OUTPUT 709 ;"F1R-1Z0N4T1"
750 ENTER 709 ; A4
760 P1=(A4-V4)/V3*P0
770 KEY LABEL
780 DISP USING 790 ; P1
790 IMAGE /,"PRESSURE= ",MDDDDD.D
800 GOTO 750
810 !
820 ! ... read the force
830 OUTPUT 709 ;"CLS6"
840 OUTPUT 709 ;"F1R-1Z0N4T1"
850 ENTER 709 ; A6
860 F1=(A6-V6)/V5*F0
870 KEY LABEL
880 DISP USING 890 ; F1
890 IMAGE "RAM FORCE = ",MDDDDD.D
900 GOTO 850
910 !
920 ! ... re-zero the force
930 OUTPUT 709 ;"CLS6"
940 OUTPUT 709 ;"F1R-1Z0N4T2"
950 ENTER 709 ; V6
960 GOTO 490
970 ! *************************
980 !    MAIN TEST
990 ! *************************
1000 CLEAR
1010 OFF KEY# 1
1020 OFF KEY# 2
1030 OFF KEY# 3
1040 OFF KEY# 5
1050 ON KEY# 4," END" GOTO 1290
1060 ON KEY# 8,"ABORT" GOTO 420
1070 KEY LABEL
1080 OUTPUT 709 ;"LS6,8"
1090 I=0
1100 !
```

```
1110 ! take the curve data
1120 !
1130 I=I+1
1140 OUTPUT 709 ;"F1RA1Z0N4T3"
1150 X(I,3)=TIME
1170 ENTER 709 ; A6,A8
1180 X(I,1)=(A6-V6)/V5*F0
1190 X(I,2)=(A8-V8)/V7*D0
1200 !
1210 PLOT X(I,2)-X(1,2),X(I,1)
1220 !
1230 OUTPUT 709 ;"CLS6"
1240 OUTPUT 709 ;"F1R-1Z0N4T1"
1250 ENTER 709 ; A6
1260 F2=(A6-V6)/V5*F0
1270 IF ABS(F2-X(I,1))>50 THEN GOTO 1130
1280 GOTO 1250
1290 ON KEY# 6,"FILE" GOSUB 1350
1300 I2=I
1310 DISP "TEST OVER"
1320 BEEP
1330 DISP I2;" DATA POINTS TAKEN"
1340 GOTO 490
1350 ! filing subroutine, records information about the test
1360 MASS STORAGE IS ".DATA"
1370 REDIM X(I2,3)
1380 !
1390 CLEAR
1400 DISP "DATA FILE NAME:"
1410 INPUT N$
1420 DISP "TODAY'S DATE:"
1430 INPUT D$
1440 DISP "ROCK DESCRIPTION:"
1450 INPUT R$
1460 DISP "COMMENTS:"
1470 INPUT C$
1480 N=INT((I2*24+384)/256+1)
1490 CREATE N$,N
1500 ASSIGN# 1 TO N$
1510 PRINT# 1 ; N$,D$,R$,I,P1,T1,C$,X(,)
1520 ASSIGN# 1 TO *
1530 CLEAR
1540 BEEP
1550 DISP N$;" FILED"
1560 KEY LABEL
1570 MASS STORAGE IS ".TESTER"
1580 REDIM X(500,3)
1590 RETURN
1600 END
```

```
5 MASS STORAGE IS ".DATA"
7 PRINTER IS 1
10 OPTION BASE 1
20 REAL X(500,3)
30 DIM N$[6],D$[8],R$[20],C$[311]
35 INTEGER I,N,L
40 DISP "WHICH FILE DO YOU WANT?"
50 INPUT N$
60 ASSIGN# 1 TO N$
70 READ# 1 ; N$,D$,R$,N,P1,T1,C$
75 REDIM X(N,3)
76 READ# 1 ; X(,)
80 ASSIGN# 1 TO *
90 CLEAR
100 PRINT "FILE NAME: ";N$
105 PRINT "CORRECTED ACCORDING"
106 PRINT "TO X=C1*Y^(C2+C3*Y)"
107 PRINT "MODEL"
110 PRINT "CREATED ON ";D$
115 PRINT "ROCK: ";R$
116 PRINT "PRESSURE = ";P1;" PSI"
117 PRINT "POSITION = ";T1
120 PRINT "COMMENTS:"
130 PRINT C$
135 D9=X(1,2)
136 E9=X(1,3)
140 FOR I=1 TO N
150 X(I,2)=X(I,2)-D9-.000141884*X(I,1)^(.62032-.0000083744*X(I,1))
160 X(I,3)=X(I,3)-E9
170 NEXT I
180 CLEAR
190 PRINT "OLD NAME: ";N$
200 PRINT "ENTER NEW NAME"
210 INPUT A$
211 L=INT((N*24+384)/256+1)
212 CREATE A$,L
220 ASSIGN# 1 TO A$
230 PRINT# 1 ; A$,D$,R$,N,P1,T1,C$,X(,)
240 ASSIGN# 1 TO *
250 BEEP
260 PRINT A$;" FILED"
270 END
```

```
10 DEG
20 OPTION BASE 1
30 MASS STORAGE IS ".DATA"
40 !
50 DIM N$[6],D$[8],C$[311],R$[20]
60 REAL X(800,3),P,T,Z,L1,L2,L3,L4
70 INTEGER N,I
80 !
90 DISP "MAX X, TIC INCREMENT"
100 INPUT L1,L2
110 DISP "MAX Y, TIC INCREMENT"
120 INPUT L3,L4
130 !
140 GCLEAR
150 SCALE -(.2*L1),1.2*L1,-(.2*L3),1.1*L3
160 AXES L2,L4
170 LDIR 0
180 LORG 6
190 CSIZE 3
200 FOR Z=0 TO L1 STEP L2
210 MOVE Z,-(.03*L3)
220 LABEL Z
230 NEXT Z
240 LORG 8
250 FOR Z=0 TO L3 STEP L4
260 MOVE -(.03*L1),Z
270 LABEL Z/1000
280 NEXT Z
290 LORG 5
300 CSIZE 6
310 MOVE L1/2,-(.15*L3)
320 LABEL "DISPLACEMENT (IN)"
330 LDIR 90
340 MOVE -(.15*L1),L3/2
350 LABEL "FORCE (KIPS)"
360 !
370 DISP "WHICH DATA SET?"
380 INPUT N$
390 ASSIGN# 1 TO N$
400 READ# 1 ; N$,D$,R$,N,P,T,C$
410 REDIM X(N,3)
420 READ# 1 ; X(,)
430 ASSIGN# 1 TO *
440 MOVE 0,0
450 FOR I=1 TO N
460 PLOT X(I,2)-X(1,2),X(I,1)
470 NEXT I
480 PENUP
490 DISP "ANOTHER ONE? (Y/N)"
500 INPUT A$
510 IF A$="Y" THEN GOTO 370
520 END
```

```
/*                              program cone .c
    Uses a finite-difference approximation to solve the equations of
    plasticity and the slip line field for the problem of indentation
    of a rigid-plastic material.

    Reference:  L. L. Karafiath and E. A. Nowatski, SOIL MECHANICS FOR
                OFF-ROAD VEHICLE ENGINEERING, Trans Tech Publications,
                Clausthal, Germany (1978).                              */

#include <stdio.h>
#include <math.h>

                /************************************
                * Note:  point1 file operations are  *
                *        NOT commented out in this   *
                *        version.                    *
                ************************************/


/* note these variables will be global (declared before main): */

     double z[601][201],x[601][201],sigma[601][201],theta[601][201];
     double pi,phi,sinphi,tanphi,mu;
     double tan(),sin();
     FILE *point1;

main()
{
     int i,j,h,k,itmax,iter;
     double w,c,deltheta,m,z0,pressure;
     double linner,louter,eps,length,b,beta,alpha;
     double exp();
     void recur();
     char fname[8],f2name[8];
     FILE *point2;

    printf("File name for state variables:  \"        \"\b\b\b\b\b\b\b\b\b\b");
        scanf("%s", fname);
    printf("File name for tool pressures:  \"        \"\b\b\b\b\b\b\b\b\b\b");
        scanf("%s", f2name);


pi=3.1415926535;  /* approximately !                        */
eps=0.001;        /* tolerance for final point position */
itmax=20;         /* max iterations on length              */

/* set the fineness of the mesh */

        printf("Enter the number of j-lines (k):\n");
        scanf("%d",&k);
        h=3*k;              /* highest i-index */

/* define physical characteristics   */

c=1000.0;    /* use this value always, then scale pressures by c */

        printf("Coulomb friction angle (rad):  ");
        scanf("%lf",&phi);

            sinphi=sin(phi);    /*        these calculations      */
```

```
            tanphi=tan(phi);     /*          should prevent many      */
            mu=pi/4.0-phi/2.0;   /*          function calls           */

w=0.0;              /* see c* argument */

        printf("Enter wedge half-angle, beta (radians):\n");
        scanf("%lf",&beta);

b=1.0;              /* for convenience                                 */
z0=b/tan(beta);     /* penetration depth (unitless for a sharp cone)   */
iter = 0;           /* haven't started yet                             */

/* guess limits for the extent of the slip-line field */

linner=0.0;         /* gotta be too small */
louter=8.0;         /* gotta be too big   */

/*************************************************************************/

newguess:
        iter = iter +1;                 /* start of a new iteration      */
        if (iter > itmax)
           {
             printf ("\n\n\n\n\n\n\n\n");
             printf ("Completed %d iterations without convergence!\n", itmax);
             printf ("On final iteration:\n\n");
             goto finish;  /* print values for the 'itmax'th iteration */
           }


        point1=fopen(fname,"w");        /* reopen (and clear) ascii file */


        fprintf(point1,"%d %d\n",h,k); /* record mesh density            */
        length=(linner+louter)/2.0;    /* (generally) a new guess        */


/* set boundary conditions (geometry, confining pressure known) */

     for(j = 0; j <= k; j++)
        {
         i=k-j;
         z[i][j]=0.0;
         x[i][j]=b+length*j/k;
         sigma[i][j]=(c/tanphi+w)/(1.0-sinphi); /* Mohr-Coulomb only! */
         theta[i][j]=0.0;

         fprintf(point1,"%lf %lf %lf %lf\n",x[i][j],
                        z[i][j],theta[i][j],sigma[i][j]);
        }


/* now solve for the passive field */

     for(i = 1; i <= k; i++)
        {
             for(j = k-i+1; j <= k; j++)
                {
                  recur(i,j);
                }
```

```
        }


/* compute values at the singular point [k--->2k][0] */

         deltheta=beta/k;   /* equal increments of theta */
         j=0;
      for(i = k+1; i <= 2*k; i++)
         {
         theta[i][0]=theta[i-1][0]+deltheta;
         sigma[i][0]=sigma[k][0]*exp(2.0*tanphi*(theta[i][0]-theta[k][0]));
         x[i][0]=x[i-1][0];
         z[i][0]=z[i-1][0];
         fprintf(point1,"%lf %lf %lf %lf\n",x[i][j],
                        z[i][j],theta[i][j],sigma[i][j]);

         }


/* compute the other stresses in the radial zone */

      for(i = k+1; i <= 2*k; i++)
         {
          for(j = 1; j <= k; j++)
             {
              recur(i,j);
             }
         }


/* now solve the active field */

          m=tan(pi/2.0-beta);       /* the slope of the boundary */
     for(i = 2*k+1; i <= h; i++)
        {
/* ................solve the boundary point first.....................*/

         j = i-2*k;
         theta[i][j]=beta;         /* for no friction ! */
         z[i][j]=(z[i-1][j]+(z0/m-x[i-1][j])*tan(theta[i-1][j]-mu))
                 /(1.0+tan(theta[i-1][j]-mu)/m);
         x[i][j]=(z0-z[i][j])/m;

         if(x[i][j] < 0.0)   /* x is beyond axis of symmetry:  danger! */
             {
                 fclose(point1);
                 louter=length;
                 goto newguess;
             }

         alpha=sinphi*(x[i][j]-x[i-1][j])-tanphi*(1.0-sinphi)*
                                          (z[i][j]-z[i-1][j]);

         sigma[i][j]=sigma[i-1][j]+2.0*sigma[i-1][j]*tanphi*
             (theta[i][j]-theta[i-1][j])-sigma[i-1][j]*alpha/x[i-1][j];

          fprintf(point1,"%lf %lf %lf %lf\n",x[i][j],
                         z[i][j],theta[i][j],sigma[i][j]);
```

```
/* ..............now do the rest for this i.............................*/

        for(j = i-2*k+1; j <= k; j++)
           {
             recur(i,j);
           }
        }


    fclose(point1);

/* check to see if the final point is in the right place (within a margin
   of error.  If so, stop.  Otherwise, modify the guess for 'length'
   and start again at 'newguess:'. */

if (x[h][k] > eps)    /* too small */
     {
      linner=length;
      goto newguess;
     }

/* =========> If here, then we have an acceptable solution. */

/* write the wedge boundary pressures (scaled by c) to file f2name */

        point2=fopen(f2name,"w");      /* open pressure curve file  */
                fprintf(point2,"%d\n",k);

        for(j = k; j >= 0; j--)
            {
                i=j+2*k;
                pressure=(sigma[i][j]*(1.0+sinphi)-c/tanphi)/c;
                fprintf(point2,"%lf %lf\n",x[i][j],pressure);
            }


        fclose(point2);


     printf("\n\n\n\n\nSolution ran to completion. Error tolerance %f\n", eps);
     printf("Took %d iterations\n\n",iter);

finish:
    printf("Physical problem characteristics:\n");
    printf("          Cone half-angle, beta = %lf (rad)\n", beta);
    printf("          Friction angle, phi = %lf (rad)\n", phi);
    printf("          Confining pressure, w = %lf (psi)\n\n", w);


     printf("Mesh size: %d X %d\n",h,k);

     printf("Slip line field extends to x = %f\n\n", x[0][k]);

     printf("Singular point at cone/free boundary interface:\n");
```

```
      printf("     sigma[%d][0] = %10.5f     theta[%d][0] = %10.5f\n",
              2*k,sigma[2*k][0],2*k,theta[2*k][0]);

      printf("         x[%d][0] = %10.5f         z[%d][0] = %10.5f\n\n",
              2*k,x[2*k][0],2*k,z[2*k][0]);


      printf("Values on axis of symmetry (cone tip):\n");

      printf("     sigma[%d][%d] = %10.5f     theta[%d][%d] = %10.5f\n",
              h,k,sigma[h][k],h,k,theta[h][k]);

      printf("         x[%d][%d] = %10.5f         z[%d][%d] = %10.5f\n\n",
              h,k,x[h][k],h,k,z[h][k]);
      printf("\n");

     printf("Pressure profile located in file %s\n\n\n", f2name);

}

/************************ function recur ***************************
*                                                                  *
*                  (finite difference implementation)              *
*                                                                  *
*******************************************************************/
void recur(i,j)
     int i,j;
{
     double alpha1,alpha2,abar,bbar;

     alpha1=tan(theta[i][j-1]+mu);
     alpha2=tan(theta[i-1][j]-mu);

     x[i][j]=(z[i-1][j]-z[i][j-1]+alpha1*x[i][j-1]-alpha2*x[i-1][j])/
             (alpha1-alpha2);

     z[i][j]=z[i-1][j]+alpha2*(x[i][j]-x[i-1][j]);

     abar=sinphi*(x[i][j]-x[i-1][j])-
            tanphi*(1.0-sinphi)*(z[i][j]-z[i-1][j]);

     bbar=sinphi*(x[i][j]-x[i][j-1])+
            tanphi*(1.0-sinphi)*(z[i][j]-z[i][j-1]);


     sigma[i][j]=(2.0*sigma[i-1][j]*sigma[i][j-1]*(1.0-tanphi*(theta[i-1][j]-
                  theta[i][j-1]))-
                  sigma[i-1][j]*sigma[i][j-1]*(abar/x[i-1][j]+bbar/x[i][j-1]))
                 /(sigma[i][j-1]+sigma[i-1][j]);

     theta[i][j]=(sigma[i][j-1]-sigma[i-1][j]+2.0*tanphi*(sigma[i-1][j]*
                  theta[i-1][j]+sigma[i][j-1]*theta[i][j-1])
                  +(sigma[i-1][j]*abar/x[i-1][j]-sigma[i][j-1]*bbar/x[i][j-1]))
                  /(2.0*tanphi*(sigma[i-1][j]+sigma[i][j-1]));

         fprintf(point1,"%lf %lf %lf %lf\n",x[i][j],
                        z[i][j],theta[i][j],sigma[i][j]);

         return;
```

PROGRAM bluntcone.c

```
/*                      program bluntcone.c
    Uses a finite-difference approximation to solve the equations of
    plasticity and the slip line field for the problem of indentation
    of a rigid-plastic material.

    Reference:  L. L. Karafiath and E. A. Nowatski, SOIL MECHANICS FOR
                OFF-ROAD VEHICLE ENGINEERING, Trans Tech Publications,
                Clausthal, Germany (1978).                              */

#include <stdio.h>
#include <math.h>

                /************************************
                * Note:  point1 file operations are  *
                *        commented out in this       *
                *        version.                    *
                ************************************/


/* note these variables will be global (declared before main): */

     double z[601][201],x[601][201],sigma[601][201],theta[601][201];
     double pi,phi,sinphi,tanphi,mu;
     double tan(),sin();


main()
{
     int i,j,h,k,itmax,iter;
     double w,c,deltheta,m,z0,pressure;
     double linner,louter,eps,length,start,b,beta,alpha;
     double exp();
     void recur();
     char finame[8],f2name[8];
     FILE *point1,*point2;

/*    printf("File name for state variables:  \"        \"\b\b\b\b\b\b\b\b\b");
        scanf("%s", finame);*/
    printf("File name for tool pressures:  \"        \"\b\b\b\b\b\b\b\b\b");
        scanf("%s", f2name);


pi=3.1415926535;  /* approximately !                        */
eps=0.001;        /* tolerance for final point position */
itmax=20;         /* max iterations on length              */

/* set the fineness of the mesh */

        printf("Enter the number of j-lines (k):\n");
        scanf("%d",&k);
    .   h=3*k;            /* highest i-index */

/* define physical characteristics   */

c=1000.0;    /* use this value always, then scale pressures by c */

        printf("Coulomb friction angle (rad):  ");
        scanf("%lf",&phi);

            sinphi=sin(phi);    /*        these calculations      */
```

```
            tanphi=tan(phi);     /*         should prevent many      */
            mu=pi/4.0-phi/2.0;   /*         function calls           */

w=0.0;                    /* see c* argument */

        printf("Enter wedge half-angle, beta (radians):\n");
        scanf("%lf",&beta);

b=1.0;            /*                                    */
        printf("Enter penetration depth:");
        scanf("%lf",&z0);

                  /************************************
                  *  Solve the cone part first to      *
                  *  the extent of its field.          *
                  ************************************/

iter = 0;         /* haven't started yet                                  */

/* guess limits for the extent of the slip-line field */

linner=0.0;       /* gotta be too small */
louter=12.0;       /* gotta be too big   */


again:
        iter = iter +1;                /* start of a new iteration      */
        if (iter > itmax)
           {
             printf ("\n\n\nConical part:\n");
             printf ("Completed %d iterations without convergence!\n", itmax);
             printf ("On final iteration:\n\n");
             goto finish;  /* print values for the 'itmax'th iteration */
           }


        start=(linner+louter)/2.0;    /* (generally) a new guess        */


/* set boundary conditions (geometry, confining pressure known) */

     for(j = 0; j <= k; j++)
        {
         i=2*k-j;
         z[i][j]=0.0;
         x[i][j]=b+z0*tan(beta)+start*j/k;
         sigma[i][j]=(c/tanphi+w)/(1.0-sinphi); /* Mohr-Coulomb only! */
         theta[i][j]=0.0;
        }


/* now solve for the passive field */

     for(i = k; i <= 2*k; i++)
        {
             for(j = 2*k-i+1; j <= k; j++)
                {
                  recur(i,j);
                }
```

```
        }

/* compute values at the singular point */

         deltheta=beta/k;    /* equal increments of theta */
         j=0;
      for(i = 2*k+1; i <= 3*k; i++)
         {
         theta[i][0]=theta[i-1][0]+deltheta;
         sigma[i][0]=sigma[2*k][0]*exp(2.0*tanphi*(theta[i][0]-theta[2*k][0]));
         x[i][0]=x[i-1][0];
         z[i][0]=z[i-1][0];
         }


/* compute the other stresses in the radial zone */

      for(i = 2*k+1; i <= 3*k; i++)
         {
          for(j = 1; j <= k; j++)
             {
              recur(i,j);
             }
         }


/* now solve the active field */

          m=tan(pi/2.0-beta);       /* the slope of the boundary */
     for(i = 3*k+1; i <= 4*k; i++)
        {
/* .................solve the boundary point first.....................*/

        j = i-3*k;
        theta[i][j]=beta;          /* for no friction ! */
      z[i][j]=(z[i-1][j]+((z0+b/tan(beta))/m-x[i-1][j])*tan(theta[i-1][j]-mu))
                /(1.0+tan(theta[i-1][j]-mu)/m);
        x[i][j]=b+(z0-z[i][j])/m;

        if(x[i][j] < b-eps)    /* x is beyond ridge:  too big! */
            {
                louter=start;
                goto again;
            }

        alpha=sinphi*(x[i][j]-x[i-1][j])-tanphi*(1.0-sinphi)*
                                          (z[i][j]-z[i-1][j]);

        sigma[i][j]=sigma[i-1][j]+2.0*sigma[i-1][j]*tanphi*
            (theta[i][j]-theta[i-1][j])-sigma[i-1][j]*alpha/x[i-1][j];


/* ..............now do the rest for this i.............................*/

        for(j = i-3*k+1; j <= k; j++)
           {
             recur(i,j);
           }
        }
```

```
if (x[4*k][k] > b+eps)   /* too small */
     {
      linner=start;
      goto again;
     }


/* ========> If here, then conical part is solved. */

                /*************************************
                *  Value of start is known.  Now     *
                *  solve the rest of the field to the *
                *  flat part.                        *
                *************************************/

iter = 0;         /* haven't started yet                                  */

/* guess limits for the extent of the slip-line field */

linner=0.0;       /* gotta be too small */
louter=12.0;       /* gotta be too big   */


newguess:
        iter = iter +1;              /* start of a new iteration      */
        if (iter > itmax)
           {
             printf ("\n\n\nFlat part:\n");
             printf ("Completed %d iterations without convergence!\n", itmax);
             printf ("On final iteration:\n\n");
             goto finish;  /* print values for the 'itmax'th iteration */
           }


        length=(linner+louter)/2.0;   /* (generally) a new guess       */


/* set boundary conditions (geometry, confining pressure known) */

     for(j = k+1; j <= 2*k; j++)
        {
         i=2*k-j;
         z[i][j]=0.0;
         x[i][j]=b+z0*tan(beta)+start+length*(j-k)/k;
         sigma[i][j]=(c/tanphi+w)/(1.0-sinphi); /* Mohr-Coulomb only! */
         theta[i][j]=0.0;
        }


/* now solve for the passive field */

     for(i = 1; i <= k; i++)
        {
             for(j = 2*k-i+1; j <= 2*k; j++)
                {
                  recur(i,j);
                }
        }
```

```
        for (i=k+1;i<=4*k;i++) {
            for (j=k+1;j<=2*k;j++) {
                recur(i,j);
            }
        }

/* compute values at the singular point */

         deltheta=(pi/2.0-beta)/k;    /* equal increments of theta */
         j=k;
      for(i = 4*k+1; i <= 5*k; i++)
         {
         theta[i][j]=theta[i-1][j]+deltheta;
         sigma[i][j]=sigma[4*k][j]*exp(2.0*tanphi*(theta[i][j]-theta[4*k][j]));
         x[i][j]=x[i-1][j];
         z[i][j]=z[i-1][j];
         }


/* compute the other stresses in the radial zone */

       for(i = 4*k+1; i <= 5*k; i++)
          {
           for(j = k+1; j <= 2*k; j++)
              {
               recur(i,j);
              }
          }


/* now solve the active field */

     for(i = 5*k+1; i <= 6*k; i++)
        {
/* ................solve the boundary point first.....................*/

        j = i-4*k;
        theta[i][j]=pi/2.0;          /* for no friction ! */
        z[i][j]=z0;
        x[i][j]=x[i-1][j]+(z[i][j]-z[i-1][j])/tan(theta[i-1][j]-mu);

        if(x[i][j] <= 0.0)    /* x is beyond axis of symmetry: too big! */
            {
                louter=length;
                goto newguess;
            }

        alpha=sinphi*(x[i][j]-x[i-1][j])-tanphi*(1.0-sinphi)*
                                          (z[i][j]-z[i-1][j]);

        sigma[i][j]=sigma[i-1][j]+2.0*sigma[i-1][j]*tanphi*
            (theta[i][j]-theta[i-1][j])-sigma[i-1][j]*alpha/x[i-1][j];


/* .............now do the rest for this i.............................*/

        for(j = i-4*k+1; j <= 2*k; j++)
           {
            recur(i,j);
```

```
            }
        }

if (x[6*k][2*k] > eps)   /* too small */
    {
     linner=length;
     goto newguess;
    }


/* ========> If here, then flat part is solved. */

/* write state variables */
/*      point1=fopen(f1name, "w");
        fprintf(point1,"%d %d\n",h,k);
        j=0;
        for (i=2*k;i<=3*k;i++) {
            fprintf(point1,"%lf %lf %lf %lf\n",x[i][j],z[i][j],
                        theta[i][j],sigma[i][j]);
        }
        for (j=1;j<=k;j++) {
            for (i=2*k-j;i<=j+3*k;i++) {
            fprintf(point1,"%lf %lf %lf %lf\n",x[i][j],z[i][j],
                        theta[i][j],sigma[i][j]);
            }
        }
        for (j=k+1;j<=2*k;j++) {
            for (i=2*k-j;i<=k;i++) {
            fprintf(point1,"%lf %lf %lf %lf\n",x[i][j],z[i][j],
                          theta[i][j],sigma[i][j]);
            }
        }
        for (i=k+1;i<=4*k;i++) {
            for (j=k+1;j<=2*k;j++) {
                fprintf(point1,"%lf %lf %lf %lf\n",x[i][j],z[i][j],
                        theta[i][j],sigma[i][j]);
            }
        }

        j=k;
        for (i=4*k+1;i<=5*k;i++) {
            fprintf(point1,"%lf %lf %lf %lf\n",x[i][j],z[i][j],
                        theta[i][j],sigma[i][j]);
        }
        for (j=k+1;j<=2*k;j++) {
            for (i=4*k+1;i<=j+4*k;i++) {
            fprintf(point1,"%lf %lf %lf %lf\n",x[i][j],z[i][j],
                        theta[i][j],sigma[i][j]);
            }
        }
        fclose(point1);*/


/* write the boundary pressures (scaled by c) to file f2name */

        point2=fopen(f2name,"w");      /* open pressure curve file  */
                fprintf(point2,"%d\n",2*(k+1)); /* number of points
                                                   written */
        for(j = 2*k; j >= k; j--)
```

```
            {
                i=j+4*k;
                pressure=(sigma[i][j]*(1.0+sinphi)-c/tanphi)/c;
                fprintf(point2,"%lf %lf\n",x[i][j],pressure);
            }
        for (j=k;j>=0;j--) {
            i=j+3*k;
                pressure=(sigma[i][j]*(1.0+sinphi)-c/tanphi)/c;
                fprintf(point2,"%lf %lf\n",x[i][j],pressure);
        }


        fclose(point2);


     printf("\n\n\n\n\nSolution ran to completion. Error tolerance %f\n",eps);
     printf("Took %d iterations\n\n",iter);

finish:
    printf("Blunt-ended single cone:\n");
    printf("          Cone half-angle, beta = %lf (rad)\n", beta);
    printf("          Friction angle, phi = %lf (rad)\n", phi);
    printf("          Confining pressure, w = %lf (psi)\n", w);
    printf("          Indentation depth, z0 = %lf\n",z0);



     printf("Mesh size: %d X %d\n",h,k);

     printf("Slip line field extends to x = %f\n\n", x[0][2*k]);

     printf("Singular point at cone/free boundary interface:\n");
     printf("     sigma[%d][0] = %10.5f     theta[%d][0] = %10.5f\n",
            2*k,sigma[2*k][0],2*k,theta[2*k][0]);

     printf("          x[%d][0] = %10.5f          z[%d][0] = %10.5f\n\n",
            2*k,x[2*k][0],2*k,z[2*k][0]);


     printf("Values on axis of symmetry (cone tip):\n");

     printf("     sigma[%d][%d] = %10.5f     theta[%d][%d] = %10.5f\n",
            6*k,2*k,sigma[6*k][2*k],6*k,2*k,theta[6*k][2*k]);

     printf("          x[%d][%d] = %10.5f          z[%d][%d] = %10.5f\n\n",
            6*k,2*k,x[6*k][2*k],6*k,2*k,z[6*k][2*k]);
     printf("\n");


}

/************************ function recur ****************************
*                                                                   *
*                  (finite difference implementation)               *
*                                                                   *
*******************************************************************/
void recur(i,j)
     int i,j;
{
     double alpha1,alpha2,abar,bbar;
```

```
        alpha1=tan(theta[i][j-1]+mu);
        alpha2=tan(theta[i-1][j]-mu);

        x[i][j]=(z[i-1][j]-z[i][j-1]+alpha1*x[i][j-1]-alpha2*x[i-1][j])/
                (alpha1-alpha2);

        z[i][j]=z[i-1][j]+alpha2*(x[i][j]-x[i-1][j]);

        abar=sinphi*(x[i][j]-x[i-1][j])-
               tanphi*(1.0-sinphi)*(z[i][j]-z[i-1][j]);

        bbar=sinphi*(x[i][j]-x[i][j-1])+
               tanphi*(1.0-sinphi)*(z[i][j]-z[i][j-1]);


        sigma[i][j]=(2.0*sigma[i-1][j]*sigma[i][j-1]*(1.0-tanphi*(theta[i-1][j]-
                     theta[i][j-1]))-
                     sigma[i-1][j]*sigma[i][j-1]*(abar/x[i-1][j]+bbar/x[i][j-1]))
                    /(sigma[i][j-1]+sigma[i-1][j]);

        theta[i][j]=(sigma[i][j-1]-sigma[i-1][j]+2.0*tanphi*(sigma[i-1][j]*
                     theta[i-1][j]+sigma[i][j-1]*theta[i][j-1])-
                     +(sigma[i-1][j]*abar/x[i-1][j]-sigma[i][j-1]*bbar/x[i][j-1]))
                     /(2.0*tanphi*(sigma[i-1][j]+sigma[i][j-1]));

            return;

}
```

PROGRAM force.c

```
/*                    program force.c
        Read a pressure-radius file to determine the total
        vertical force on a tool.    */

#include <stdio.h>
#include <math.h>

main()
{
    int i,k;
    double r[303],p[303],pi=3.141592654;
    double a1,a2,c1,c2,force,rflat,rbar;

    FILE *point1;
    char fname[20];

/* ask what pressure file to read */

    printf("What file do you want to read?\n");
    scanf("%s",fname);

/* get tool size */

    printf("What is actual flat radius (in)?\n");
    scanf("%lf",&rflat);

/* open the file */

    point1=fopen(fname,"r");

/* read the number of data pairs */

    fscanf(point1,"%d",&k);

/* read the radii and pressures */

    for (i=1;i<=k;i++) {
        fscanf(point1,"%lf %lf",&r[i],&p[i]);
        r[i]=r[i]*rflat;    /* scale to correct size */
    }
    r[0]=0.0;
    p[0]=p[1];

/* close the file */
    fclose(point1);


/* use trapezoidal rule with Pappus-Guldinus to get total force */
    force=0.0;

    for (i=1;i<=k;i++) {
        a1=(r[i]-r[i-1])*p[i];          /* rectangle area */
        c1=(r[i]+r[i-1])/2.0;           /* rectangle centroid */
        a2=0.5*(r[i]-r[i-1])*(p[i]-p[i-1]); /* triangle area */
        c2=r[i-1]+(r[i]-r[i-1])/3.0;        /* triangle centroid */

        /* find net centroid */
        if ((a1+a2) == 0.0) {
            rbar=c1;
            goto skip;
```

```
        }

        rbar=(c1*a1+c2*a2)/(a1+a2);
skip:
        force=force+2.0*pi*rbar*(a1+a2);
    }

   printf("force/c* = %lf lbf/psi for flat radius = %lf in\n",force,rflat);
}
```